NASA TT F-10,030

CONTRIBUTION TO THE ANALYSIS OF LIGHT ELEMENTS USING X-FLUORESCENCE EXCITED BY RADIOELEMENTS

André Robert

Translation of "Contribution à l'analyse des éléments légers par fluorescençe X excitée au moyen de radioéléments". Commissariat à l'Energie Atomique, Rapport CEA - R 2539, 1964.

NATIONAL AERONAUTICS AND SPACE ADMINISTRATION
WASHINGTON MARCH 1966

Report CEA R No.2539

CONTRIBUTION TO THE ANALYSIS OF LIGHT ELEMENTS USING X-FLUORESCENCE EXCITED BY RADIOELEMENTS

André Robert

(Thesis, Conservatory of Liberal Arts)

1964

LIST OF ILLUSTRATIONS

TABLE OF CONTENTS

CONTRIBUTION TO THE ANALYSIS OF LIGHT ELEMENTS USING X-FLUORESCENCE EXCITED BY RADIOELEMENTS

*/1

André Robert

In order to study the possibilities of using radioactive sources for the X-fluorescence analysis of light elements, the principle is given, after a brief description of X-fluorescence, of the excitation of this phenomenon by X, β, and α emission from radioelements. The operation and use of the proportional gas counter for X-ray detection is described. [illegible] device has been studied for analyzing the elements of the 2nd and 3rd periods of the Mendeleev table. It makes it possible to excite the fluorescence with a radioactive source emitting X-rays or α particles; the X-ray fluorescence penetrates into a windowless proportional counter, this being made possible by the use of the auxiliary electric field in the neighborhood of the sample. The gas detection pressure leading to the maximum detection yield is given. The spectra are given for the K_α lines of the 3rd period elements excited by ^{55}Fe, $^{3}H/Zr$ and ^{210}Po sources; for the 2nd period the K_α spectra of carbon and of fluorine excited by the α particles of ^{210}Po.

INTRODUCTION

Under certain physical conditions, the peripheral electrons of a given

---

* Numbers in the margin indicate pagination in the original foreign text.

atom may pass from one energy level to another. Such transitions are accompanied by an electromagnetic radiation whose wavelength may extend from the visible spectrum to the X-ray spectrum, depending on the atomic number of the element and on the electron orbits considered.

About 100 years ago, Bunsen and Kirchhoff designed a practical spectrograph and, by deriving fundamental laws with respect to the emission of the characteristic spectrum of an element, demonstrated the possibility of using this spectrum for analytical purposes.

Starting with the XIX Century, spectroscopy developed further and finally became one of the foremost methods of qualitative analysis. Experiments by Moseley in 1913, Coster, and Hevesy in 1923 demonstrated the possibility of using the X-ray radiation spectra, emitted by the atoms, for general analysis. This work permitted to free the field of spectrometry of the difficulties in working up the optical lines emitted in large number by the atom.

The quality of the electronic apparatus and the detection techniques, over several decades, permitted a considerable progress in analytical methods by X-ray fluorescence. The measurement of the intensity and frequency of fluorescence radiation is applied to a quantitative and qualitative analysis of various elements, starting from magnesium, for physical states such as solids, liquids, and powders.

X-ray fluorescence analysis forms part of the great variety of physical analytical methods that make use of the properties of radiations. In these various methods, X-ray fluorescence occupies a position among those in which the element to be determined emits a characteristic secondary radiation, including:

analysis by neutron activation; /2

analysis by detection of gamma rays emitted by the nucleus during capture of a neutron;

analysis by detection of secondary radiation at the reactions (γ, n) $(\alpha, n\gamma)$, $(\alpha, p\gamma)$.

Of this enumeration, we will retain the analyses by neutron activation and by X-ray fluorescence, as proved and currently applied methods.

The high sensitivity of an analysis by neutron activation has made this a method of choice for research on traces. The theoretical limits of this method are imposed by the effective cross section of the element to be determined and by the period of the nuclide formed. The necessity of an intense neutron source (nuclear reactor) may present a practical limit, while awaiting the possibility of using small deuteron accelerators that produce 14-Mev neutrons by nuclear reaction.

Over a period of several years, numerous studies have been made on replacing the X-ray tube, in X-ray fluorescence analysis, by a radioactive source. This yielded various advantages.

The radiation spectrum of the radioactive source is invariant, and the intensity of its emission is affected only by statistical fluctuations inherent to the random character of the nuclide disintegration and by the decrease in activity, in obedience to a well-known law which is a function of time and of the half-life of the nuclide.

The elimination of the exciter tube and of its stabilized feed presents an economical advantage, in view of the cost of a radioactive source.

Reduced cost price, small dimensions, ruggedness, and absence of maintenance of the exciter system by radioisotopes generally makes this technique useful for nondestructive testing of strength or thickness of coatings of industri-

al products.

In industrial laboratories, it will become possible to design various equipment with this technique, for determining, for example,

tungsten in steels to within 1%, in 20 sec;

cobalt in hydrocarbons to within 0.01%, in 3 min;

uranium in solutions with a sensitivity of 50 ppm;

calcium and iron in cores of Lorraine iron ore, with a sensitivity of 3% absolute.

In practical application, the limit of analysis at low atomic numbers is shifted toward magnesium, for the two excitation techniques, namely, by X-ray

bility and the use conditions of radioelements in the X-ray fluorescence analysis of light elements, specifically of the first of the third period in the /3 periodic table, as well as those of the second period, i.e., from lithium to fluorine.

To reduce this analysis limit of light elements, several practical advantages can be obtained with an excitation by radioelements that could be selected on the basis of preceding studies. However, some theoretical interest may lie in the use of α-radiation for excitation of light elements.

After a brief review of several general principles of X-ray fluorescence, this paper will give the considered solutions in their basic principles and the difficulties presented by an analysis of light elements.

Using the described means, the experimental conditions and the obtained results will be discussed in Part II of this report.

PART I

I. THE PHENOMENON OF FLUORESCENCE /7

I.1 Quantization of Electron Levels

According to Bohr's atomic theories, complemented by Sommerfeld, the electrons are distributed about the nucleus in quantized energy levels. Schrödinger associated a wave function, independent of time, with the electron. The solutions of this equation introduce whole numbers, known as quantum numbers; these fix the "position" of the electron in the atom.

---

the electron.

n = principal quantum number, able to assume integral values: 1, 2, 3, 4, ...; these values correspond, respectively, to the shells K, L, M, N, ...;

l = azimuthal quantum number, able to assume the values 0, 1, 2, ..., n - 1, corresponding to the subshells s, p, d, f, ...; the half-integer of the electron spin decomposes the value of l such that $l \pm 1/2$, but must always yield a positive number. Thus, l and the spin determine the subshells;

m = magnetic quantum number, able to assume the values -l, -(l - 1), ..., -1, 0, 1, ..., (l - 1), l.

The latter intervenes in the Stark as well as the Zeeman effect, where a slight variation in the radiation frequency is observed.

Each group of these four quantum numbers defines a single electron in the atom, in accordance with Pauli's exclusion principle.

If a peripheral electron receives an energy quantum of a value sufficient for being ejected from the shell it occupies, a vacancy is created which can be filled by an electron coming from a shell less rigidly bound to the nucleus and having a higher energy level.

The transition of an electron from one shell to another modifies the energy of the atom. The law of the conservation of energy is obeyed by the appearance of X-ray radiation, known as fluorescence, or by the emission of an electron.

An electron transition gives rise to an electromagnetic radiation of the energy $h\nu$, defined by the levels in question. /8

Here, ν is the radiation frequency $\nu = \frac{c}{\lambda}$, and h is Planck's constant

$$h = 6.625 \times 10^{-27} \text{ erg-sec.}$$

Transitions between levels, having the same value of l, are forbidden.

A fluorescence radiation is designated by two letters. The first letter indicates the shell where the vacancy had been created while the second letter denotes the shell where the transition electron originated. These two letters can be supplemented by a number that defines the subshells; examples are $L_{III}\alpha_1$; $K\beta_1$. Figure 1, according to Brown, shows the numerous possible transitions in a uranium atom.

I.2 Qualitative Analysis

For a given transition, the energy of the X-ray fluorescence quantum is characteristic of the excited element. Thus, it will be possible to associate an element with the detected fluorescence energy. Table 2 gives the X-ray fluorescence energy of the $K\alpha_1$ line for the second and third period.

The frequency ν of K-fluorescence radiation, as a function of the atomic number Z, obeys the following law established by Moseley: /10

$$\sqrt{\frac{\nu}{R}} = 0.874\ (Z - 1.13)$$

where R is the Rydberg constant and R = 109,737 cm^{-1}.

Figure 2 presents this energy variation as a function of Z (Bibl.1).

Period	Z	Elements	Line $K\alpha_1$ ev	Å
2nd	3	Li	52	238.3
	4	Be	110	112.7
	5	B	185	67
	6	C	282	44.9
	7	N	392	31.8
	8	O	523	23.8
	9	F	677	18.3
3rd	11	Na	1 041	11.9
	12	Mg	1 254	9.88
	13	Al	1 487	8.34
	14	Si	1 740	7.12
	15	P	2 015	6.15
	16	S	2 308	5.37
	17	Cl	2 622	4.72
	18	A	2 957	4.19

I.3 Fluorescence Yield

The term "Auger effect" is used for the phenomenon in which the fluorescence radiation, by photoelectric effect with a peripheral electron of the atom, is converted into the emission of an electron.

For example, let an atom be excited at the K level and let us assume that it can emit the X-$K\alpha_1$ fluorescence radiation of an energy $E_K - E_{L_{III}}$ (here, E denotes the energy level of the shell under consideration). Certain of these photons, again by photoelectric effect in the shell L_{II}, may decay by ejecting

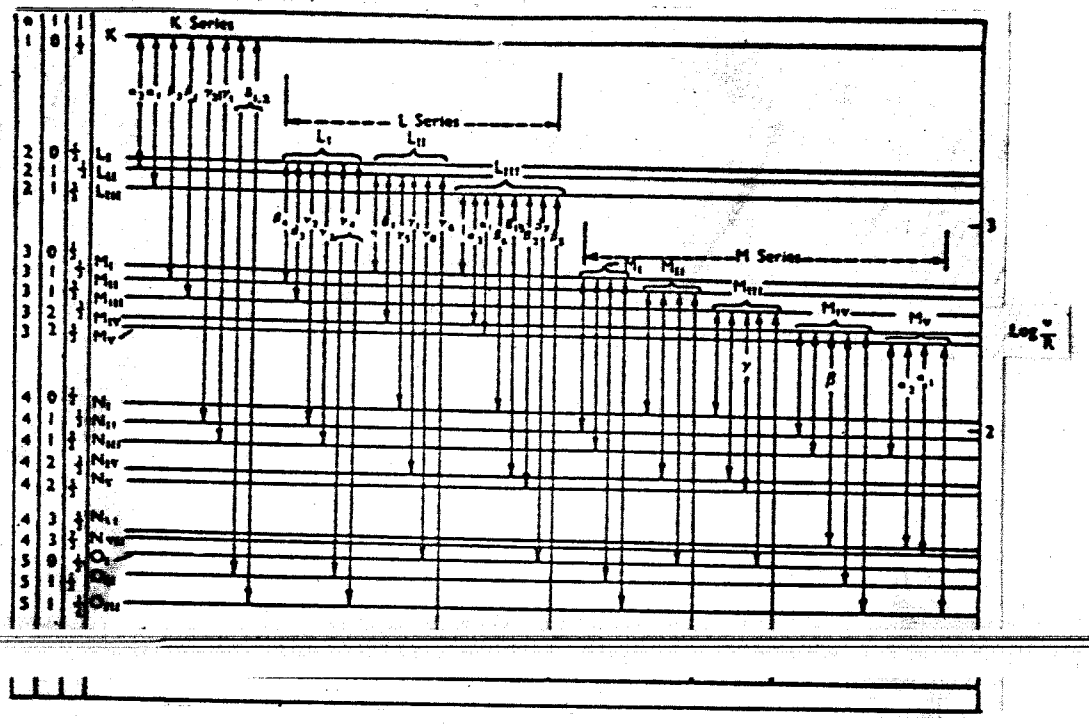

Fig.1 Diagram of Energy Levels of X-Ray Lines for the Uranium Atom, according to Brown

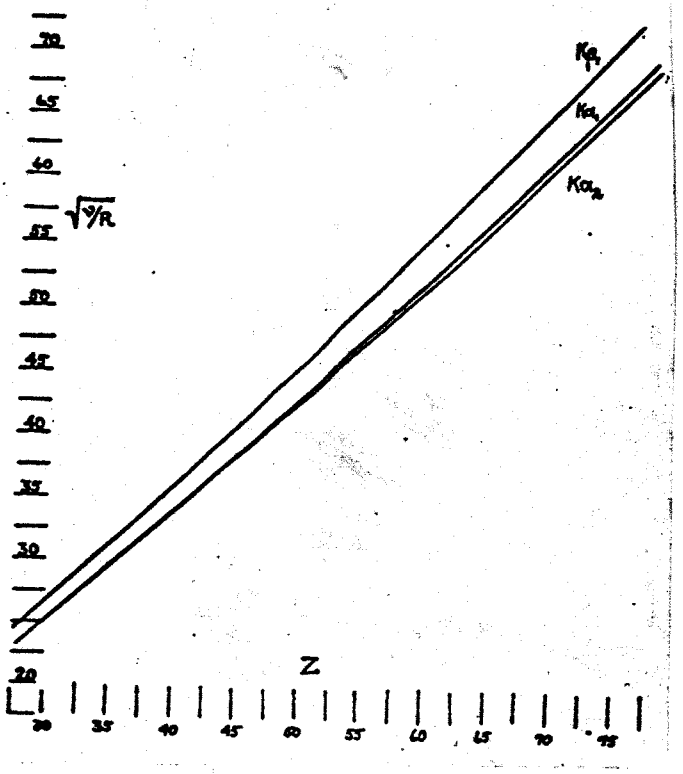

Fig.2 Moseley Curve

an electron from this shell. The emitted electron or "Auger electron" will have the energy

$$E_K - E_{L\,III} - E_{L\,II} .$$

Thus, in the de-excitation of the atom, the emission of a photon and that of an electron are two concurrent processes.

Let us take the simplifying hypothesis of a target consisting of a single type of atoms, irradiated by an X-ray beam. Let n_q be the atoms excited in unit time at the level q, and let n_q^i, f be the number of atoms emitting the line i of the series q, in unit time.

The following ratio is designated as the fluorescence yield ω_q, corresponding to this level q:

$$\omega_q = \frac{\sum_i n_q^i}{n_q}$$

where ω_q is proportional to the probability of fluorescence emission from the shell q.

This yield is a function of the atomic number Z of the excited element. The following relation

/11

empirically derived by Arends (Bibl.5), reduces to that derived by Wentzel, who established his expression by a wave-mechanical expansion.

I.4 Quantitative Analysis

Let a monoenergetic X-ray beam of a frequency ν_1 and an intensity I_1 irradiate a target of a surface s and a thickness d, at an angle of incidence φ. For simplifying the description, let us assume that the target consists of a binary compound of the elements A and B. In studying the fluorescence radiation of

the series q of the element A, produced in the target by the primary radiation, we can obtain a relation of proportionality between the intensity of isotropic

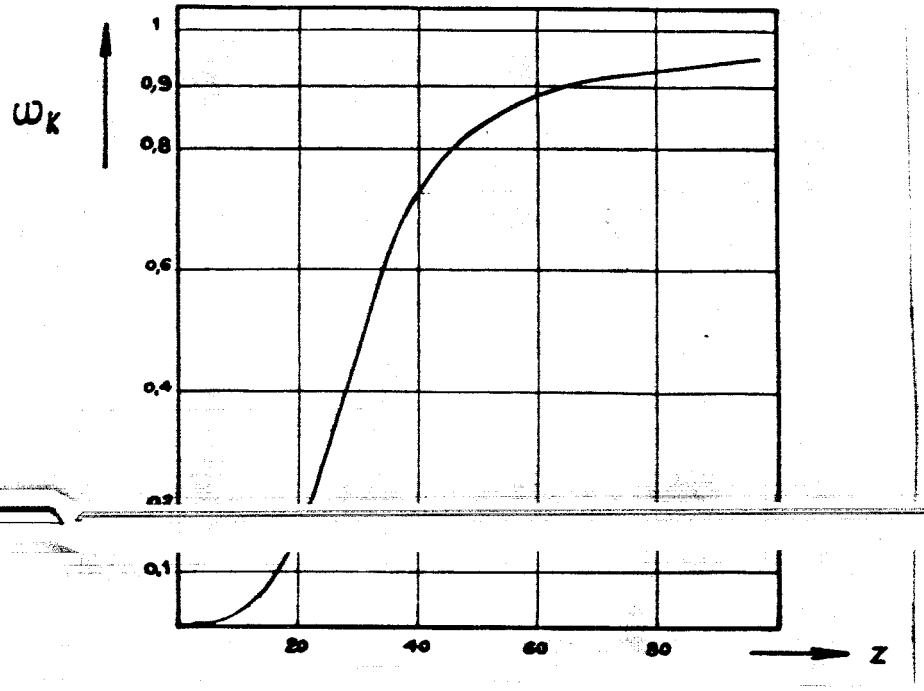

emission of A and its concentration in the target. The accompanying diagram and the following definitions will define the notations.

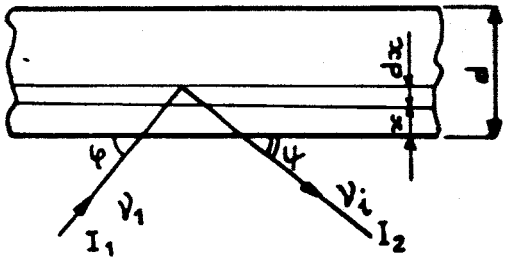

In the target, M_A and M_B, respectively, denote the volume masses of the /12 elements A and B; μ is the linear absorption coefficient, corresponding to $\mu = \zeta + \sigma$; ζ and σ, respectively, are the partial absorption coefficients, of the photoelectric and the diffusion type.

For the traversal of a binary medium, we have

$$\mu = \mu_m (A) \cdot M_A + \mu_m (B) \cdot M_B$$

where

μ_m = mass absorption coefficient, connected with μ by the general relation $\mu_m = \frac{\mu}{\rho}$;

ρ = density;

μ_1 = linear absorption coefficient of the target, linked to the incident radiation of a frequency ν_1;

r_q = ratio of the values of ζ at the extremities of the absorption discontinuity q.

The intensity of the incident energy flux, at a depth x of the target, will be reduced to

$$I_{1(x)} = I_1 e^{-\frac{\mu_1 \cdot x}{\sin \Phi}}.$$

The absorption due to the photoelectric effect, over a thickness dx, by the element A will be

$$d I_1 = - I_1 e^{-\frac{\mu_1 \cdot x}{\sin \Phi}} \cdot \frac{\zeta_{1\,A}}{\rho A} \cdot N_A \frac{dx}{\sin \Phi}$$

The corresponding energy absorbed in the layer dx by the specimen will be

$$d E_{1\,A} = I_1 e^{-\frac{\mu_1 \cdot x}{\sin \Phi}} \cdot \frac{\zeta_{1\,A}}{\rho A} \cdot N_A \cdot \frac{dx}{\sin \Phi} \cdot s \cdot \sin \Phi$$

and, for exciting the level q,

$$(d E_{1\,A})_q = \frac{r_q - 1}{r_q} \cdot \frac{\zeta_{1\,A}}{\rho A} \cdot I_1 \cdot e^{-\frac{\mu_1 \cdot x}{\sin \Phi}} \cdot N_A \cdot s \cdot dx.$$

The number of primary photons absorbed by the level q of the atoms A in the layer dx is

$$\frac{(d E_{1\,A})_q}{h \nu_1} = \frac{\lambda_1}{hc} (d E_{1\,A})_q$$

to which corresponds the number $n_q \cdot s \cdot dx$ of atoms A excited in the volume

s • dx, i.e.,

/13

$$\frac{\lambda_1}{hc}\ \frac{r_q - 1}{r_q}\ \frac{\zeta_{1A}}{\rho A} \cdot I_1 e^{-\frac{\mu_1 \cdot x}{\sin \varphi}} \cdot M_A \cdot s \cdot dx$$

where ω_q is the fluorescence yield of A at this level; p_i is the probability that an atom excited at the level q emits the line i.

The number of atoms emitting the radiation i will be

$$(n_q^i)_A \cdot s \cdot dx = \omega_q \cdot p_i \cdot \frac{\lambda_1}{hc}\ \frac{M_A}{\rho A}\ \frac{r_q - 1}{r_q} \cdot \zeta_{1A} \cdot I_1 \cdot e^{-\frac{\mu_1 \cdot x}{\sin\varphi}} \cdot s \cdot dx$$

The volume s • dx emits secondary X-ray fluorescence radiation in all directions, of the line i at the frequency ν_i, with an energy of

$$(d E_2\ A)_i = h \nu_i \cdot n_q^i \cdot s \cdot dx = \frac{\lambda_1}{\lambda_i}\ \frac{r_q - 1}{r_q}\ \frac{M_A}{\rho A}$$

$$\tau_{1A} \cdot \omega_q \cdot p_i \cdot I_1 \cdot e^{-\frac{\mu_1 \cdot x}{\sin\varphi}} \cdot s \cdot dx .$$

We will determine the fluorescence intensity I_2, i of A at a distance R from the target ($R \gg d$) over a surface of 1 cm^2 and perpendicular to the X-ray emission at an angle ψ.

Here, μ_i is the absorption coefficient of the target for the frequency ν_i:

$$(I_2\ ,\ A)_i = \int_0^d \frac{I_1}{4 \pi R^2}\ \frac{\lambda_1}{\lambda_i}\ \frac{r_q - 1}{r_q}\ \frac{M_A}{\rho A} \cdot \zeta_{1A} \cdot \omega_q \cdot p_i \cdot e^{-\left(\frac{\mu_1}{\sin\varphi} + \frac{\mu_i}{\sin\psi}\right) x} \cdot s \cdot dx$$

$$(I_2 \cdot A)_i = \frac{I_1}{4\pi R^2} \cdot \omega_q \cdot p_i \frac{r_q - 1}{r_q} \frac{\zeta_{1A}}{\mu_1} \cdot s \cdot \frac{M_A}{\rho A} \sin\Phi \times \frac{\lambda_1 / \lambda_i}{1 + \frac{\sin\Phi}{\sin\Psi} \frac{\mu_i}{\mu_1}} \cdot \left[1 - e^{-\left(\frac{\mu_1}{\sin\Phi} + \frac{\mu_i}{\sin\Psi}\right) \cdot d}\right]$$

/14

For the total emission of the level q, we have

$$(I_2 \cdot A)_q = \sum_i (I_2 \cdot A)_i .$$

If d is sufficiently large, all of the X-rays will be absorbed in the target, and

$$(I_2 \cdot A)_i = \frac{I_1}{4\pi R^2} \cdot \omega_q \cdot p_i \frac{r_q - 1}{r_q} \cdot \frac{\zeta_{1A}}{\mu_1} \cdot s \cdot \frac{M_A}{\rho A} \sin\Phi \times \frac{\lambda_1 / \lambda_i}{1 + \frac{\sin\Phi}{\sin\Psi} \frac{\mu_i}{\mu_1}} .$$

In first approximation, the fluorescence radiation emitted by the element A can be considered proportional to its concentration in the target.

I.4.1 Matrix Effect

The values μ_1 and μ_i are functions of various volume masses M_A, M_B, M_C, ..., of the constituent elements of the specimen. If A is the element to be determined, a variation in M_B, M_C, ..., will influence the expression of $(I_2, A)_i$ (Bibl.59, 60, 61). The photoelectric absorption of the incident radiation ν_1 by the elements B, C, ..., may generate a secondary radiation of an energy sufficient for contributing to the excitation of the element A. By attenuation

or by reinforcing the investigated ray, the variation in the matrix composition introduces a supplementary parameter into the quantitative analysis.

L.S.Birks and D.L.Harris (Bibl.62) demonstrated an unusual matrix effect. An analysis of the iron in chromite-olivine ore (Cr and Fe) shows that the intensity Kα-Fe decreases with increasing iron concentration.

Various factors may influence the intensity of the fluorescence radiation. For low energies, the detected fluorescence radiation concerns only the surface portion of the specimen and thus will impart a satisfactory homogeneity of /15 the element to be analyzed.

Considerations of statistics and geometry indicate that, for a pelleted specimen, a granulometry of the order of one micron is to be preferred.

I.4.2 Calibration

Since the matrix effect does not permit a simple linear relation between the fluorescence intensity of a given element and its concentration in a given matrix, various analytical methods have been investigated.

It is possible to make a systematic study as to the influence of each individual element on the radiation of the element to be analyzed. If the composition of the matrix is known, it becomes possible to mathematically derive the corrections to be made for the analysis. This tedious method, of only moderate accuracy, presupposes that the exciting spectrum is known.

An almost complete elimination of the matrix effect can be obtained by diluting the specimen with very light elements.

The method most frequently used because of its simplicity and accuracy consists in a comparison of the specimen with standards having the same matrix and in which the content of the element to be analyzed spans the content to be

determined.

II. DETECTION OF X-RAY RADIATION BY PROPORTIONAL COUNTER

The analysis by X-ray fluorescence is based on the possibility of selectively measuring a single ray of the characteristic radiation of the investigated element.

In classical X-ray fluorescence analysis, a crystal known as the analyzer diffracts the radiation emitted by the specimen. This diffraction of the wave radiation associated with the photons takes place in accordance with Bragg's relation: $2d \sin \theta = n\lambda$.

/16

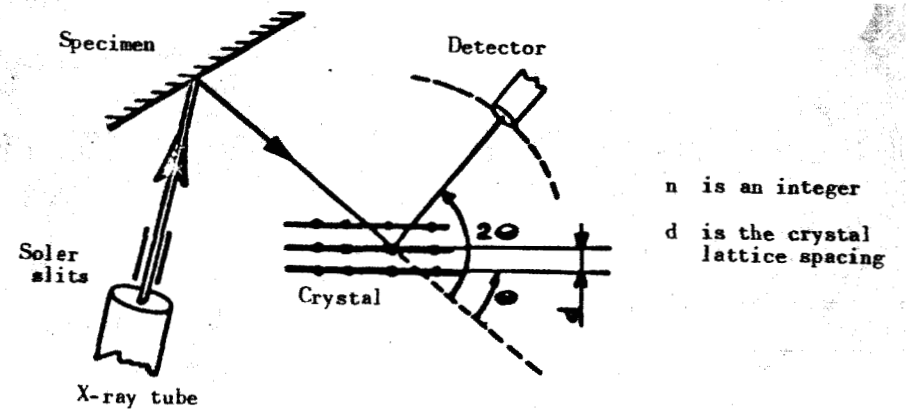

This process permits a fine resolution in studying a given spectrum. The X-ray tube abundantly irradiates the specimen and thus compensates the poor yield of the crystal.

At the limiting condition of $\theta = 90^{\circ}$, the first order of the Kα line will be diffracted if $d \geq \lambda/2$.

At low energies, this raises the difficulty of finding crystals with a sufficient lattice spacing, starting from sodium. For aluminum and magnesium, synthetic EDDT and ADP_2 crystals* are in common use.

---

* EDDT = d-ethylenediamine tartrate; ADP = ammonium dihydrogen phosphate.

For extremely low energies, the radiation is diffracted by a grating formed of superposed films (Bibl.21, 33).

L.G.Dowell designed a diffraction grating, formed of 135 single layers of lead stearate, with an effective spacing of about 51 Å. This diffracting system permits an analysis of C, N, and O.

Nondispersive X-ray radiation can be ensured by a detector whose response is an electric pulse of an amplitude proportional to the absorbed energy. Scintillation detectors, gas-filled proportional counters, and semiconductors have this property.

The energy distribution of the detected X-ray radiation is obtained by spectrometry of the pulse heights, furnished by the detector.

This analytical technique, at low energies, prevents the difficulties encountered in diffraction.

Semiconductor detectors can be used at present only for energies higher than several tens of Kev. For low energies, the proportional counter is preferable over /17 a scintillation counter which has a higher background and a less satisfactory resolution. On the other hand, the selection of a thin window for the scintillation counter is limited by the requirement that this window be light-tight.

II.1 Operating Principle of the Proportional Counter

Detection of X-ray radiation of an energy E proceeds by ionizing the gas in the counter, after which the produced photoelectrons are collected on the anode.

A system of concentric electrodes creates a convergent electric field of the form

where

V = potential difference between the electrodes;

r_c and r_a = radii of the cathode and anode, respectively.

If ω_i is the ionization energy of the gas, the number of photoelectrons produced will be $\frac{E}{\omega_i}$. In proportional operation, the photoelectrons in the electric field acquire a kinetic energy sufficient for ionizing other atoms so that, for a quantum E, the anode will collect $A \cdot \frac{E}{\omega_i}$ electrons. Here, A denotes the gas multiplication factor.

Rose and Korff (Bibl.12) formulated the first theory of gas amplification and derived the following expression for A:

$$A = \exp\left\{2\,(a \cdot N_m \cdot C_c \cdot r_a \cdot V)^{1/2} \cdot \left[\left(\frac{V}{V_o}\right)^{1/2} - 1\right]\right\}$$

where

a = gas constant;

N_m = number of molecules per unit volume;

C_c = capacity of the counter per unit length;

V_o = threshold of the proportional region.

However, several hypotheses limit this theory:

The ultraviolet radiation emission and the photoelectric effect on the cathode are negligible.

The secondary electron emission, produced by the positive ions on the cathode, is absent. /18

The fluctuations in the specific ionization of the filling gas and electron attachment to the electronegative impurities are insignificant.

A modified theory, formulated by Diethorn, is expressed by the relation

$$\text{Log } A = \frac{V \text{ Log } 2}{\overline{\Delta V} \text{ Log } \frac{r_c}{r_a}} \cdot \text{Log} \left[\frac{V}{\overline{K} \cdot p \cdot r_a \cdot \text{Log } \frac{r_c}{r_a}} \right]$$

where

p = pressure;

$\overline{\Delta V}$ and $\overline{K}$ = characteristic coefficients of the gas.

Kiser (Bibl.13) demonstrated that this theory agreed best with the experimental results; he also measured $\overline{\Delta V}$ and $\overline{K}$.

Gas Filling	$\overline{\Delta V}$ volts	$\overline{K}$ V/mm Hg	ω_i ev
99,8 % CH_4 + 0.2 % A	38.3	225	28.9
CH_4	40.3	190	28.9
7,9 % CH_4 + 92.1 % A	30.2	102	26.7
90,3 % CH_4 + 9.7 % A	28.3	287	28.7

The maximum amplitude V_a of the pulse collected at the anode depends on the law of the collection of charges as a function of time which, in turn, depends primarily on the transit time of the sheath of positive ions created in the vicinity of the anode. In fact, the mobility of the electrons is 10^3 to 10^4 times that of the heavy positive ions.

For an infinite charge resistance R, we have the asymptotic value

$$V_a = \frac{E \cdot A \cdot e}{\omega_i \cdot C} .$$

On giving a sufficient value to the time constant R_c with respect to the rise time of the pulse, we will have (Bibl.14):

$$Vt = \frac{A \cdot E \cdot e}{2 \cdot \omega_i \cdot C \operatorname{Log} \frac{r_c}{r_a}} \cdot \operatorname{Log} \left(1 + \frac{t}{t_o}\right)$$

with

$$t_o = \frac{p \cdot r_a^2 \operatorname{Log} r_c/r_a}{2 V \cdot \mu}$$

/19

where

μ = mobility of the positive ions;

C = capacitance distributed between anode and ground, from the filament to the grid of the first tube.

The dispersion in the arrival time of the electrons at the anode will be decisive for the validity of this relation. On the other hand, at high values of A, the space charges may perturb the function V_t.

II.2 Filling Gas

Under the effect of the ionizing radiation, the filling gas of the counter becomes an electron generator. These photoelectrons and the secondary electrons are grouped in the time of collection on the anode. The induced pulse amplitude represents the energy of the absorbed radiation. The number of these pulses per unit time will be the mirror image of the intensity of this same radiation. Various phenomena may disturb this mechanism and falsify the test results. The main error source usually is an incomplete collection of the electrons on the anode, or the fact that the ionizing particle transfers its energy to the gas in a form different from ionization. Thus, in a gas containing electronegative molecules such as O_2 and H_2O, the free electron would have a non-negligible probability of attachment $\frac{\alpha}{\rho\omega}$, as indicated in Fig.3 (Bibl.15).

If the ionization of the gas is intense, recombination of the electron with a positive ion becomes possible.

Figure 25 gives the mass absorption coefficients for the gas mixtures A + + 10% CH_4 and He + 10% CH_4, as a function of the wavelength of the X-rays.

Disregarding the two preceding phenomena, the amplitude fluctuation P of the pulse, furnished by the proportional counter, can be written in the form

$$\left(\frac{\sigma P}{P}\right)^2 = \left(\frac{\sigma N}{N}\right)^2 + \frac{1}{N}\left(\frac{\sigma A}{A}\right)^2$$

where

N = number of primary electrons created by the ionizing particle;

A = number of secondary electrons created by a primary electron.

a) Primary Ionization /20

The term $\left(\frac{\sigma N}{N}\right)^2$, studied by Fano, was found equal to $\frac{F}{N}$, where F is known as the Fano coefficient.

For hydrogen, we have $1/3 < F < 1/2$.

The energy of the ionizing particle to be detected cannot be entirely converted for ionizing the detector gas. In fact, a relatively large number of gas molecules may be excited, often at a metastable state. The optimum gas detector is one in which the major portion of the particle energy is used for ionizing this gas. Certain gas mixtures have the property of reconverting the energy fraction, used for the excitation, into ionization energy by secondary effect.

This phenomenon had been demonstrated by Korolev (Bibl.16) for CH_4 contents of less than 6% in the argon. In Fig.4, the function Log A = f(V), given by this author, is plotted for various mixtures of A and CH_4.

From 0 to 6% of CH_4, the increase in the coefficient A is due to secondary ionization, produced by collision between the excited argon and methane atoms, such that

$$A^* + CH_4 \longrightarrow A + CH_4^+ + e^- \pm \Delta E$$

where ΔE denotes the variation in kinetic energy of the incident particle. This phenomenon of de-excitation is made possible by the fact that argon has more than hundred excitation levels above the ionization potential of methane.

For methane contents above 6%, it should be recalled that there is an inverse effect due to the known fact that the addition of a polyatomic gas to a monatomic gas causes the mean energy of the free electrons to decrease. Simultaneously, the multiplication factor also decreases. A large portion of the excitation photons, produced in the Townsend avalanche, is absorbed by the heavy gas; however; the slope of the function Log A = F(V), on descending, yields a greater operating stability.

b) Gas Amplification

The term $\frac{1}{N}\left(\frac{\sigma A}{A}\right)^2$ is introduced by gas amplification of the primary electrons. Frish and Snyder give a value of $\left(\frac{\sigma A}{A}\right)^2 = 1$; however, Curran's theory, experimentally verified, reduces the quantity $\left(\frac{\sigma A}{A}\right)^2$ to 2/3.

In first approximation, according to the above statements, it will be possible to write $\left(\frac{\sigma P}{P}\right)^2 \sim \frac{1}{N}$.

This number N becomes principal, and an attempt should be made to increase it. The quantity N is linked to the ionization potential of the gas: $N = \frac{E}{\omega_i}$. /22

Thus, the gas used should have the lowest possible ω_i.

In the gas amplification, the probability of secondary ionization will

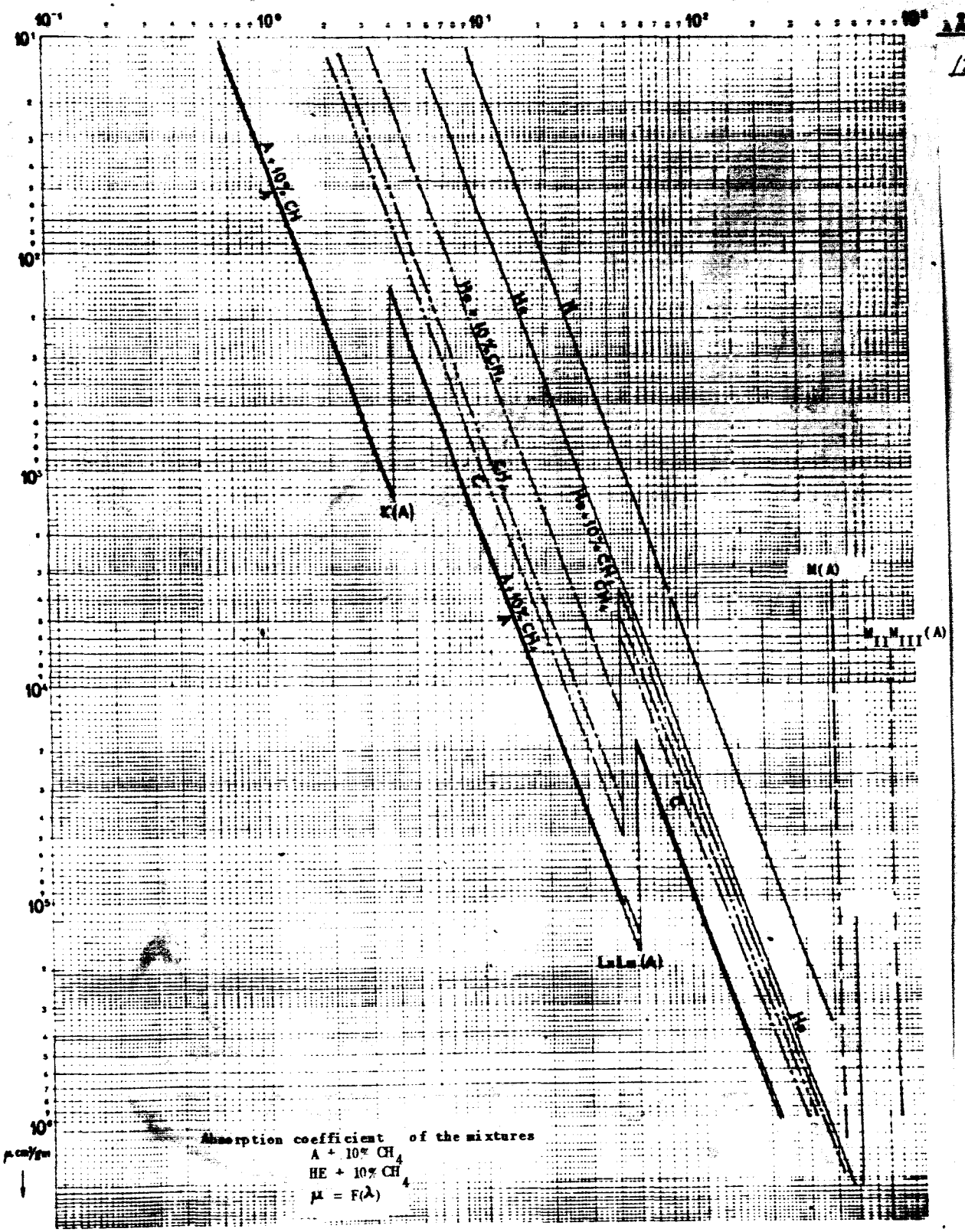

Fig.25 Absorption Coefficients of the Detector Gas

also be a function of ω_i (Bibl.17), as indicated in Fig.5.

II.3 Possibilities of Detection by Proportional Counter

Gas-filled proportional counters have been in wide use as detectors, furnishing a response proportional to the energy. The progress made in the field of photomultipliers has led to replacement of scintillation counters by proportional counters, in numerous cases. However, for soft X-rays (energy below 10 Kev), the proportional counter remains the detector of choice. This type of detector has the advantage of a resolution 2 - 3 times better than that of a scintillation counter; in addition, its background is less and its recovery time is short.

The possibility of determining, at will, the nature and the pressure of the filling-gas mixture permits varying the efficiency of detection and, with the same token, obtaining a selective efficiency for a given energy.

Resolution

We will attempt to derive the theoretical resolving power of proportional counters from the previously obtained relation:

$$\left(\frac{\sigma P}{P}\right)^2 \sim \frac{1}{N}$$

$$N = \frac{E}{\omega_i}$$

E = energy of the detected particle

$$\frac{\sigma P}{P} = \sqrt{\frac{\omega_i}{E}}$$

ω_i = ionization energy of the gas

The resolving time is defined as the ratio of the width of the peak at

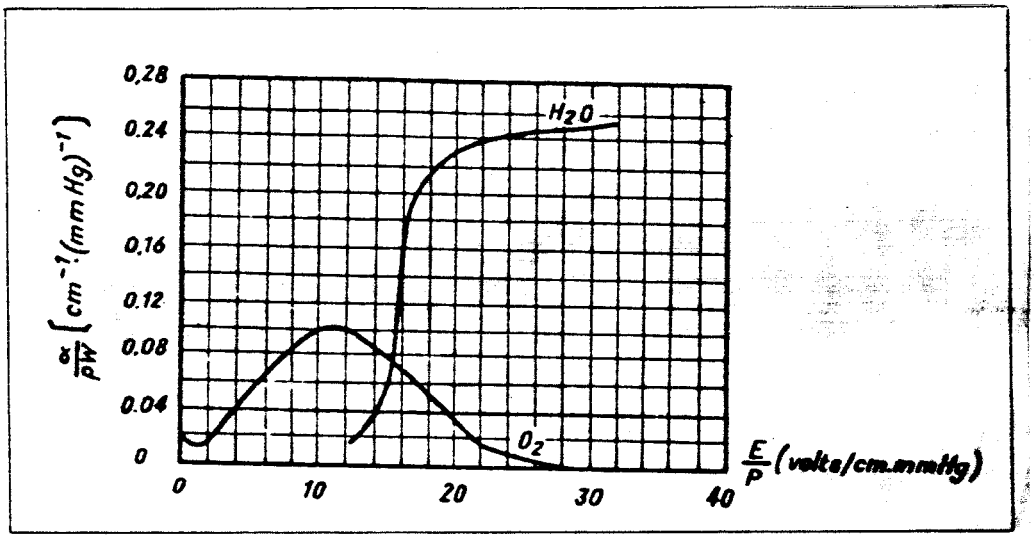

Fig.3 Probability of Electron Attachment per Centimeter of Path α/pW, at 1 mm Pressure

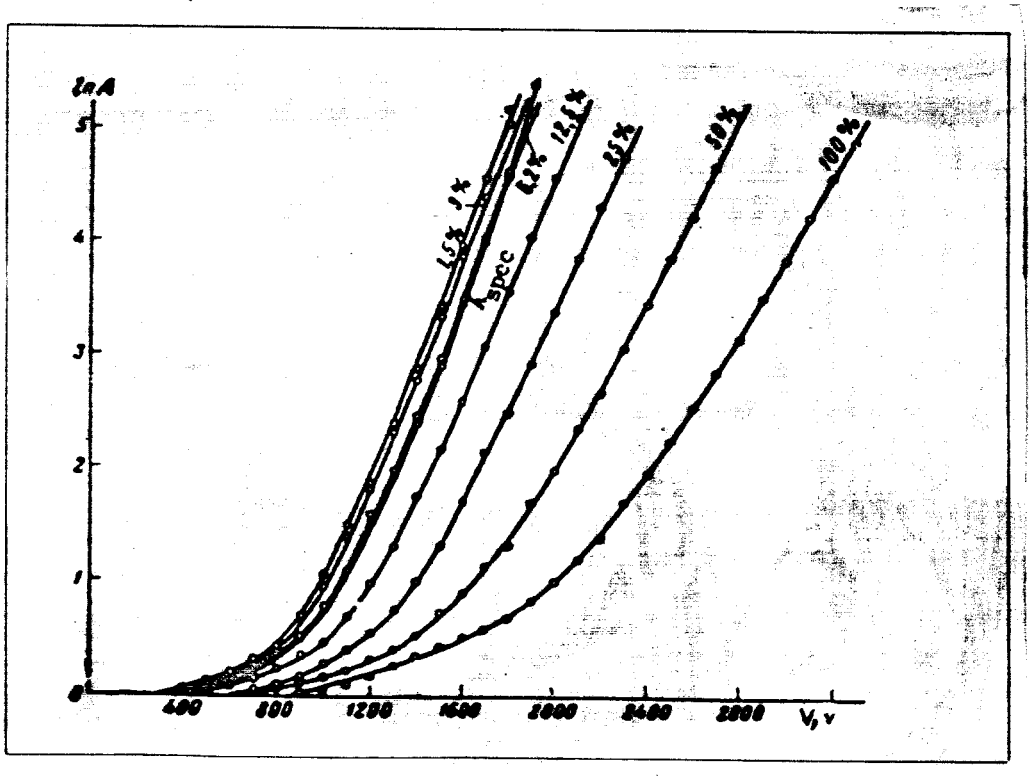

Fig.4 Gas Amplification Factor as a Function of the Anode Voltage, for Various Gas Mixtures of Argon and Methane

midheight to the abscissa of the peak.

The width of the peak at midheight will be equal to the dispersion σP, with the coefficient 2.354.

From this, we obtain the expression for the resolution /24

$$\frac{\Delta P}{P} = 2.354 \sqrt{\frac{\omega_i}{E}} .$$

For the gas mixture of A + 10% CH_4, we have ω_i = 26.7 ev and

$$\frac{\Delta P}{P} = \frac{0.384}{\sqrt{E_{Kev}}} .$$

The factor 0.384 appears higher than expected from the experimental results (Bibl.63) obtained for the value of $\frac{\sigma A}{A}$.

A possible expression for the theoretical resolution will be

$$\frac{\Delta P}{P} = \frac{0.35}{\sqrt{E_{Kev}}} .$$

Too intense an ionization of the gas produces space charges and deteriorates the resolution. Pontecorvo (Bibl.18) places a limit A_{cr} on the gas amplification factor up to which resolution will be maintained:

$$E \cdot A_{cr} \simeq 10^8 \text{ ev}$$

Stability of the very high voltage (VHV) of at least $\frac{1}{10,000}$ is recommended. The end effects may produce a rise at low energy and influence the resolving time.

Still other causes may affect the resolution, including:

phenomena of attachment and recombination in the detection gas (II.2);

surface finish of the anode filament.

We have proved that a minimal mechanical tension of the anode filament is neces-

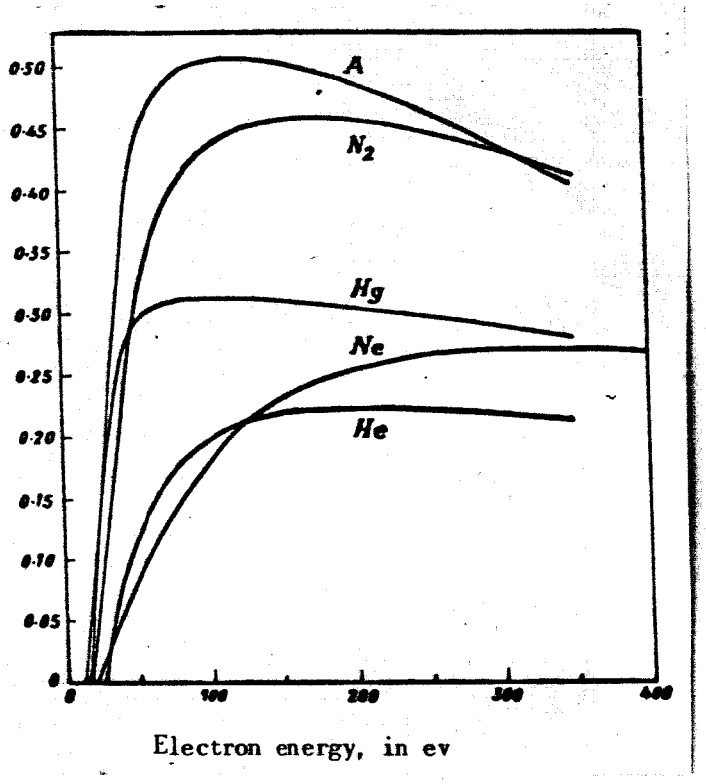

Fig.5 Probability of Ionization

λ_i = 8.3 Å

λ_K = 7.9 Å

r K = 12.6

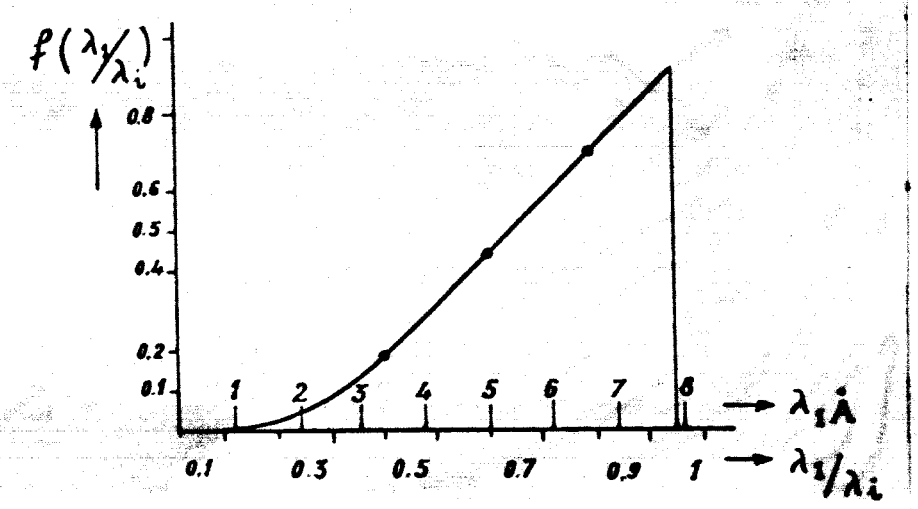

Fig.6 Probability of Excitation for the Al-Kα Line as a Function of λ_1/λ_i

sary.

Spectra of very low energy have been detected with proportional counters; one merely needs mention the X_K line of carbon of 282 ev, excited by Dolby (Bibl.20) with a microprobe; the X_L line of chlorine of 238 ev, excited by M.Langevin (Bibl.19); the oxygen line of 523 ev, excited by B.L.Henke (Bibl.21). J.E.Holliday (Bibl.31) detected the X_K emission of beryllium of 110 ev.

These performances at low energies demonstrate the potentialities of the proportional counter and the usefulness of such a detector for the energies that we wish to investigate here.

III. EXCITATION OF FLUORESCENCE BY MEANS OF RADIOISOTOPES /26

The supply of energy to the atom, permitting the expulsion of an electron from the shell that is to be excited, basically proceeds in accordance with two modes.

The first mode utilizes the energy furnished by the sufficiently accelerated thermal electrons. In the mode of direct emission, these electrons strike the specimen and excite its fluorescence radiation. This process is used in the microprobe which focuses the electron beam on an area of μm^2 of the specimen. More often, the electron beam strikes a metal surface (anticathode) where the deceleration of the electrons generates an X-ray radiation of continuous spectrum, to which the fluorescence line spectrum of the anticathode is superposed. This X-ray radiation then excites the fluorescence of the specimen.

The second mode of energy supply consists in using the radiation of radioactive isotopes.

The excitation of fluorescence will take place under different conditions, that must be defined in accordance with the type of nuclear radiation used.

However, all of these sources have several properties in common:

a) The energy of the particle or of the quantum emitted by the source must satisfy the imposed conditions for obtaining a satisfactory efficiency of fluorescence excitation of a given element.

b) The half-life of the radioisotope must be sufficiently long.

c) As high as possible a specific activity should be selected.

d) The radioactive source must not be contaminated.

III.1 Excitation by Photons

The interaction of a photon with the atom may take various forms; a dozen of processes are theoretically possible. However, for photons of energies below 100 Kev, these processes are restricted to inelastic Compton scattering, to the photoelectric effect, and - in the case of soft X-rays - to elastic Rayleigh scattering.

The photoelectric effect, in accordance with the process indicated in Section I.4, will excite fluorescence of the specimen.

In the investigated shell, the energy $h\nu$ of the photon is transmitted as/27 follows:

$$h\nu = E_e + E_q$$

where

E_e = kinetic energy of the electron ejected from the shell q;

E_q = binding energy of the shell q.

This energy E_q can be converted, during de-excitation of the atom, into X-ray fluorescence radiation or into an Auger electron.

Influence of the Excitation Energy

Returning to the formula that gives the intensity of fluorescence radiation

excited in a binary target (Section I.4), we have

$$(I_2, A)_i = \frac{I_1}{4 \pi R^2} \cdot \omega_q \cdot p_i \cdot \frac{r_q - 1}{r_q} \cdot \frac{\zeta_{1\,A}}{\mu_1} \cdot s \cdot \frac{M_A}{f A} \cdot \sin \Phi \cdot \frac{\lambda_1 / \lambda_i}{1 + \frac{\sin \Phi}{\sin \Psi} \frac{\mu_i}{\mu_1}} \cdot$$

For a target, formed of a single element, we have $M_A = \rho_A$.

In μ_1, for soft X-rays, the component ζ_1 is principal so that we obtain

$$(I_2)_i = \frac{I_1}{4 \pi R^2} \cdot \omega_q \cdot p_i \cdot \frac{r_q - 1}{r_q} \cdot s \cdot \sin \Phi \cdot \frac{\lambda_1 / \lambda_i}{1 + \frac{\sin \Phi}{\sin \Psi} \frac{\mu_i}{\mu_1}}$$

It seems that $I_{2,i}$ increases with increasing λ_1; however, λ_1 must be lower than λ_q (value corresponding to the absorption discontinuity q). The double condition $\lambda_1 < \lambda_q < \lambda_i$ requires a value of $\frac{\lambda_1}{\lambda_i}$ below 1.

Assuming that the absorption coefficient μ is proportional to λ^3 and neglecting the scattering, we have

$$\frac{\mu_i}{\mu_1} \approx \left(\frac{\lambda_i}{\lambda_1}\right)^3 \cdot 1 / r_q \cdot$$

Posing /28

$$f\left(\frac{\lambda_1}{\lambda_i}\right) = \frac{(\lambda_1 / \lambda_i)^4}{\left(\frac{\lambda_1}{\lambda_i}\right)^3 + \frac{1}{r_q} \frac{\sin \Phi}{\sin \Psi}}$$

we obtain

$$I_{2,i} \sim R \cdot f (\lambda_1 / \lambda_i) \cdot$$

Thus, Fig.6 shows the course of $f\left(\frac{\lambda_1}{\lambda_i}\right)$ as a function of $\frac{\lambda_1}{\lambda_i}$, for the K line of aluminum (Bibl.11).

Selection of the Radioisotope

The importance of proper selection of the radiation λ_1, which excites the fluorescence radiation λ_i, is quite obvious.

The accompanying Table gives the X-ray generating isotopes of an energy below 10 Kev.

TABLE OF X-RAY SOURCES BELOW 10 Kev

Isotopes	T	Emission Mode	X-Ray Energy	Radioactive Descendant
Be^7	53 days	12 % 478 Kev, EC	0.052	
Ca^{41}	$1,1.10^5$ yrs	EC	3.31	
Ti^{44}	10^3 yrs	γ 70 Kev, EC	4.09	Se^{44} β^+ ; γ 1,16 Mev & EC
V^{49}	1 yr	EC	4.51	
Cr^{51}	27 days	γ 323 Kev 10 %, e^-, EC	4.95	
Mn^{54}	300 days	γ 835 Kev 100 %, EC 100 %	5.41	
Mn^{53}	2.10^6 yrs	EC	5.41	
Fe^{55}	2.94 yrs	EC	5.90	
Co^{57}	270 days	γ $^{123}_{14}$ Kev, e^-, EC	6.40	
Co^{58}	72 days	β^+ 14 %; γ 800 Kev; EC 86 %	6.40	
Ni^{59}	$7,5.10^5$ yrs	EC	6.93	
Zn^{65}	250 days	β^+ 2 %; γ 46 % 1,11 Mev EC	8.05	
Ge^{71}	11.4 days	EC	9.25	
As^{73}	76 days	EC	9.89	Ge^{73} ⟶ γ 53 Kev
Se^{75}	127 days	β^- ; γ 10 % 265 Kev, EC	10.84	

Most of these sources emit, by K capture, the line of the lower element Z. This line spectrum yields satisfactory peaking ratios. Consequently, the /29 number of energy sources below 6 Kev is limited. The period, the purity of the X-ray spectrum, the specific activity, and the possibilities of conditioning make it preferable to use Fe^{55} for elements with an atomic number Z below 25. As will be demonstrated below, the emitters of charged particles can use the

low-energy relay for producing X-rays by secondary effects. The α and β particles are able to excite the characteristic X-ray radiation of a given radiator. The betas produce, in addition, a continuous X-ray background by bremsstrahlung.

III.2 Excitation by β-Particles

An ionization of the atom, in its most rigidly bound shells K, L, ..., by β-particles will produce the emission of characteristic lines of this atom. This line spectrum will be superposed by a continuous X-ray spectrum known as bremsstrahlung, produced by acceleration of the particle in the Coulomb field of the nucleus.

When using this excitation process and in the case of a nondispersive analysis, it is suggested to prevent the β-particles, back-scattered by the specimen, from penetrating into the detector. This is readily obtained by using a magnetic field (Bibl.22). The X-ray bremsstrahlung, although it does contribute to exciting the fluorescence radiation of the target, might deteriorate the contrast of the characteristic peaks, due to the continuous background which it imparts to the detected spectrum.

An indirect technique of utilizing β-sources consists in using these for producing X-rays in an intermediary target. Different variants of this method have been applied (Bibl.7, 8, 9, 10).

The mean output of energy radiated through bremsstrahlung by an electron of energy E, in a target with an atomic number Z, is represented by the formula confirmed by Wyard:

$$E_B = 5.8 \cdot 10^{-4} Z \cdot E^2$$

where E_B and E are expressed in Mev.

For the entire β-spectrum we will have

$$E_B = 5{,}8 \cdot 10^{-4} Z \cdot E^2 \int_0^1 \psi^2 N(\psi)\, d\psi$$

where

$$\psi = \frac{E}{E_\beta};$$

/30

$N(\psi)d\psi$ = proportion of the β-particle spectrum in the energy interval E to E + dE, such that

$$\int_0^1 N(\psi)\, d\psi = 1.$$

The intensity of the internal bremsstrahlung has the form

$$E_{IB} = 3{,}7 \cdot 10^{-4} E^2 \beta.$$

If, in first approximation, the direct excitation of characteristic X-rays by the betas is independent of the production of bremsstrahlung, the excitation of fluorescence will depend directly on the intensity of the bremsstrahlung spectrum, having an energy greater than the energy of the fluorescence line under consideration.

The number of photons I_q, produced by the β-particles over excitation of the level q, will be

$$I_q = \int_0^E \phi_q(E)\, I_\beta(E)\, dE.$$

Here, $I_\beta(E)$ is the normalized β-particle distribution:

$$\phi_q(E) = \omega_q \int_{E_q}^E \sigma_q(E) \left(\frac{dR}{dE}\right) dE$$

where

σ_q = effective cross section for excitation;

R = mean free path of monoenergetic electrons.

For energies below 0.1 Mev, we have

$$R(E) = 1.5 E^2 \text{ gm/cm}^2.$$

The accompanying Table compiles the results of experimental studies on the

efficiency of production of X-ray radiation by β-sources. The validity of these results is limited to the experimental conditions described by the authors.

/31

Authors and Bibliography	Source	Target	X / β	χ_K/ Σbrem.
STARFELT (Bibl.23)	Pr^{143}	Pb	4.3 %	1
LEVEQUE (Bibl.24)	$(Sr+Y)^{90}$	Pb	3.9 %	Peak K: 10 times the height X of stopping
CAMERON, RHODES (Bibl.8)	H^2 / Ti		1.3×10^{-2} %	2.2
REIFFEL (Bibl.6)	Sr^{90}	Sn	3.5 %	1

These experimental results confirm the theory: The use of β-sources of low energy, exciting radiators of low atomic number, is characterized by low yield.

The following Table lists the β^- emitting radionuclides of low energy.

Isotopes	T	Emission
H^3	12.26 years	β^- 18 Kev
Ni^{63}	80 years	β^- 63 Kev and XK of Ni and Cu, 7.47, & 8 Kev
Re^{187}	5.10^{10} years	63 % $\beta^- \leq$ 8 Kev isometric transition Y 0.133 Mev
Ac^{227}	21.8 years	98 % β^- 45 Kev 1 %. α 4.9 Mev and numerous emitting descendants α and Y
Pb^{210}	19.4 years	β^- 17 Kev and Y of 46 Kev

An original type of source-plus-radiator unit is composed of a zirconium or titanium foil (radiators) in which tritium (β-emitter) is fixed by adsorption.

Figure 7 gives the spectrum of a H^3/Zr source, described in the second portion of Section III.2.

/32

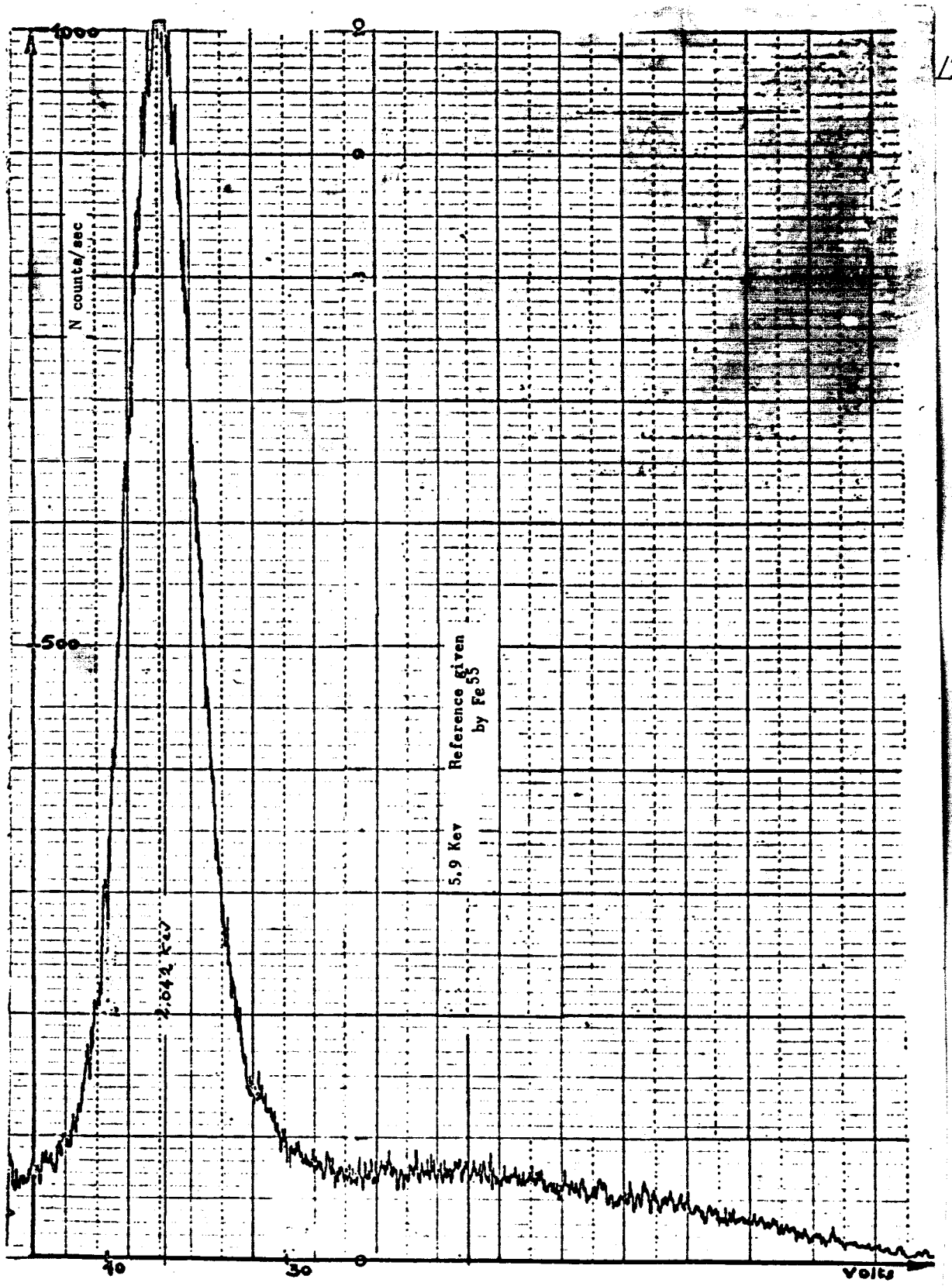

Fig.7 Spectrum of the H^3/Zr Source
The peak L_α of Zr becomes detached at 2.042 Kev

The sources of adsorbed tritium, developed and used in British Laboratories (Bibl.8, 9), have come into general use for excitation of elements of low atomic number. For the analysis, G.Seibel (Bibl.25), using 2.4 curies of H^3/Zr, a radiation path in vacuum, and detection and analysis by proportional counter, obtained the results shown in the accompanying Table.

/33

Standards	Fe	Co_3Ca	SiO_2	Al_2O_3	MgO
X-ray radiation	Fe_K	Ca_K	Si_K	Al_K	Mg_K
Energy (Kev)	6.39	3.69	1.74	1.48	1.25
Intensity (cts/sec)	1100	1050	710	330	180
Background (cts/sec)*	19	15	11	12	8

* Background noise measured on either side of the line.

III.3 α-Sources

The production of an X-ray fluorescence radiation, from α-particles, has been demonstrated and investigated since the beginnings of nuclear physics (Bibl.29, 66, 67, 68, 69, 70).

Born's method (Bibl.66) for treating collision processes is valid only if the velocity of the incident particle is large with respect to the rate of revolution of the knock-on electron. Although this condition is not satisfied in the case of α-particles and electrons of the K shell, Born's method does yield satisfactory results. Henneberg (Bibl.69) explains this by the fact that the expression of the excitation probability, derived by Born, is only a first approximation and that it will suffice only as long as its value remains small with respect to unity. Thus, this condition is still satisfied for aluminum where the probability is 1/1000, which decreases even further for heavier atoms.

In accordance with Henneberg's theory, Bühring and Haxel (Bibl.28) derived an expression of the effective cross section σ for emission of X-K rays, as a function of the energy of the incident particle α:

$$\sigma(E) = 1.408 \cdot 10^{-15} \cdot \omega_K (Z^4 \theta)^{-1} \varphi(n) \quad \text{in cm}^2$$

where

ω_K = fluorescence yield K for the atom of an atomic number Z;

$\theta = \frac{E_K (ev)}{13.53\ Z^2}$ = ratio of real to ideal ionization energies K;

$\varphi_0(n)$ = a dimensionless function; /34

$$\varphi_0(n) = 0.1 \cdot e^{-\frac{4n}{1+n}} \cdot \left(\frac{4n}{1+n}\right)^4 \cdot \left[1 + \frac{1}{3}\left(\frac{4n}{1+n}\right) + \ldots\ldots\right]$$

$n = \frac{4E}{\alpha^2 M} \frac{E}{rd}$ E = energy in Rydbergs (1 Rydberg = 13.5 ev)

$\alpha^2 = 0.68\ Z^2$

$M = \frac{M_\alpha \cdot M_{atom}}{M_\alpha + M_{atom}}$ reduced mass of the α-particle, in unit electron mass.

Bothe and Franz (Bibl.32), on the basis of their experiments, found the production yield of characteristic X-rays excited by the α-particles of Po^{210}, where this yield by α-particles ranges from 54×10^{-3} for magnesium to $2.4 \times \times 10^{-3}$ for zinc.

Bühring and Haxel (Bibl.28) studied the production of characteristic X-rays of nickel, copper, and molybdenum under the following experimental conditions: A source of Po^{210} of 5 mC*, in the transmission mode, excites the fluorescence of a radiator. The influence of the energy E of the α-particle on the intensity I of the X-rays is expressed by the relation

$$I_{(E)} \sim E^n.$$

If Ψ is the number of quanta emitted per single α-particle of 5.3 Mev, the

* mC = millicurie.

authors give the following results:

Excited Element	Z	Ψ	n
Ni	28	$18.7 \cdot 10^{-4}$	4.8
Cu	29	$14.8 \cdot 10^{-4}$	4.8
Mo	42	$0.61 \cdot 10^{-4}$	5.3

These studies and experiments show that the yield of X-ray fluorescence increases toward elements with a low atomic number; magnesium is the lightest element used in these experiments.

The short mean free path of the α-particles and the influence of the energy of the particle on the fluorescence excitation requires special precautions for the irradiation of a given specimen by such a source.

Among radioelements emitting α-particles of sufficient energy, we can /35 mention: Po^{210}, Pu^{238}, Pu^{239}, Am^{241}, Th^{229}, Cf^{250}, Cm^{242}, etc. Preference will be given to radioisotopes without parasite γ, X, β radiations.

Although Po^{210} has a relatively short half-life of 138 days, it is preferentially used because of the purity of its emission of α-particles of 5.3 Mev.

Various authors (Bibl.26, 27, 30) have used the α-emission of Po^{210} for exciting fluorescence of light elements and for obtaining a low-energy reference X-ray source. Friedman, using a deposition of Po^{210} on aluminum, obtained an X-ray intensity several thousands of counts per second, under the aluminum line.

Cook and Mellish (Bibl.9), using an analytical setup, and a Po^{210} source of 1 mC activity, obtained the results given in the accompanying Table.

Excitation of fluorescence by means of α-particles has the advantage of yielding well-contrasted peaks; in fact, α-radiation produces no extensive bremsstrahlung in the target, and the α back scattering, which is negligible for

light elements, reaches 100% only at the highest atomic numbers.

Excited Element	Target	Intensity of the Peak	r Ratio Peak/Valley
Al	Al	18	7.6
Cl	Polyvinyl chloride	6	4

IV. ANALYSIS OF LIGHT ELEMENTS

We will here discuss the difficulties of theoretical and practical order, encountered in X-ray fluorescence analyses of light elements. By light element, we mean all elements of the third period of the Periodic Table, occasionally including titanium. If special precautions are taken, present technological means will permit the range of this analysis to be extended to magnesium, inclusive.

IV.1 Difficulties of a Theoretical Nature /36

The characteristics of an analysis at low atomic numbers, presented here, most likely will not be further modified by technical variations.

a) Fluorescence Yield

The fluorescence yield W_K decreases steeply with decreasing atomic number of the target; thus, for molybdenum, we have $W_K = 0.74$ which drops to 0.26 for chromium and to 0.025 for aluminum. The number of photons emitted by the specimen decreases in favor of Auger electrons; this phenomenon was utilized by Henke (Bibl.36) who was successful in spectrometering these electrons for an analysis of very low atomic numbers.

The only possibility of compensating for this reduction in intensity of

the X-radiation would be to increase the intensity of the exciting radiation. This solution might have drawbacks, some of which are due to the phenomena discussed below.

b) Scattering of the Exciting Radiation

On exciting the specimen by X-rays having an energy corresponding to the fluorescence energy to be detected, i.e., soft X-rays in our case, the efficient cross section for Compton scattering decreases in favor of the effective cross sections for elastic Rayleigh and Thomson scattering. However, at these low energies and at the resolving power of our spectrometer, the change in energy of the Compton scattered radiation with respect to the incident radiation is negligible. For Fe^{55}, emitting photons of 2.103 Å, the Compton electron will have a minimum energy of

$$2.103 - 0.024 = 2.079 \text{ Å}.$$

Compton scattering and elastic scattering show a similar behavior with respect to increasing the background noise; this will lower the accuracy of quantitative analyses, due to a reduction in contrast of the peaks.

IV.2 Difficulties of a Practical Nature

The difficulties described here are specific for low energies. Moseley's law $\sqrt{\lambda} = f\left(\frac{1}{Z}\right)$ demonstrates the decrease in fluorescence energy at low atomic numbers (in I_2, table of Kα energies of the elements of the second and third period).

The use of these soft X-rays produces various difficulties, that will /37 be discussed below. The specific problems of exciting radiation will be discussed elsewhere.

a) Absorption Characteristics

Low-energy X-rays are characterized by high absorption coefficients that increase rapidly in inverse proportion to the energy. As a typical example, let us take, for a mean free path of 20 cm in air, the transmission T of the following Kα lines:

X Kα	Mn	Z = 25	T = 55 %
X Kα	Ca	Z = 20	T = 10 %
X Kα	Si	Z = 14	T = 10^{-4} %

Thus, the trajectory of these radiations should take place in a transparent medium. Spectrometers for low atomic numbers meet this condition by producing a vacuum along the radiation path or by replacing the air with helium. The major difficulty is encountered on traversing the window of the detector. Various techniques have been used for reducing the absorption by this window; first by decreasing its thickness and next by using materials of low density such as mica, beryllium, and plastics (Formvar, Mylar, Zapon, etc.). These latter can be obtained in minimal thickness and the constituent elements (C, H, O, etc.) have acceptable absorption coefficients. However they exhibit poor mechanical strength and, for the smallest thicknesses, must be supported on a grid. In addition, such plastic films are necessarily porous so that, for preventing a contamination of the detector gas by oxygen, the counter will have to be operated with gas circulation.

Therefore, an important purpose of our future studies will be to investigate and to design a "windowless" counter (Bibl.3) so as to eliminate an important cause for the attenuation of the fluorescence radiation intensity of light elements.

b) Radiation Spectrometry

To recapitulate, we would like to review briefly the problems encountered in dispersive spectrometry of soft X-rays. The low diffraction yield constitutes a serious drawback here. Conventional diffracting crystals cannot be used, leaving only the choice of synthetic crystals or lattices, formed by a superposition of films for producing the desired lattice spacing.

The spectrometric technique used by us is based on a suitable selection /38 of the height of the electric pulse, furnished by a detector with linear energy response. Since the proportional counter was the detector of choice, we will review the characteristics of this spectrometry for low energies. It is obvious that this type of spectrometry, at low energies, is limited by the background of the equipment. It will be necessary to obtain a signal-to-noise ratio of at most a few unities.

The background, accompanying the pulses, usually is the resultant of various and frequently independent phenomena. The counter has a natural motion, produced by the radioactivity of its constituents, by the detection of cosmic radiation, and by electrons ejected from the walls of the detector.

In the particular case of a counter without window, the intense background that might be detected will be discussed further in Part II of this report, in Chapter IV.

Other causes, both electric and electronic, may be responsible for a large portion of the background; these causes are inherent to the instrument and will be discussed in Part II (Chapter I.3).

Simultaneously with reducing the background to the lowest possible value, an attempt must be made to increase the electric pulse amplitude by the gas amplification factor, by the electron amplification, and by the reduction in

the ground-to-anode capacitance.

It seems that nondispersive spectrometry for low energies will depend on the perfection of detection and on the electron amplification.

The detector, in our case a gas-filled counter, will rapidly reach an upper limit. For example, in the case of the X-K line of 52 ev of lithium, this energy overlaps the X-ray and ultraviolet regions. The gas scintillation phenomena in the counter will cumulate to such an extent as to prevent any detection.

An analysis of the main difficulties, produced by excitation and detection of the fluorescence radiation of light elements, discussed above, resulted in the following selection:

radioactive excitation source of sufficient intensity;

proportional counter as X-ray detector;

compact geometry and elimination of the detector window, so as to ensure minimum absorption of fluorescence radiation;

spectrometry of the pulse amplitude.

The techniques used and the results obtained will be described in Part II of this paper.

PART II

I. EXPERIMENTAL UNIT /41

To increase the yield in the counting of fluorescence photons, we decided in favor of a "windowless" detector, differing from the conventionally used type. However, the absence of a window produces some perturbation in the detection; to eliminate this drawback, it was necessary to create an auxiliary electric field in the vicinity of the excitation source where ionization of the gas is intense. These two points represent the novelty in our experimental device.

Three functional parts constitute the instrument:

excitation and detection of fluorescence;

auxiliary electronic equipment;

installation for feeding the detection gas.

Figure 8 gives a schematic sketch of the overall installation.

I.1 Excitation and Detection

An auxiliary volume of the counter contains the specimen to be analyzed and the excitation radioactive source.

A lead cup, containing the source, stops the radiation of the latter in the direction of the detector.

The absence of separation between the detector and the auxiliary volume imparts a common atmosphere to the entire unit.

The irradiated sample has the form of a cylinder of 32 mm diameter and several millimeters thickness.

/42

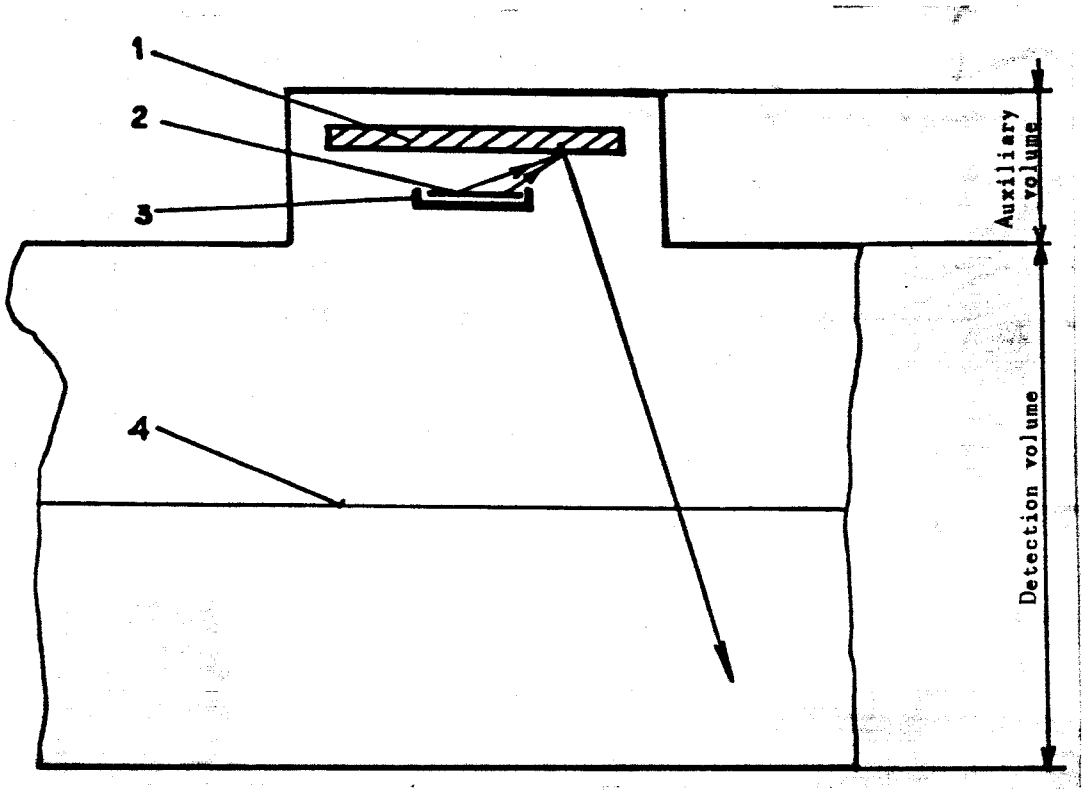

1 - X-ray radiator: specimen to be analyzed
2 - Radioactive source
3 - Cup carrying the lead source
4 - Filament of the proportional counter

The preparation of the specimen depends on the form of the matter to be analyzed. For example, a homogeneous material could be machined to desired dimensions, such as an aluminum alloy. A heterogeneous material, such as an ore sample, will first have to be crushed to a grain size below 100 μ. After this, the powder is pelleted at a pressure of 150 kg/cm^2, using a polyester resin, Acrest type 7032.

I.2 The Detector

A proportional counter, designated as CP 1, was constructed for this particular investigation (Fig.27).

The brass body prevents generation of parasite fluorescence lines in the /44

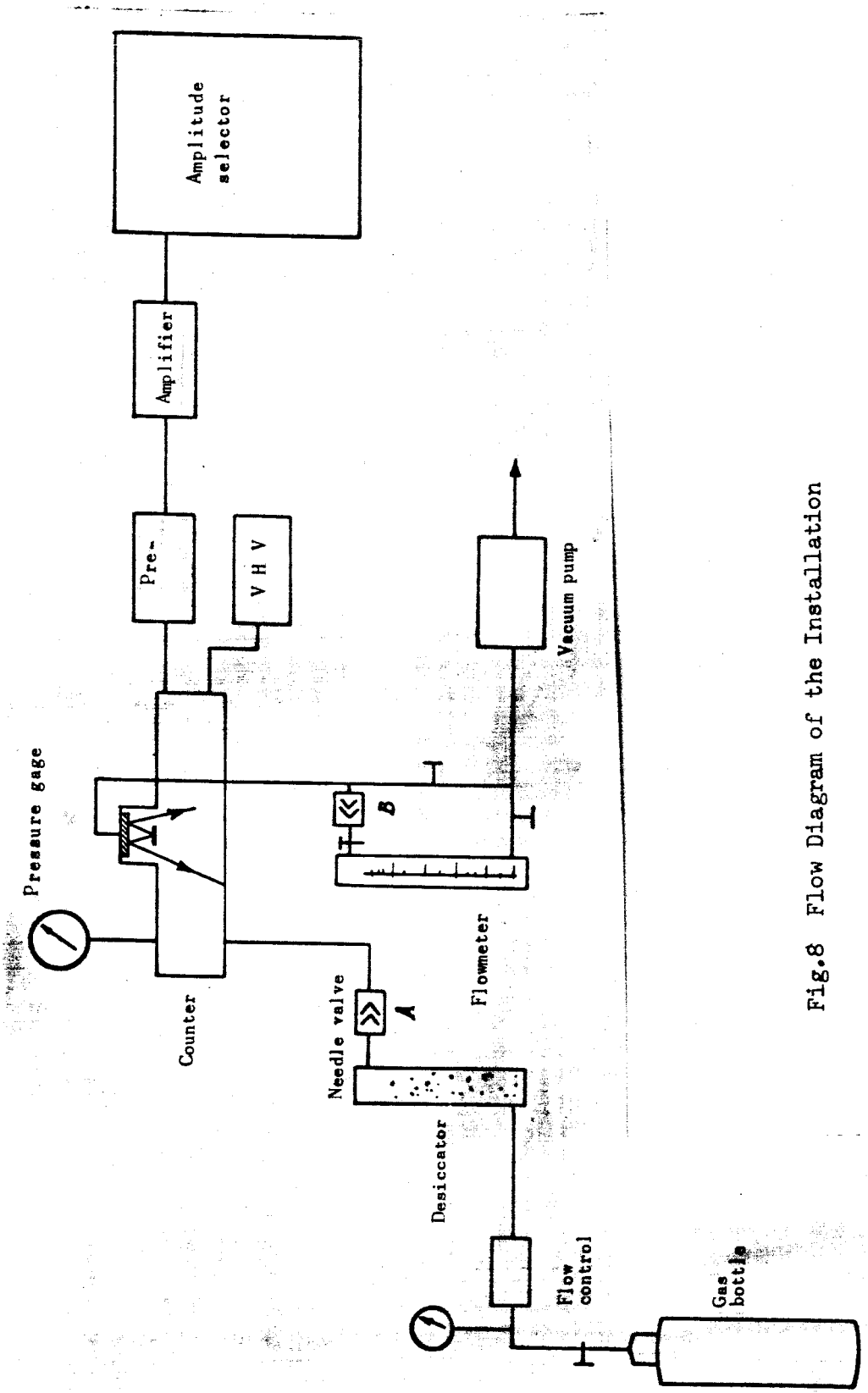

Fig.8 Flow Diagram of the Installation

range of the investigated energies. Its useful diameter of 70 mm permits satisfactory detection at the prescribed gas pressures. The length of 400 mm should be sufficient to prevent the so-called end effects produced by the distortion of the electric field at the ends.

Various anode filaments were used: stainless steel wire of 60 μ; of tungsten 50 μ; of manganese 50 μ. The anode wire must have a satisfactory surface finish, constant diameter, and sufficient mechanical strength for withstanding a stress of 100 gm on seating.

In the arrangement used, the wire is brazed at each extremity into a hypodermic needle which, in turn, is brazed to a special VHV lead-in, furnished by the S.A.I.P.; this lead-in is provided with a guard ring.

In addition, the counter is equipped with a conventional side window of beryllium of 20 mg/cm^2, with a useful diameter of 15 mm. This window permits the introduction of a reference ray or the testing of both counter and apparatus.

The charging circuit, used in the counter, is shown in the accompanying wiring diagram.

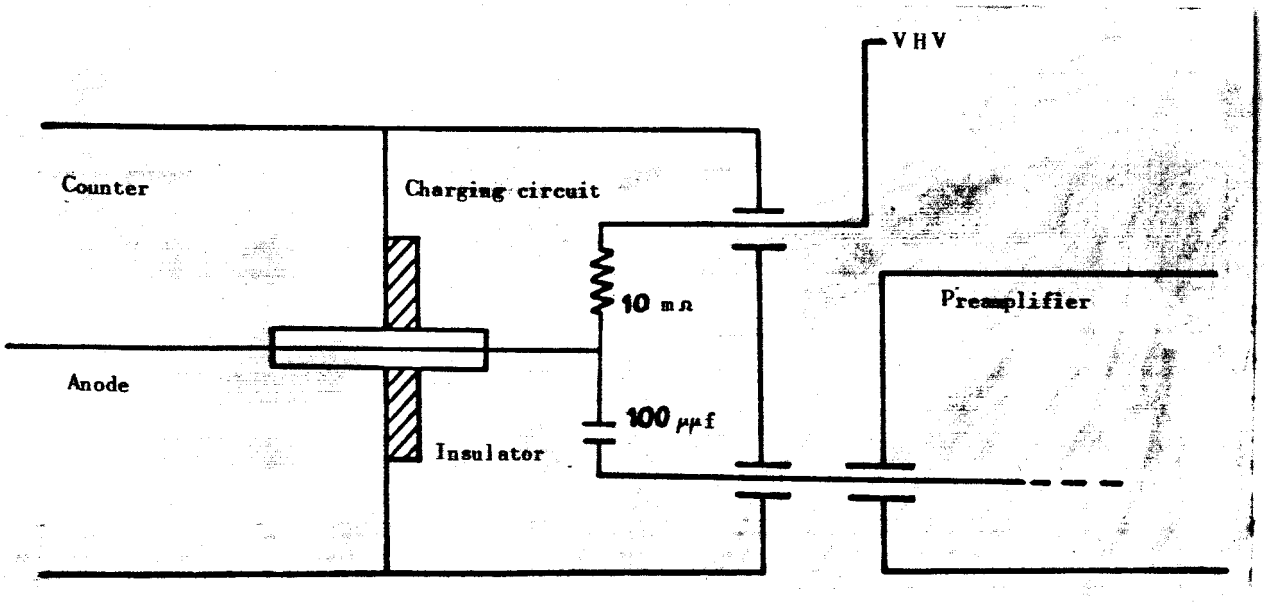

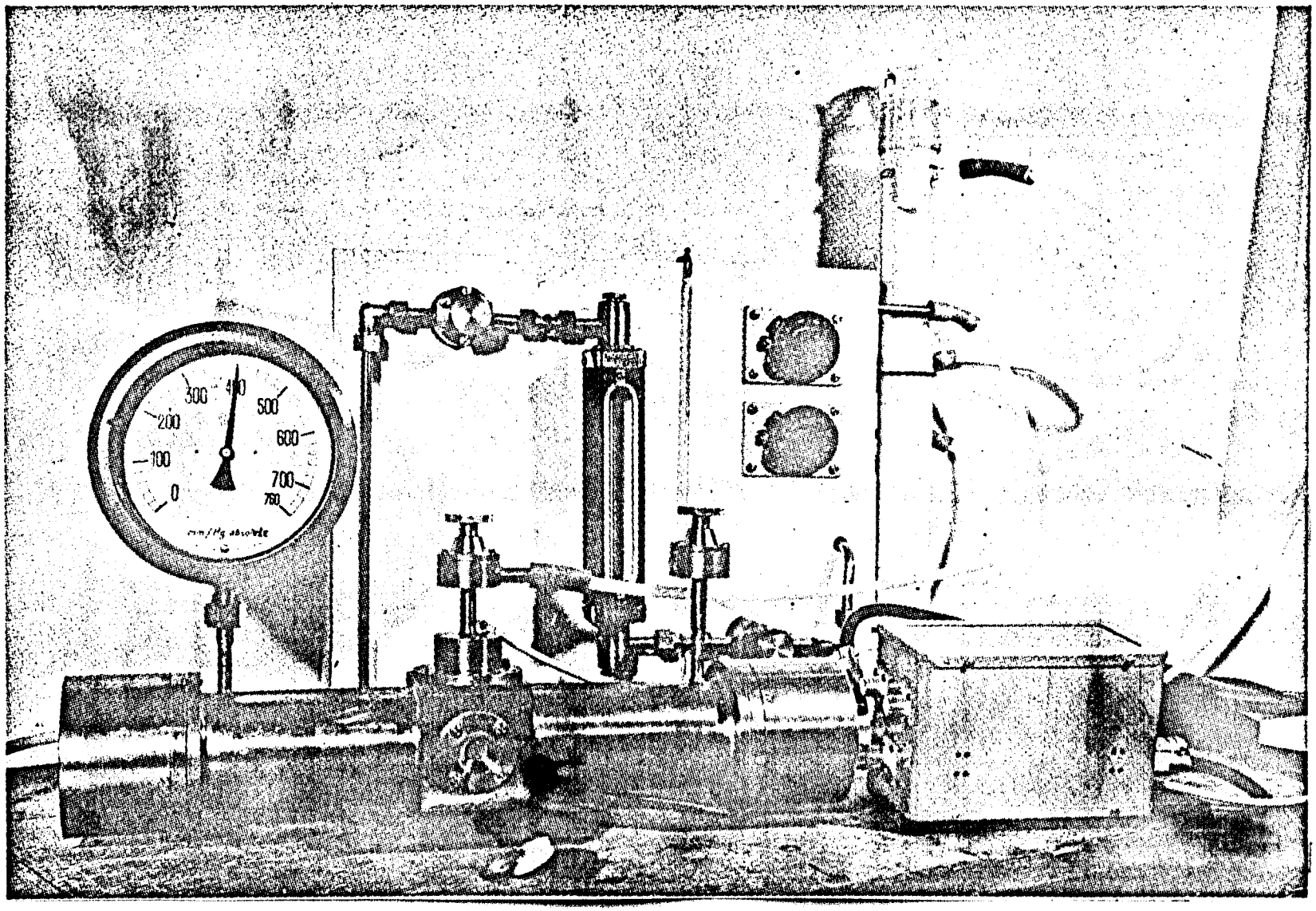

Proportional Counter and Gas Circulation Circuit

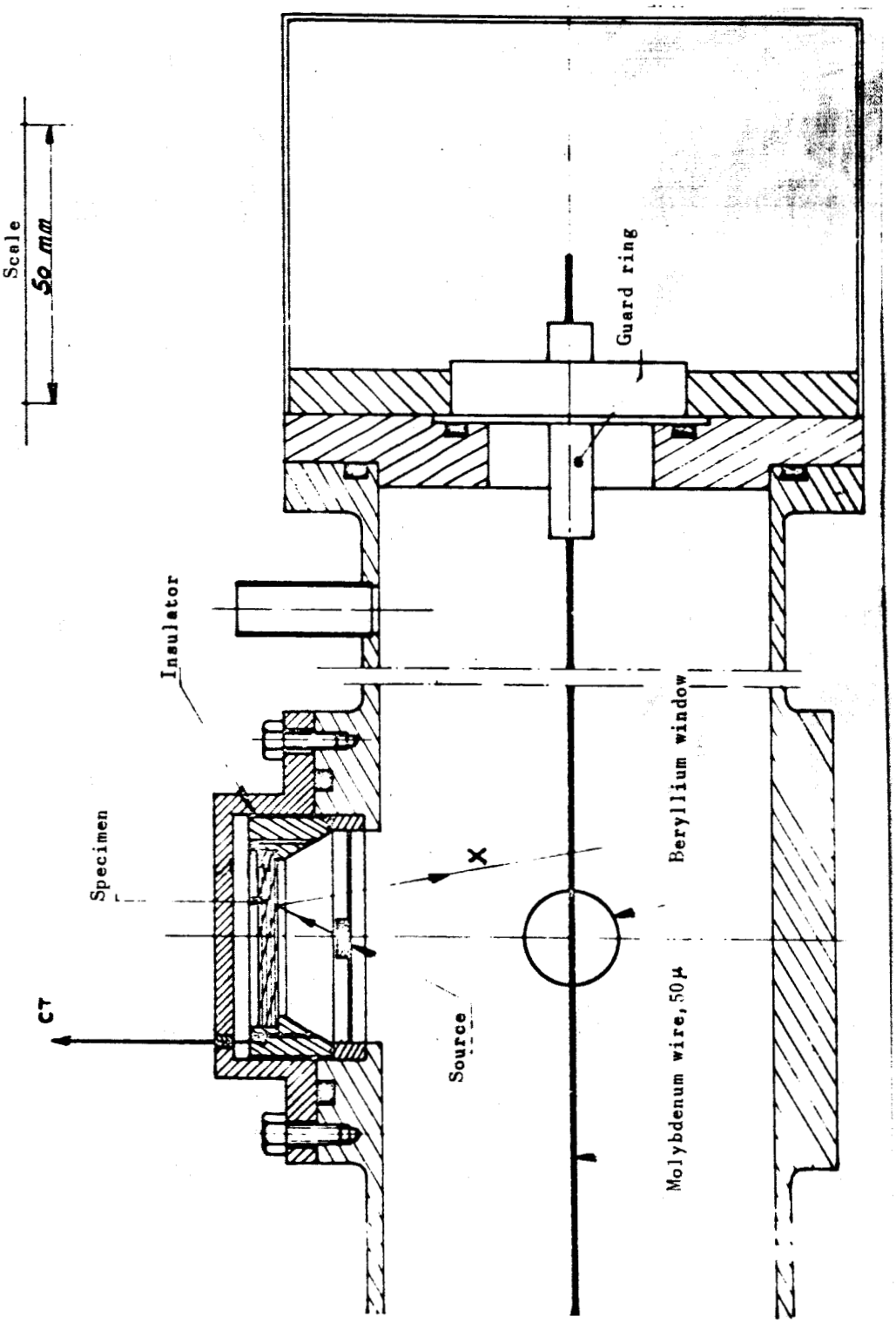

Fig.27 Proportional Counter and Specimen Irradiation Device

Characteristics /48

If ΔQ is the electric charge collected at the anode, then the variation in maximum voltage at the anode, for an infinite charge resistance R, will be $\Delta V = \frac{\Delta Q}{C}$, where C is the distributed capacitance, from the anode up to the grid of the input tube of the preamplifier:

$$C = C_C + C_{PA}$$

where

C_C = capacitance from the anode to the output terminal of the counter;

C_{PA} = capacitance of the input terminal from the preamplifier to the first tube.

These capacitances are measured at a frequency of 1 kc, with a Métrix impedance bridge.

C_C = 16 μμf

C_{PA} = 20 μμf whence C = 36 μμf .

(PAK)

The resolution of the counter was measured repeatedly with an external Fe^{55} source and a mixture of A + 10% CH_4. A resolution of 16.2% was obtained for an energy of 5.898 Kev, corresponding to the $K\alpha_1$ emission of manganese; the $K\beta_1$ radiation of 6.49 Kev is filtered through a thickness of 28.6 mg/cm^2 chromium.

Measuring the Gas Amplification Factor

The detection of an α-radiation of sufficient energy permitted defining the operating regimes of the counter by plotting (Fig.9) the relative height of the pulse as a function of a variable anode voltage.

The α-radiation, used above, was produced by a residual contamination by Po^{210}. The counting rate is about 10 c/sec and the mean detected pulse corre-

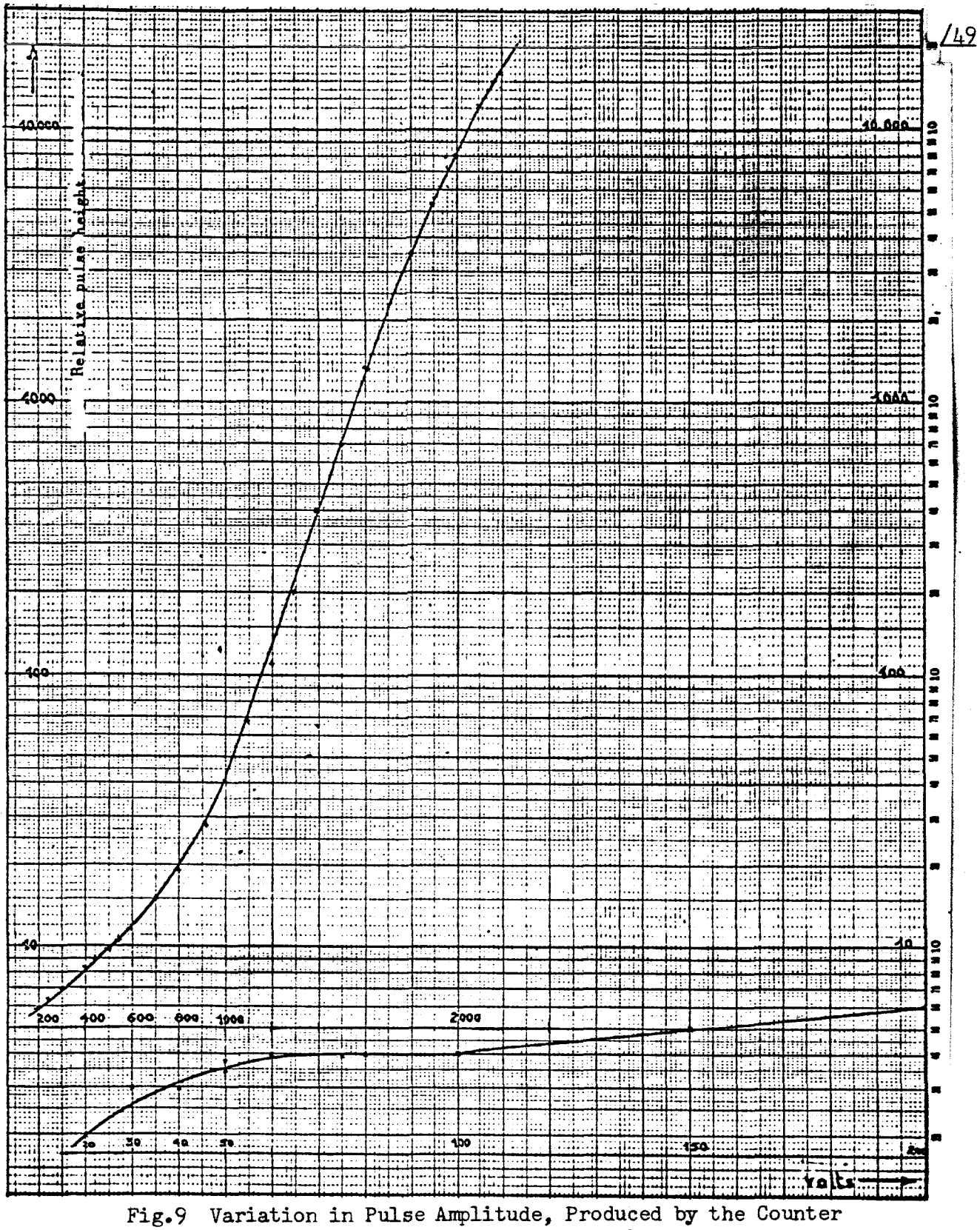

Fig.9 Variation in Pulse Amplitude, Produced by the Counter as a Function of the Anode Voltage

sponds to an energy of 2 Mev. This radiation is detected in the mixture A + + 10% CH_4, at a pressure of 700 mm Hg.

The pulse height is measured by means of a Tektronix oscilloscope, equipped with a 53 B slide-in chassis.

For a given point of the curve, the gas amplification factor A is known from the ratio of the pulse height at this point to that on the characteristic plateau curve of the ionization chamber, where A = 1.

For A = 1000, an overshoot appears on the pulse, making it necessary to modify the integration constants and the differentiation of the amplifier.

Any pulse deformation will influence the low-energy spectrum and deterio- /50 rate the resolution.

I.3 Electronic Circuits

The electronic circuits must have adequate and linear amplification, so as to ensure the lowest possible background.

The elements of this circuit are shown in Fig.8:

The VHV feed of the anode (S.A.I.P.) is regulated to within a few 10^{-4};

The preamplifier used was either the standard CEA* PJFB 1 or our own construction, designated as PAK;

The amplifier was of the AP 10 type, of the CEA standard;

The amplitude selector was of the single-channel S.A.I.P. type; toward the end of this work, we used the 400-channel Intertechnique SA 40 type.

The detection of weak electric signals requires numerous measures to eliminate the background as far as possible. The material was selected to meet this specific condition. The continuous VHV voltage must be freed of periodic or

* CEA = Atomic Energy Commission.

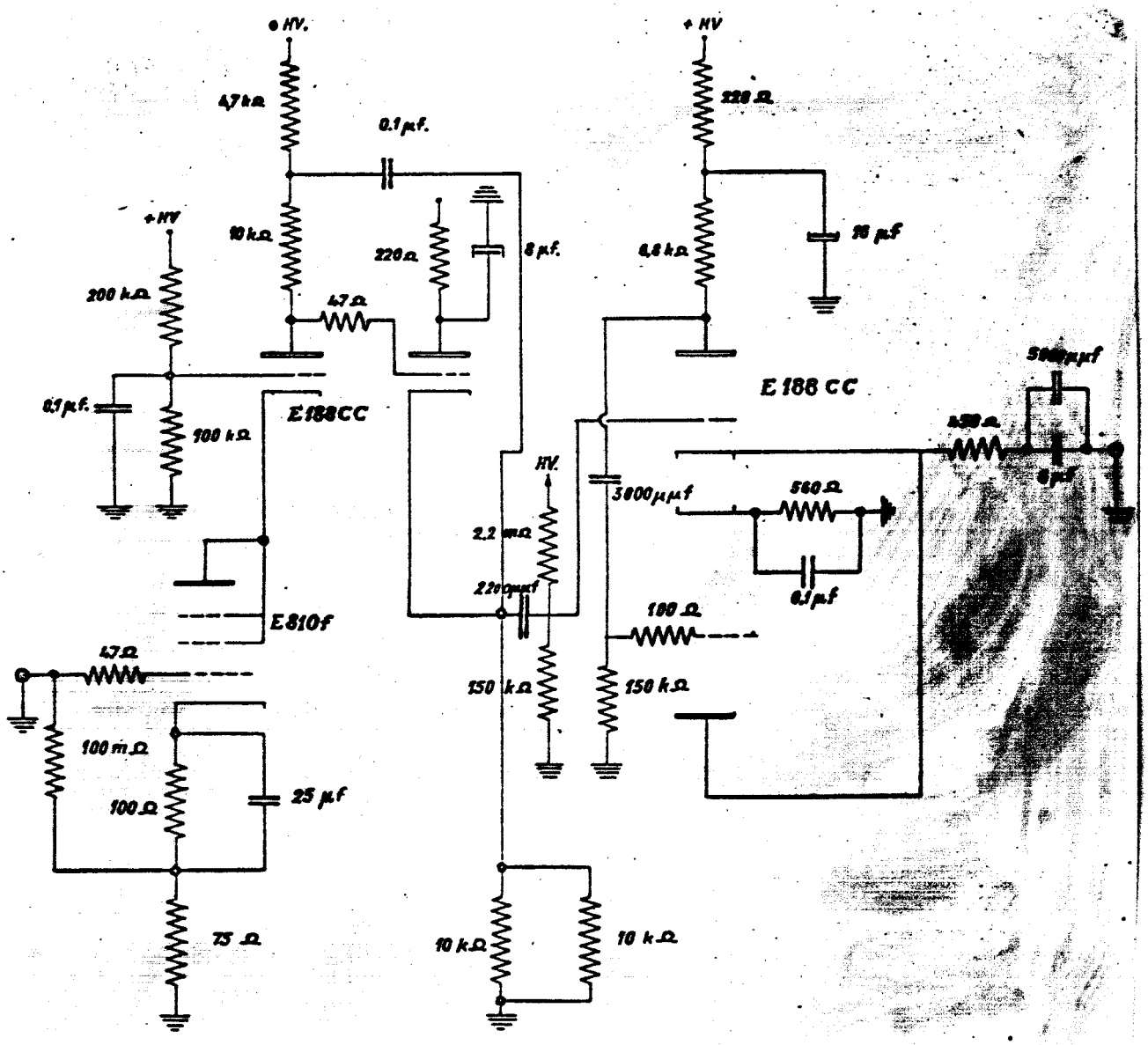

Fig.28 Wiring Diagram of the Preamplifier

random components. Since the background, due to electron amplification, is determined largely by the first preamplifier stage, special attention was paid to this circuit element.

The circuit diagram of the PAK preamplifier, constructed in our laboratory, is given in Fig.28:

Heating: 6.3 v, continuous

Gain of 65, measured to within ±10%

Input capacitance: 20 μμf

Background fed back to the input: $\frac{1 \text{ mv}}{65}$, i.e., 16 μv.

The AP 10 amplifier has a gain of 20,000, which can be regulated by a damper at the input. Pulse shaping is made possible by an RC circuit or by a delay line. A dephaser permits the output of a signal of desired sign.

We performed an energy calibration of the rise in intensity of the background at low energy. The reference energy of 4.5 Kev is furnished by a H^3/Ti source, external to the counter.

The operating conditions of the detector yield a measured gas amplification factor of 6350. /52

At the total electron gain of 650,000, the rise in background starts at an energy of 30 ev.

The filling gas for the detector CP 1 is a mixture of A + 10% CH_4, at a pressure of 600 mm Hg.

I.4 Gas-Filling of the Counter

The block diagram in Fig.8 represents the distribution circuit of the filling gas. This circuit makes it possible to operate the counter either closed or in circulation.

A vacuum pump ensures proper gas flow for pressures below atmospheric; in addition, the pump permits an evacuation of the counter before refilling with gas.

Two needle valves of the Edwards type adjust the charge of the circuit upstream and downstream of the counter. These valves permit a regulation of the pressure in the counter and adjustment of the flow, controlled by a spirometer. A metal Bourdon-type pressure gage measures the absolute pressure in the counter.

The guaranteed water and oxygen content of the gas furnished by the "Liquid Air" Corporation is less than 5 ppm; to maintain this purity, complete tightness of all tubing is essential.

A magnesium perchlorate column is used for monitoring possible dehydration of the gas flux.

Pressure Regulation of the Counter

In gas circulation, the pressure regulation of the counter over the valves A and B generally results in a deviation of the pressure value. This makes it necessary to regulate the pressure, if it is desired to work with gas circulation. A successfully tested pressure control method consists in stabilizing the "position" of the peak produced by a source of constant intensity, by modifying the pressure over the intermediary of the valve B.

The position of a given peak characterizes the power response of the installation; in a discrimination curve, the flank of this peak corresponds to the threshold D.

The integrator for this threshold D furnishes the signal S which could /54 vary by ΔS if, for the same discrimination threshold, the position of the peak varies.

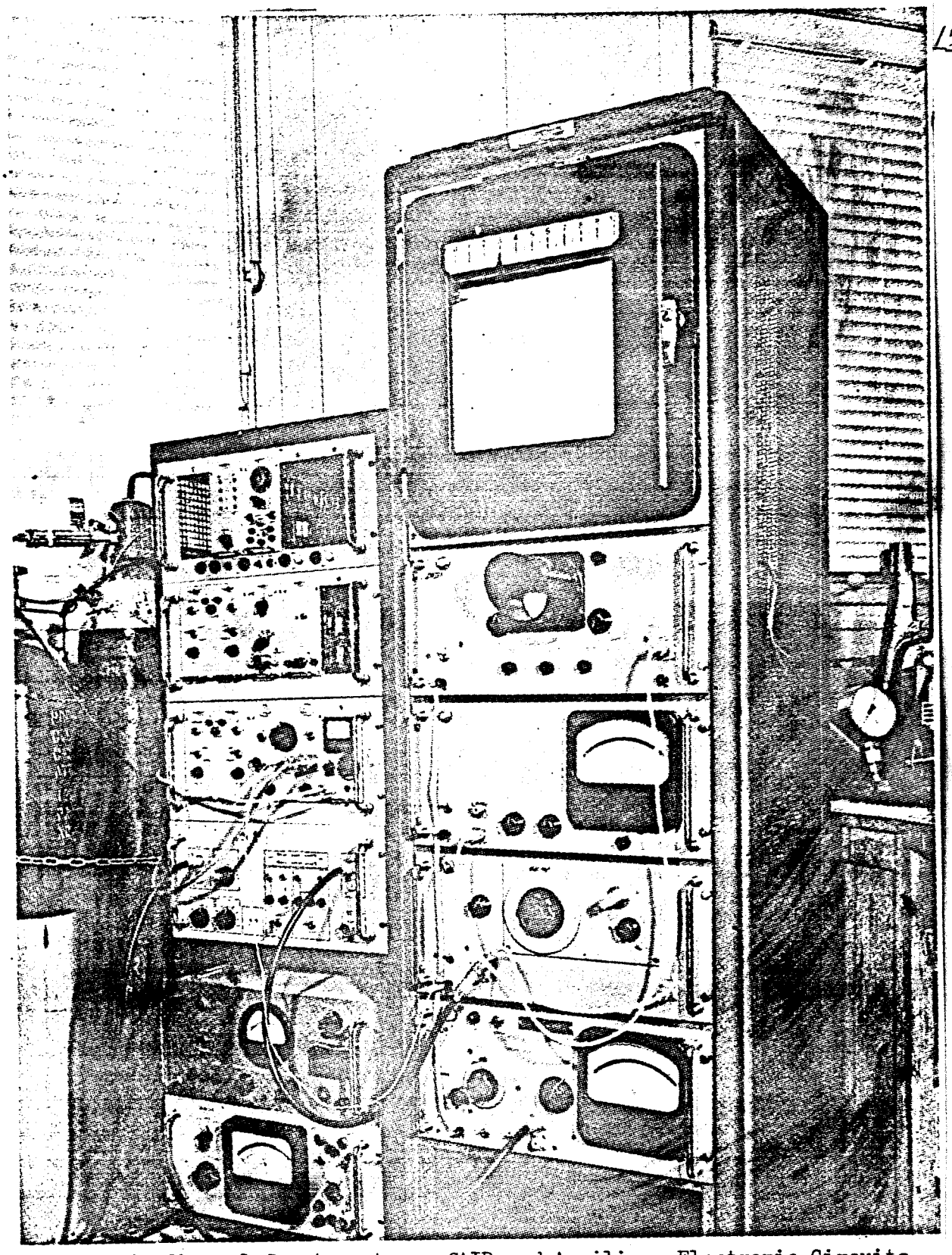

Single-Channel Spectrometer γ SAIP and Auxiliary Electronic Circuits

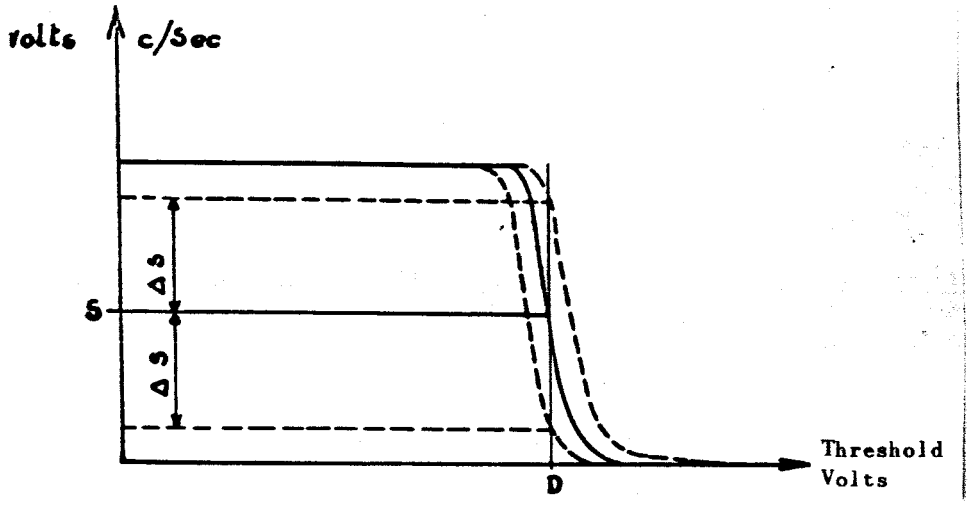

For a linear response of the system, we have

$$S = k \cdot E \cdot Ag \cdot A_{el}$$

where

k = constant

E = detected energy

Ag = gas amplification

A_{el} = electron amplification.

If P denotes the pressure of the counter, we have

$Ag = f_1(P)$ (see Section II.2 in Part I) and

$S = f_2(P)$.

Thus, it is possible to stabilize the position of the peak by influencing the pressure P; such a stabilization will be possible for any variation in the parameter affecting S.

However, this method is applicable only if the parameters other than P are subject to minor fluctuations only.

In fact, too large a variation in pressure, for compensating a variation in another parameter, will lead to a deterioration in efficiency of the counter and will cause operation outside of the proportional region.

Figure 10 shows the wiring diagram of the comparator and amplifier.

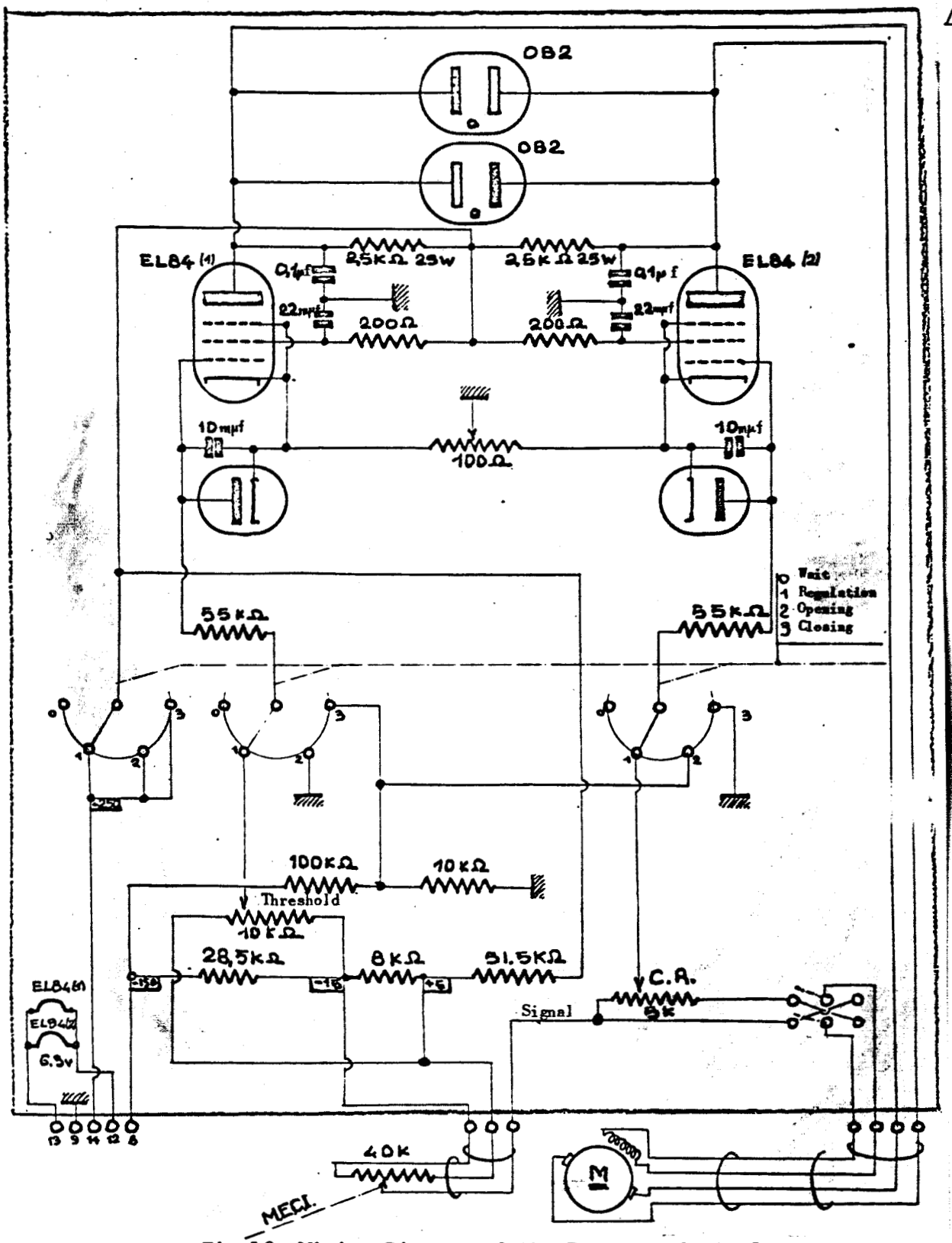

Fig.10 Wiring Diagram of the Pressure Control

/56

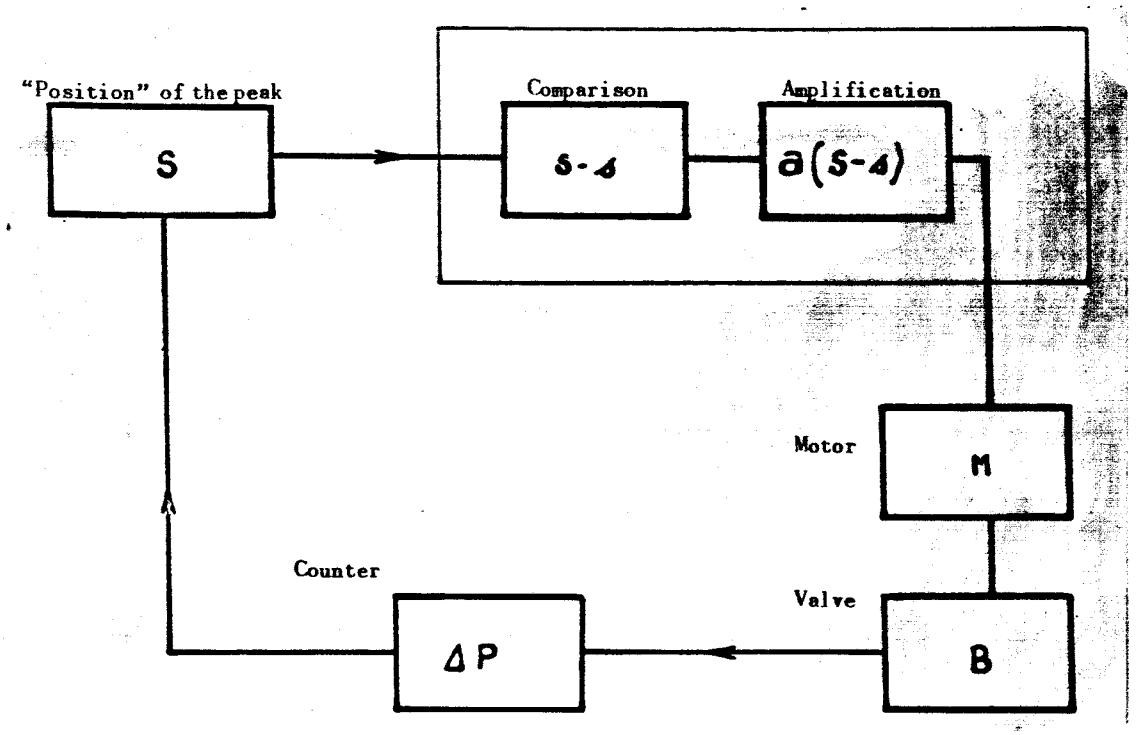

Block Diagram for Stabilization of the Energy Response of the Counter

II. EXPERIMENTAL CONDITIONS

Under the above-described conditions of fluorescence excitation of the specimen and its detection by a windowless counter, a continuous spectrum is generated which prevents spectrometry of the radiation emitted by the specimen. Under the hypothesis that this noise is due to scattering, in the detection volume, of electric charges other than those produced by the detection of fluorescence photons in the gas, we attempted to attenuate the effect by collecting these stray charges in an auxiliary electric field.

In this Section, we will investigate the influence of such an auxiliary /57 electric field, constituting an indispensable parameter. The optimum filling pressure and the excitation geometry define parameters whose influence on the counting rate or the yield of the detector will be investigated below.

We will describe experiments in which 0.5 mC of Fe^{55} was used as excitation source.

II.1 Auxiliary Electric Field

Without special precautions, a continuous spectrum is detected whose intensity decreases rapidly from zero energy to an energy largely corresponding to that of the fluorescence of the specimen. The detection of a fluorescence peak is made possible by establishing an electric field E_2 in the auxiliary volume.

The voltage V, applied to the anode of the counter, creates the electric field E_1 whose value, at a distance d from the anode, will be

$$\vec{E}_{1(d)} = \frac{\vec{V}}{d \operatorname{Log} \frac{r_c}{r_a}} .$$

In the absorption volume, the electric field will be considerably below this value of $E_{1(d)}$, because of the deformation of the lines of force.

The electric field E_2, having a direction opposite to that of E_1, is established by imparting a positive potential or a countervoltage (CV) to the electrode, composed of the specimen holder and the specimen itself, if the latter is a conductor. The resultant field $\vec{E} = \vec{E}_1 + \vec{E}_2$ will be a function of the variable CV.

Figure 11 indicates the influence of this electric field E_2 on the detection of the K lines of fluorescence of the elements Al, A, and Mn. These /58 lines are produced, respectively, by a target of pure aluminum, by the argon of the detection gas (A + 10% CH_4, pressure of 190 mm Hg), and by the radiation of the Fe^{55} excitation source.

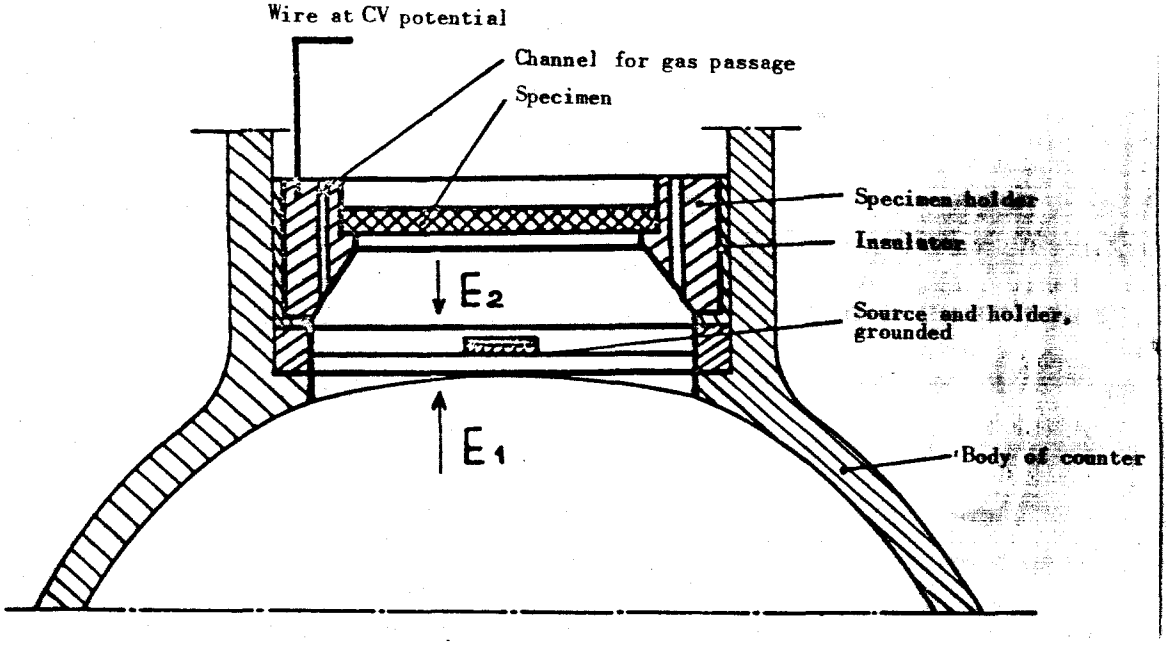

Arrangement of the Electrode Creating the Auxiliary Field

It should be mentioned here that the excitation source, in its immediate vicinity, creates a zone of high ion density, and that the presence of a weak electric field will contribute to establishing conditions favorable for intense ion recombination.

The electric field E_2 permits the collection of free electrons of low energy, which are abundantly present in this strongly irradiated zone.

In practical use, the value of CV on which E_2 depends, will be so selected as to obtain the optimum peaking ratio of the fluorescence peak.

II.2 Irradiation Geometry

The various sources used in our work are centrally arranged in the auxiliary volume, for irradiation of the specimen. A source of ring shape would also be advantageous to use.

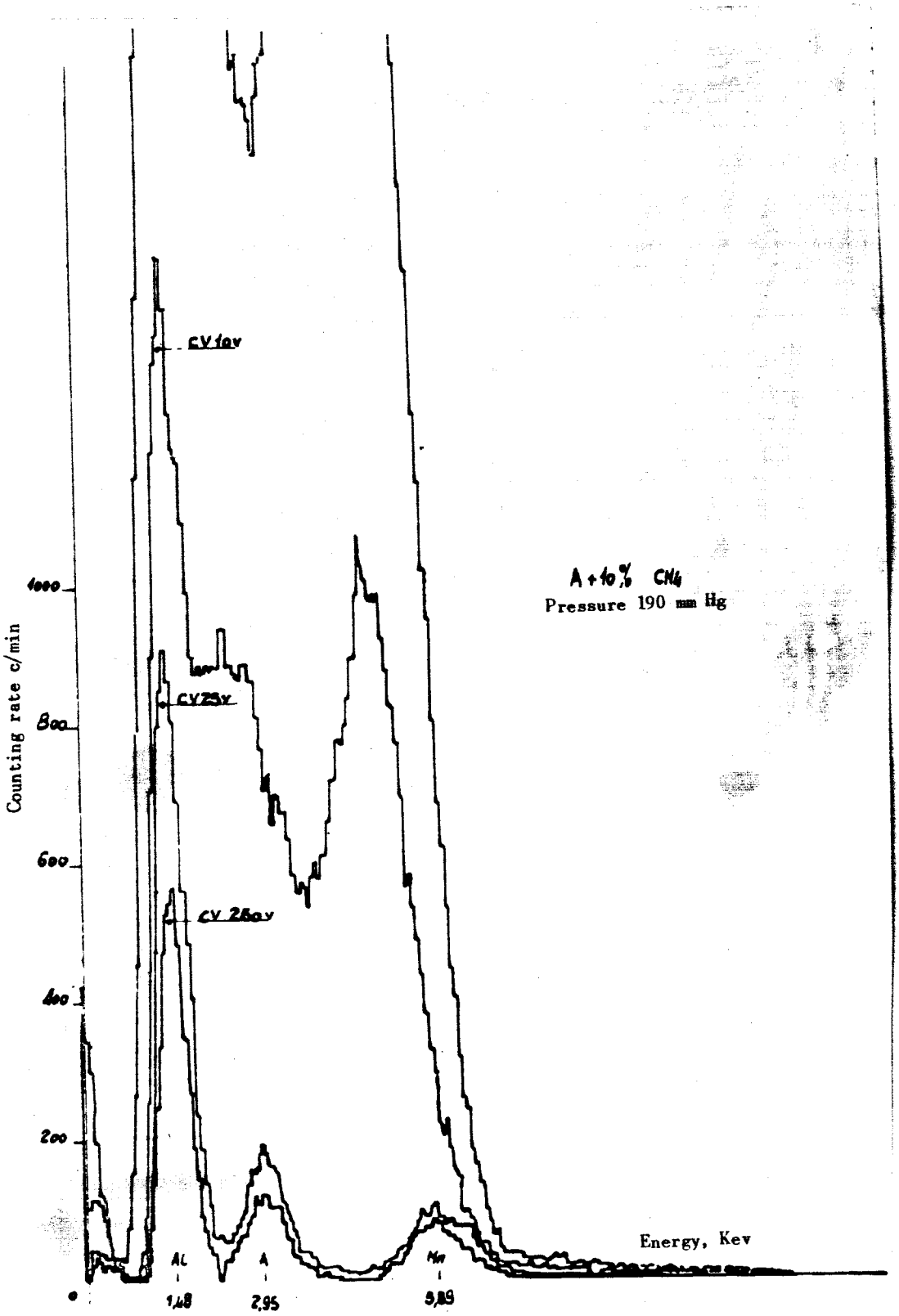

Fig.11 Influence of the Countervoltage on Detection

Below, we are giving the position of the source with respect to the specimen and the counter. /60

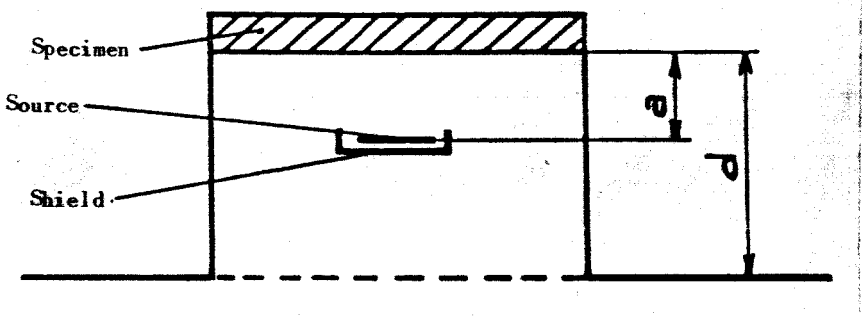

a = distance between source and specimen,
d = fictive input distance between proportional counter and specimen.

The parameters a and d define the irradiation geometry and influence the solid angles of specimen irradiation and detection.

Figure 12 shows the variations in counting rate N as a function of the values of a and d; the peaking ratio r is plotted as a function of d. These tests were made on the fluorescence peak K of an aluminum specimen, excited by an Fe^{55} source.

The other experimental conditions included

gas A + 10% CH_4 at 200 mm Hg;

countervoltage, 130 v.

The plotted value N corresponds to the height of the peak, giving the so-called low-energy background.

With the above parameters, the curve N = f(d) indicates the importance of proper positioning of the specimen. For d = 7 mm, a variation of only 1 mm in this parameter will lead to variations in the counting rate of 10%.

From Fig.12, we obtain the following optimum values, which will be used below: a = 5 mm; d = 7 mm.

/61

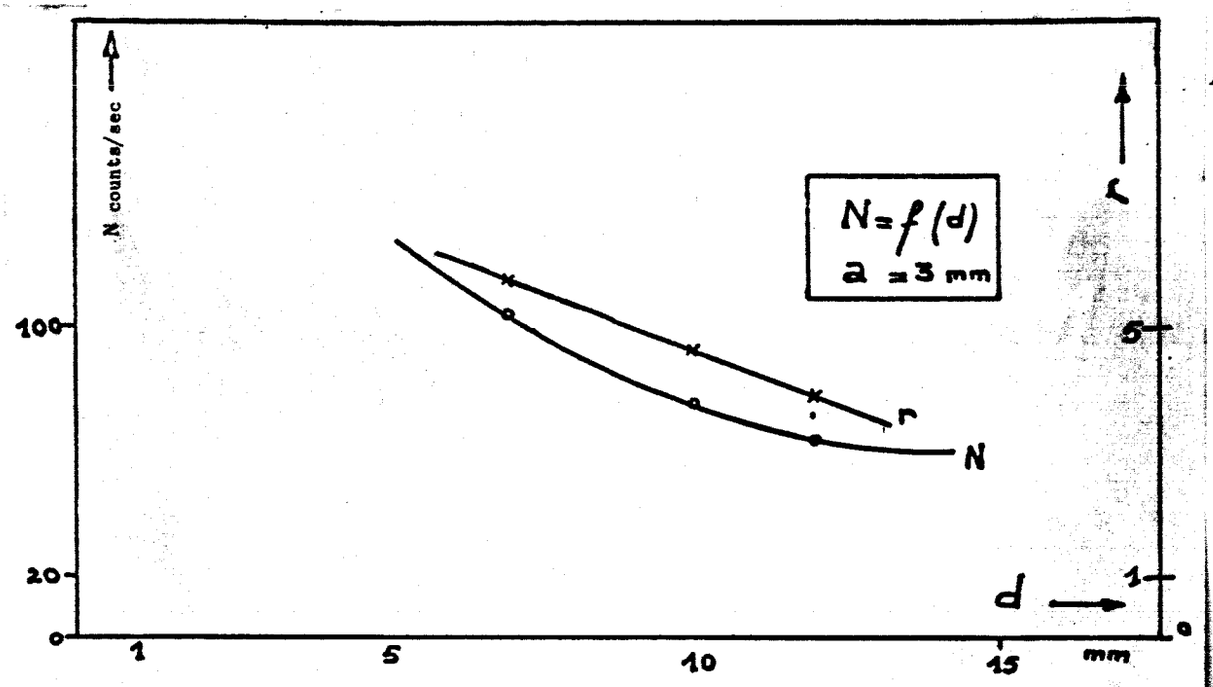

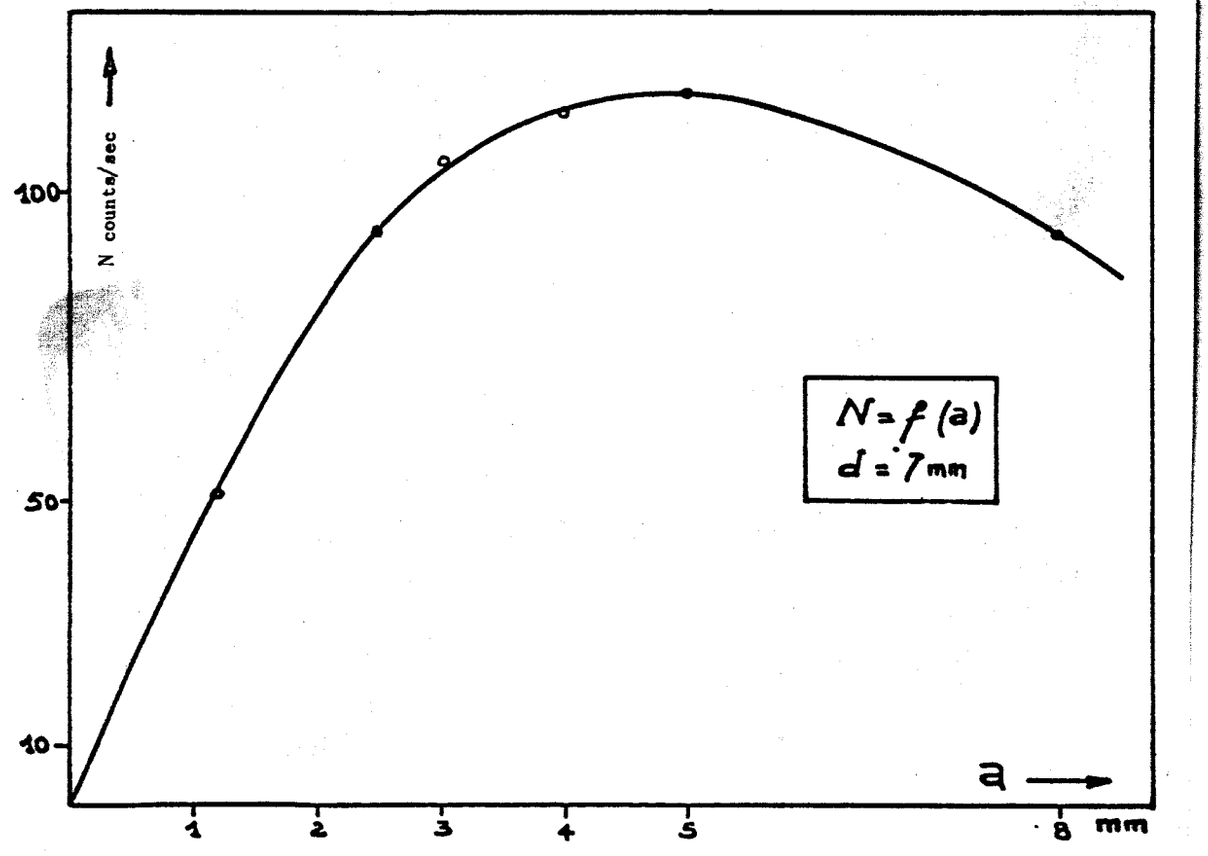

Fig.12 Influence of the Parameters a and d on the Counting Rate and the Peaking Ratio

For practical reasons, we were unable to reduce the distance d to less than 7 mm. It should be noted that the signal-to-noise ratio improves with decreasing d.

II.3 Optimum Filling Pressure /62

II.3.1 Calculation of Optimum Pressure

Below, we will calculate the pressure of the filling gas for a counter, giving maximum yield for counting of fluorescence radiation at predetermined parameter values.

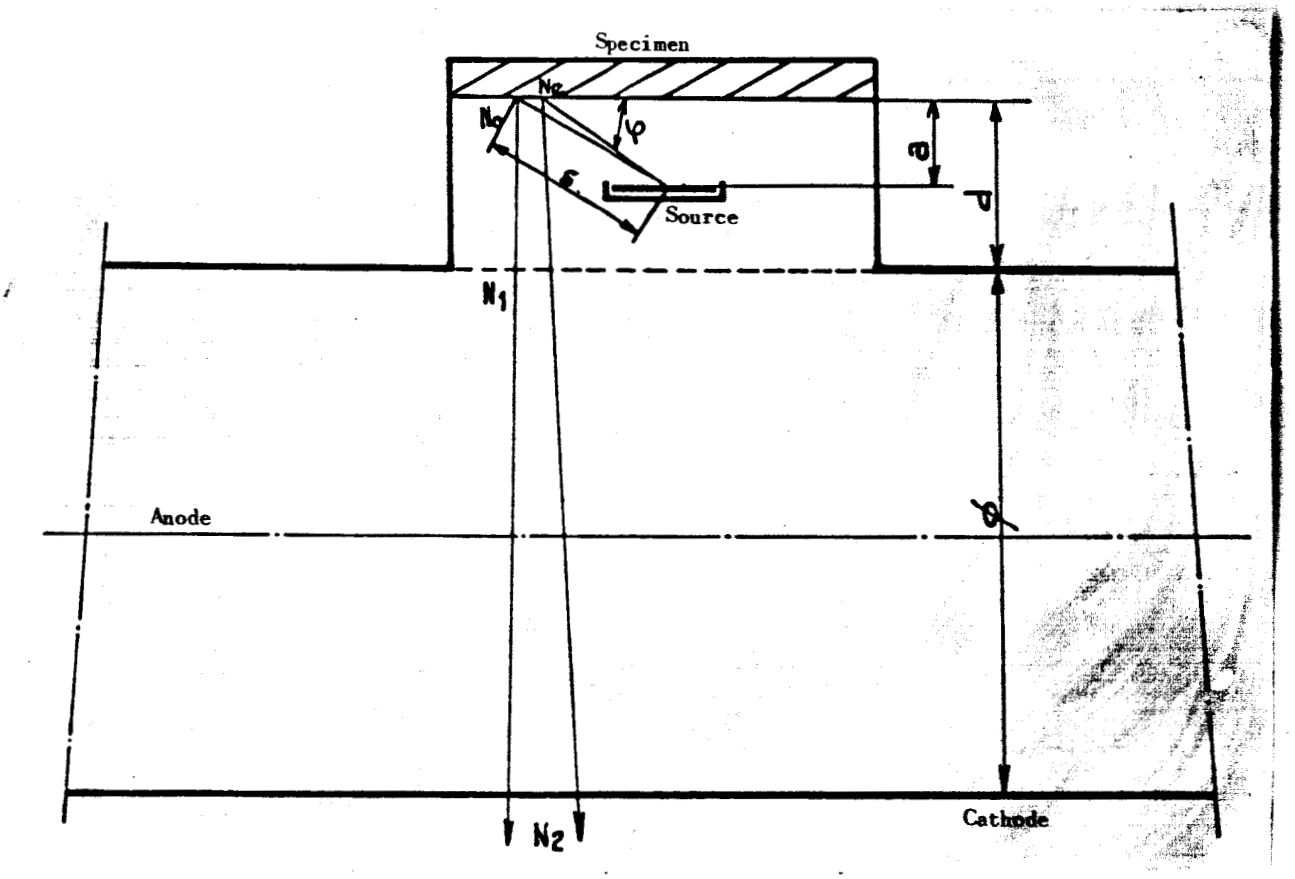

Parameters and Data

d = distance between specimen and fictive input of the counter, d =

= 0.7 cm;

a = distance between source and specimen, a = 0.45 cm;

ϕ = diameter of the proportional counter, ϕ = 7 cm;

δ = mean free path of the excitation radiation, yielding X-ray fluorescence practically perpendicular to the surface of the specimen; here, for $\varphi_m = 27^\circ$, $\delta \simeq 1$ cm;

ρ = specific mass of the gas $(P, T)_N$;

A = activity of the source. We consider here the intensity d_I emitted, in a thin beam, by the surface of the source. At the surface of the specimen, after covering a path δ in the gas, the intensity dNe of this excitation beam will be $dNe = d_I \cdot e^{-\mu_e \cdot m \cdot \delta}$; /63

μ_e = mass absorption coefficient in the gas of the exciting radiation λ_e;

μ_f = mass absorption coefficient in the gas of the fluorescence radiation λ_f;

dN_o = fluorescence flux, induced by the exciting beam and emitted at the specimen surface at an emergence angle of 90°;

dN_c = counting rate of the fluorescence $dN_c = dN_1 - dN_2$.

According to the formula obtained in Part I, Section III.1, giving the intensity of fluorescence at the surface of the specimen, we have

$$dNo = dI \cdot K \cdot e^{-\mu e \cdot m} \quad (K \text{ is a constant})$$

$$dNc = dI \cdot K \cdot e^{-\mu e \cdot m.\delta} \cdot e^{-\mu f.m.d} \cdot (1 - e^{-\mu f \cdot m.\beta}).$$

If m denotes the mass of the gas per cm^3 at a pressure P, then

$$m = \frac{P \cdot \rho}{P_N}$$

$$\frac{d\,Nc}{dI.\,K} = e^{-\frac{\rho \cdot P}{P_N}(\mu_e.\delta + \mu f \cdot d)} \times \left[1 - e^{-\mu f. \frac{\rho \cdot P}{P_N}. \beta}\right]$$

Let us define the expression of maximum dN_c as a function of P; we necessarily must have

$$\frac{d\,Nc}{d\,P} = 0$$

$$\frac{\delta\,N_c}{\delta\,P} = K \cdot e^{-\frac{\rho\,P}{P_N}(\mu_e.\delta + \mu_f \cdot d)} \cdot \mu_f \cdot \frac{\rho \cdot \phi}{P_N} \cdot e^{-\mu_f \cdot \frac{\rho\,P}{P_N}\phi}$$

$$- K \frac{\rho}{P_N}(\mu_e.\delta + \mu_f \cdot d) \cdot e^{-\frac{\rho\,P}{P_N}(\mu_e.\delta + \mu_f \cdot d)} \left[1 - e^{-\mu f \frac{\rho.P}{P_N}\phi}\right]$$

For maximum dN_c, the optimum pressure P_o will be /64

$$P_o = \frac{P_N}{\mu_f \cdot \rho \cdot \phi} \text{Log} \left[1 + \frac{\mu_f \cdot \phi}{\mu_e.\delta + \mu_f \cdot d}\right]$$

Application at the Following Conditions

Filling gas Ar + 10% CH_4 $\rho = 1.563 \times 10^{-3}$ gm/cm^3

Excitation source Fe^{55}, $\lambda_e = 2.1$ Å $\mu_e = 240$ cm^2/gm

Specimen aluminum, $\lambda_f = 8.34$ Å $\mu_f = 1100$ cm^2/gm

Countervoltage (CV) = 130 v.

With this, we find P_o = 138 mm Hg.

Figure 13 gives the variation in counting rate N_c as a function of the pressure according to the parameter d.

An experimental curve is also given, showing a deviation from the calculated curve. The optimum observed pressure P_r is 190 mm Hg, and a transfer of the observed pressure indicates that the value of d used in the calculation had been overestimated.

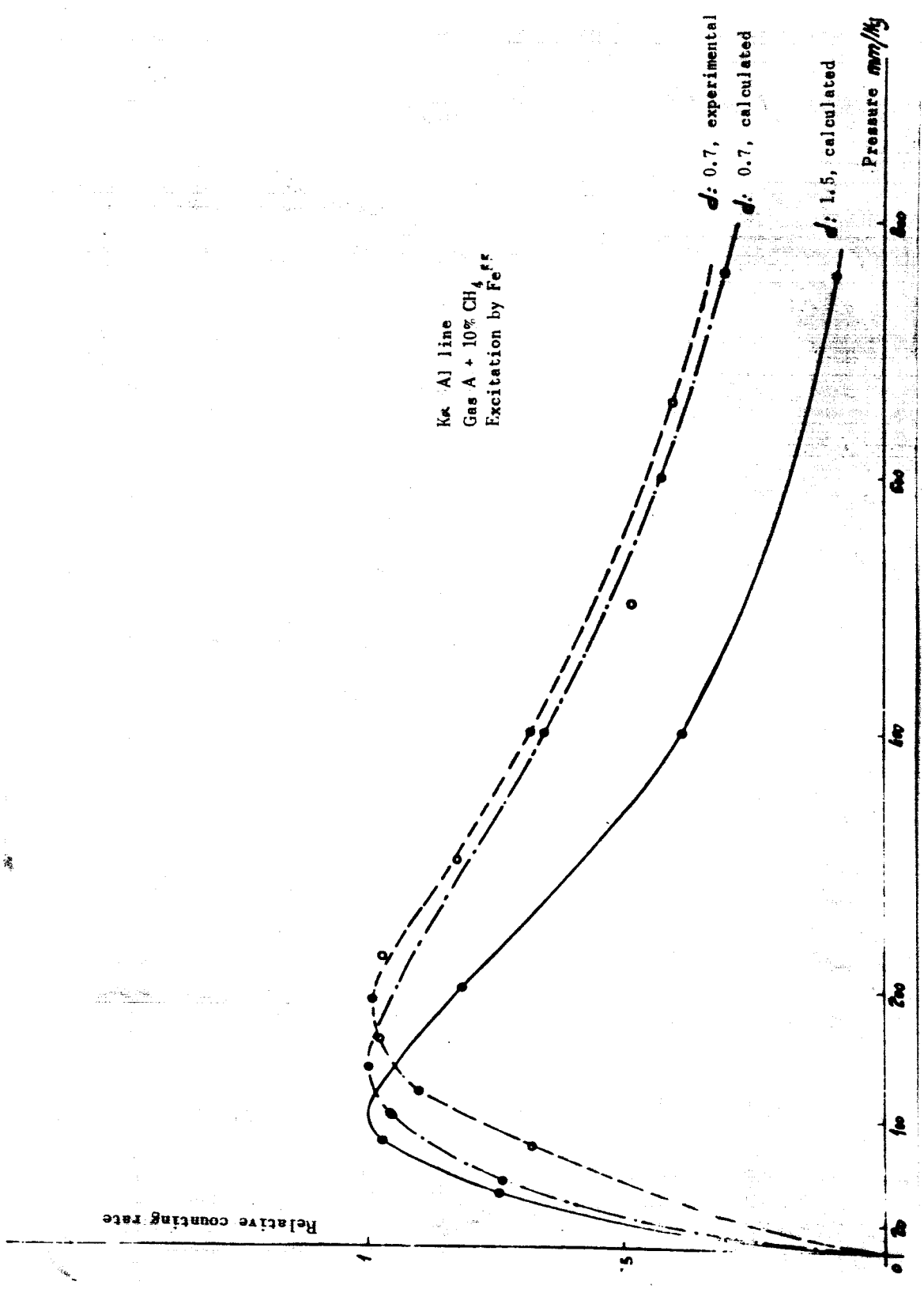

Fig.13 Detection Efficiency as a Function of the Pressure

II.3.2 Determination of the Absorption Volume

The presence of the source holder, connected to ground, creates perturbations in the resultant electric field in the vicinity of the specimen. Because of this fact, separation of the absorption and detection volumes does not occur along a plane surface. Thus, if the distance d_r from the specimen to this surface is calculated in accordance with the real optimum pressure found in Fig.13, this value of d_r will be representative only for a mean distance.

According to Fig.13, we have $P_0 = 138$

$P_r = 190$.

The detection volume is represented by

$$\beta = 7.7 - d_r$$

from which we o ... the equation /66

$$190 = \frac{760}{1100 \cdot 1.563 \cdot 10^{-3} (7.7 - d_r)} \text{Log} \left[1 + \frac{1100 (7.7 - d_r)}{240 + 1100 d_r} \right].$$

From this, we derive

$$d_r = 0.08 \text{ cm}.$$

Another determination of d_r was made by exciting a titanium target by Fe^{55}, with the geometry

$$d = 0.85 \text{ cm}$$
$$a = 0.50 \text{ cm}.$$

On separating the auxiliary volume from the proportional counter by a beryllium window of 1/10 mm thickness, the optimum pressure P_r will be found to differ little from the calculated value of P_0.

The auxiliary volume and the counter volume are under identical conditions

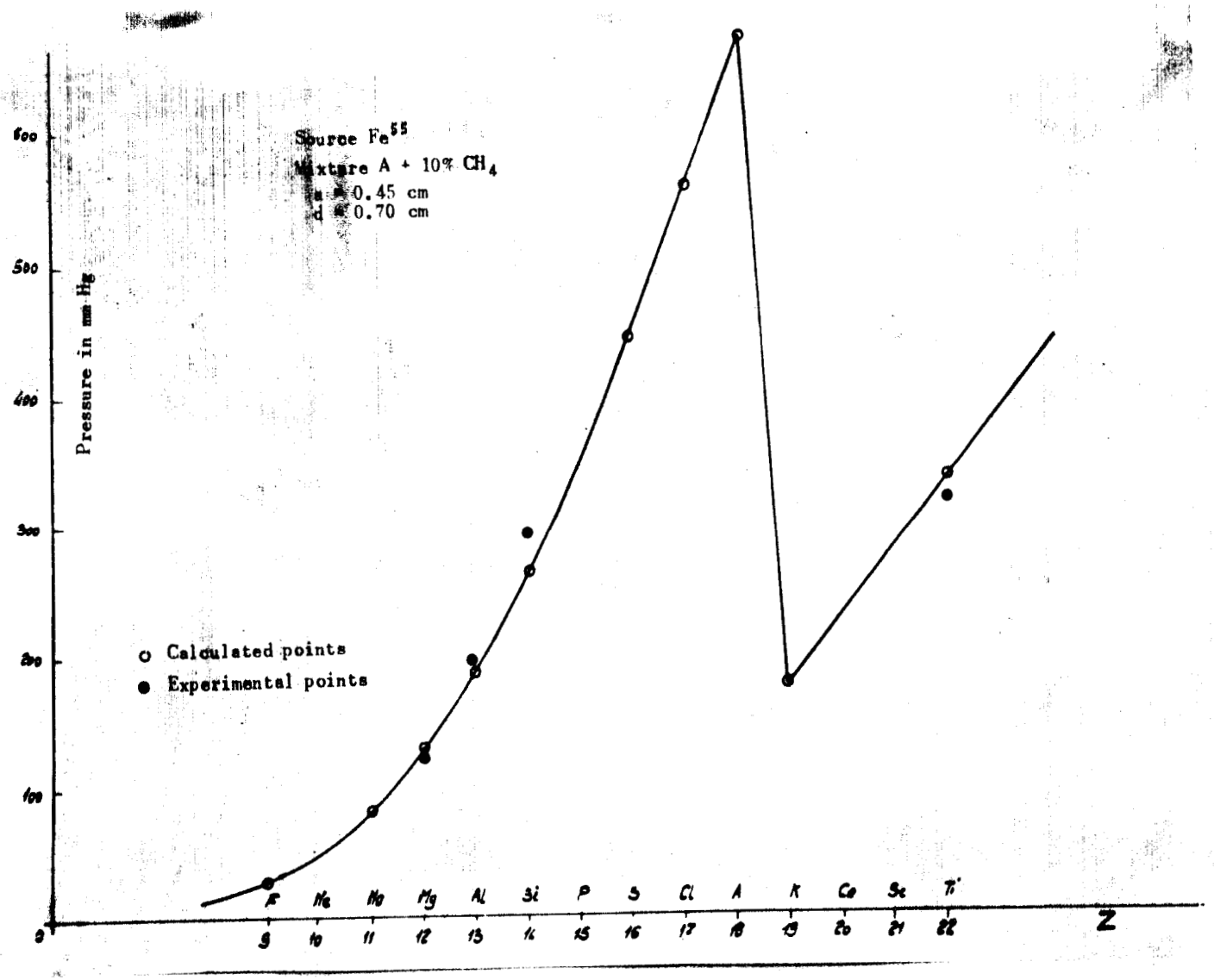

Fig.14 Optimum Pressure as a Function of the Atomic Number Z

of gas filling. A measurement of P_r, without window, yields

$$d_r \sim 0.1 \text{ cm}.$$

This value of d_r made it possible to plot the curve for the real optimum pressure as a function of the atomic number of the excited element.

This curve No.14 is valid only under the following conditions:

$a = 0.45$ cm

$d = 0.70$ cm

$d_r = 0.1$ cm.

The absorption coefficients are taken for filling of the counter with a mixture of A + 10% CH_4.

The Fe^{55} excitation source emits X-ray radiation of 2.1 Å.

For very light elements ($Z < 10$), the filling pressure will become too low; therefore, it is of advantage to use a gas of low density, such as a mixture of He and CH_4.

III. QUALITATIVE ANALYSIS OF THE ELEMENTS OF THE SECOND AND THIRD PERIODS /68

III.1 Selection of the Detector Gas

The theoretical considerations developed in Part I, Section II.2, induced us to use a mixture of rare gases and polyatomic gases; the "Liquid Air" Corporation has various mixtures of these detector gases on the market.

The element to be analyzed, depending on the energy of its fluorescence radiation, determines the selection of the gas mixture. The optimum pressure, depending on the geometry used, defines the yield of the detector. This pressure, which is a function of the density of the mixture, should be kept within reasonable limits.

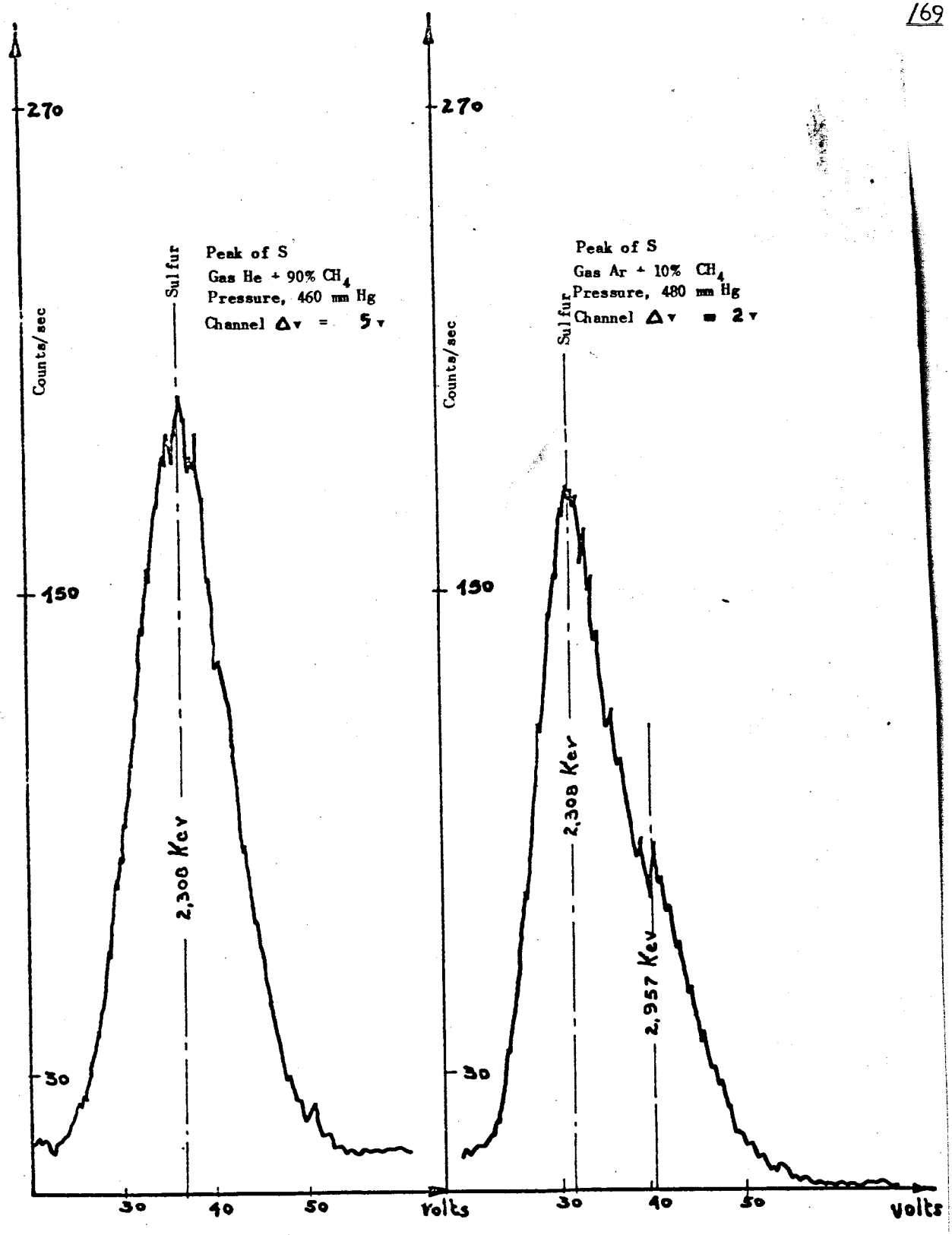

Fig.15 K Peak of Sulfur Detected with the Mixtures A + CH_4 and He + CH_4

The position of the leakage peak with respect to the energy to be detected represents still another criterion for selection of the gas.

Leakage Peak

The X-ray radiation to be detected, of an energy $h\nu$, produces ionization and excitation of the gas. By photoelectric effect, the photon $h\nu$ is able to eject an electron from the K shell of the rare gas, where the binding energy of this shell is E_K. This photoelectron loses its energy $h\nu - E_K$ by ionization of the gas.

If an Auger rearrangement of the gas atom takes place, an Auger electron of energy $E_K - 2E_L$ is emitted within 10^{-10} sec after ejection of the photoelectron. In that case, the totality of energy is collected:

$$h\nu - E_K + E_K - 2E_L \simeq h\nu.$$

If a fluorescence rearrangement is involved, the emitted photon of energy $E_K - E_L$ will have a low probability of being absorbed in the gas. In that case, the counter absorbs the energy $h\nu - E_K$.

Thus, the spectrum will contain the energy peak $h\nu$ and another peak known as "leakage peak" of an energy $h\nu - E_K$.

Fluorescence of the Gas

In the auxiliary volume, close to the source, the gas atoms are strongly excited and are able to emit fluorescence which is superposed to the detected spectrum.

For an analysis of elements of the third period, the gases A and Ne /70 permit working at admissible pressures; gases such as He and the pure poly-

atomic gases are especially suitable for elements of the second period.

If the leakage peak or the fluorescence peak of A and Ne interfere with the fluorescence of the element to be analyzed, these gases could be replaced by light gases that give no parasite peaks; in that case, a lower detection yield must be tolerated.

In Fig.15, the peak of sulfur is detected in the mixture He + 90% CH_4, with a lower detection yield, and in the mixture A + 10% CH_4 where the argon peak encroaches on that of the sulfur.

III.2 Excitation Sources Used

Various radioactive sources were used for exciting fluorescence of the elements of the third and second period:

H^3/Zr	β - X emitter
Fe^{55}	X emitter
Po^{210}	α emitter.

The sources described here were not produced specifically for this study; they were available at the laboratory or were taken from regular production.

Below, we will give the results obtained with each type of source, the conditions of their use, and the advantages or disadvantages encountered.

III.2.1 H^3/Zr Source

Tritium (half-life, 12.26 years), when adsorbed on zirconium, emits β-particles of a maximum energy of 18 Kev; these electrons induce a secondary X-ray radiation by bremsstrahlung and excitation of the fluorescence of the metal of the holder.

Figure 7 shows the detected spectrum of such a source.

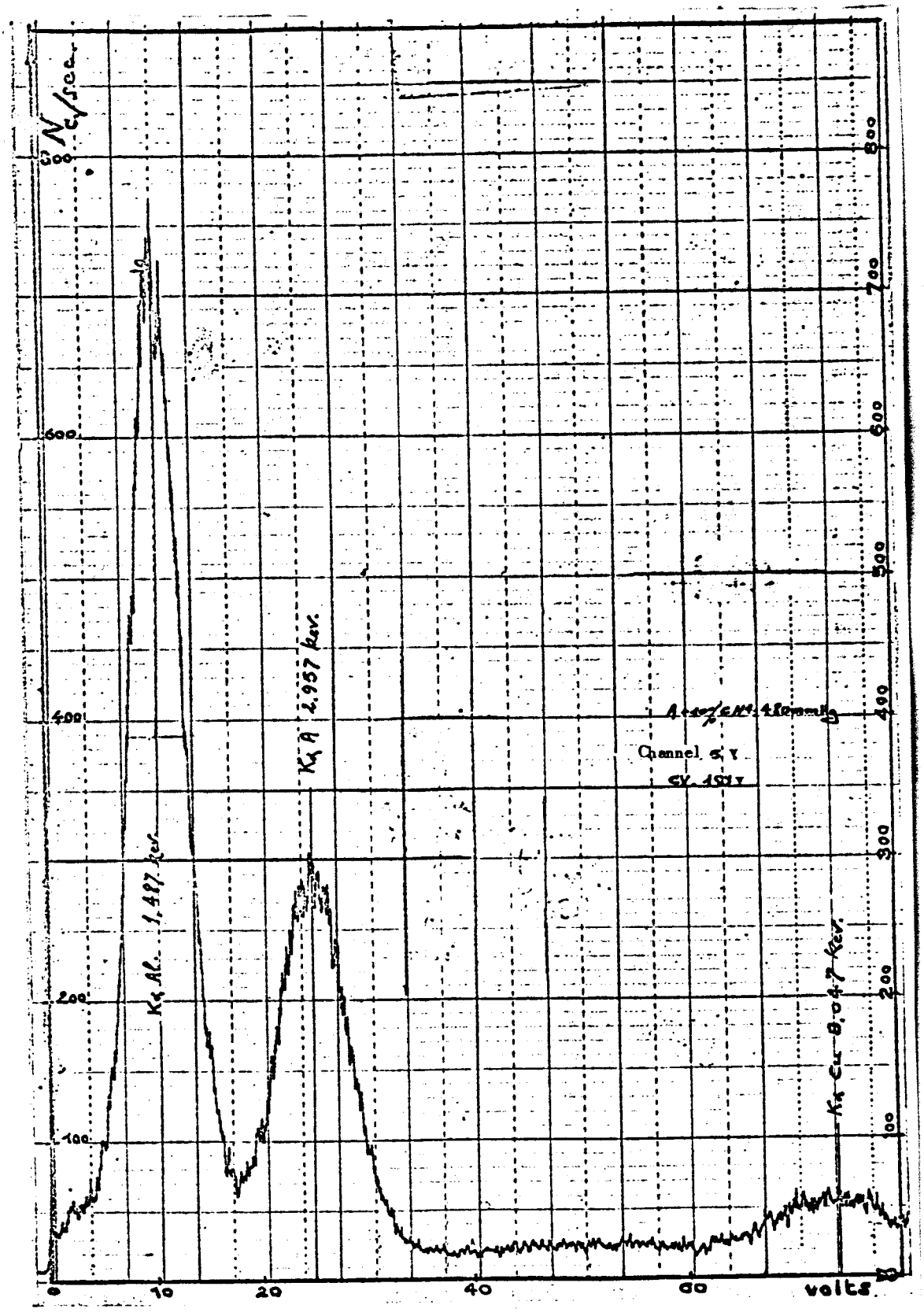

Fig.16 Kα Al Line, Excited by a H^3/Zr Source

The source used, having an activity of approximately 0.8 curie, is designed as a thin disk of 10 mm diameter.

Excitation geometry: a = 0.35 cm /72

d = 0.70 cm.

Figure 16 shows the X-Kα peak of aluminum, excited under the mentioned conditions. The diagram shows the Kα peak of copper, produced by excitation of the counter envelope, as well as the intense fluorescence peak of argon.

In Fig.17, the aluminum peak occurs at 50 v.

Figure 18 gives the intensity of this peak in accordance with the filling pressure. At constant electron gain, the position of the peak at 50 v is adjusted by variations in the very high voltage (VHV). On the other hand, the countervoltage (CV) is given a value such that the background will remain constant at 20 c/sec, at the 10-v position of the spectrum.

At a constant pressure of 480 mm Hg, Fig.19 shows the variations in the background and in the peaking ratio r, as a function of the CV.

For aluminum, the optimum pressure is located near 100 mm Hg; the preceding diagrams show the difficulty of going down to this pressure without raising the CV to a relatively high value. In the next Chapter, we will demonstrate that this difficulty apparently is due to the high activity of the source rather than to its nature.

A major drawback of this source was a contamination of the filling gas and of the counter casing by the tritium.

The liberation of tritium from the source could be reduced by not producing a vacuum before filling the counter or by using special sources with a very thin aluminum coating. In addition, circulation of gas will limit the effect of contamination.

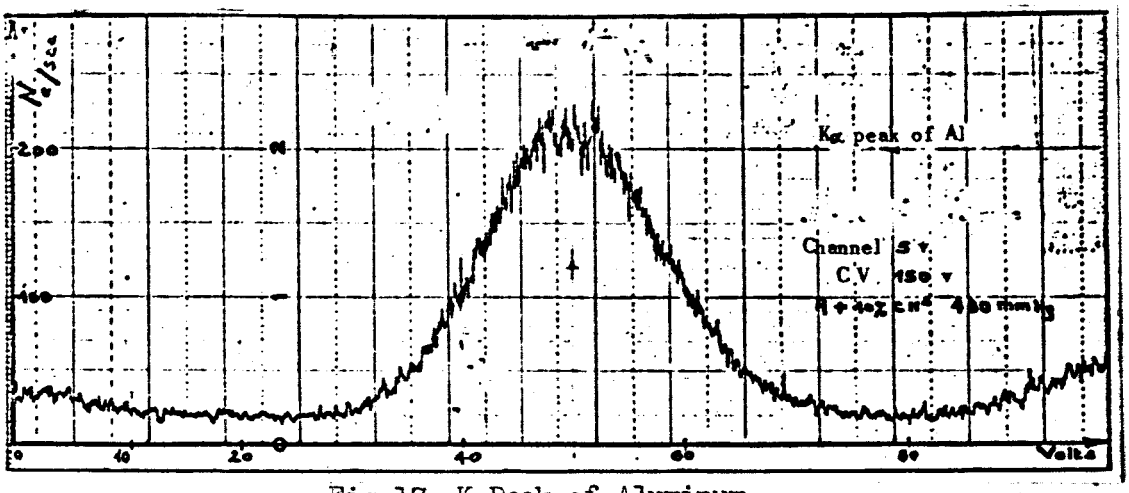

Fig.17 K Peak of Aluminum

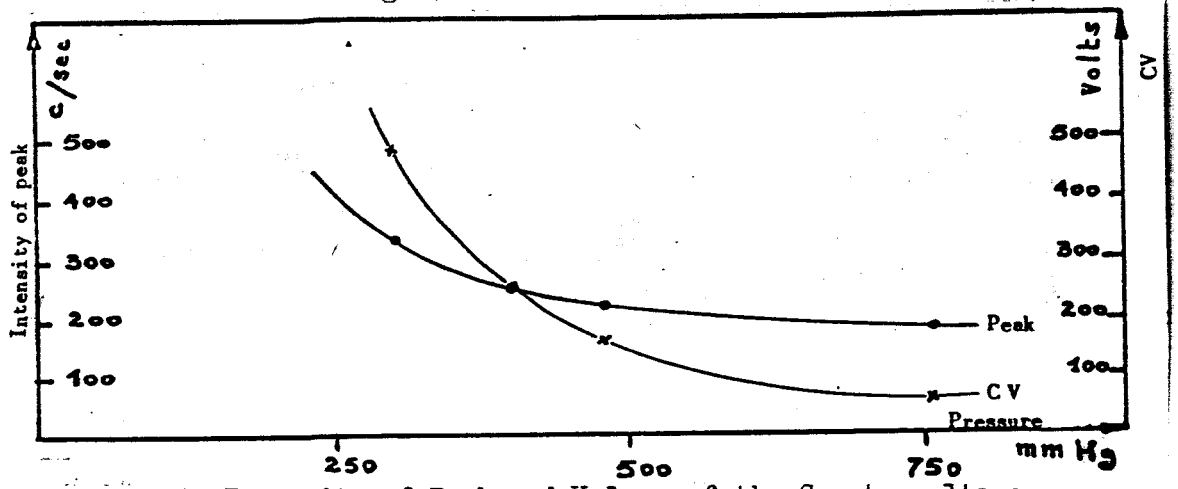

Fig.18 Intensity of Peak and Values of the Countervoltage, according to the Pressure

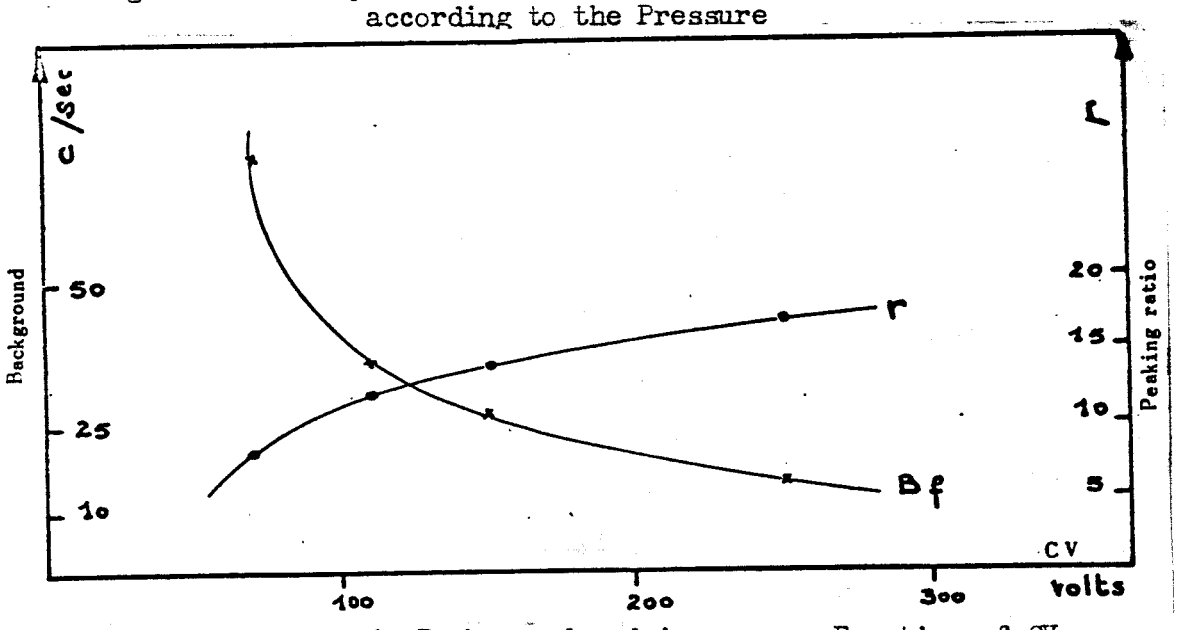

Fig.19 Variations in Background and in r, as a Function of CV

The sources of adsorbed tritium have a high specific activity and their X-ray emission has a sufficiently low energy for properly exciting the fluorescence of light elements.

III.2.2 Fe^{55} Source

The Fe^{55}, by K capture, emits

$$^{55}_{26}Fe + {}_{-1}e_K \longrightarrow {}^{55}_{25}Mn^{*} + \nu$$

which is the Kα fluorescence radiation of manganese at 5.898 Kev.

The half-life of this source is 2.7 years. /74

The source was designed as a disk of 5 mm diameter, with an activity of 0.5 mC.

Irradiation geometry: a = 0.45 cm

d = 0.70 cm.

With this source, of less activity than the other source, the background at low pressure remains acceptable, so that it is possible to trace the fluorescence spectrum of an aluminum target (Fig.20) at the optimum pressure of 190 mm Hg.

TABLE OF RECORDED SPECTRA CORRESPONDING TO THE CHARACTERISTIC PEAKS OF THE ELEMENTS OF THE THIRD PERIOD, EXCITED BY THE Fe^{55} SOURCE

Elements	Type of Target	No. of Fig.
Cl	Polyvinyl chloride	22
S	Pelleted sulfur	15
Al	Al	20
Mg	Mg	23

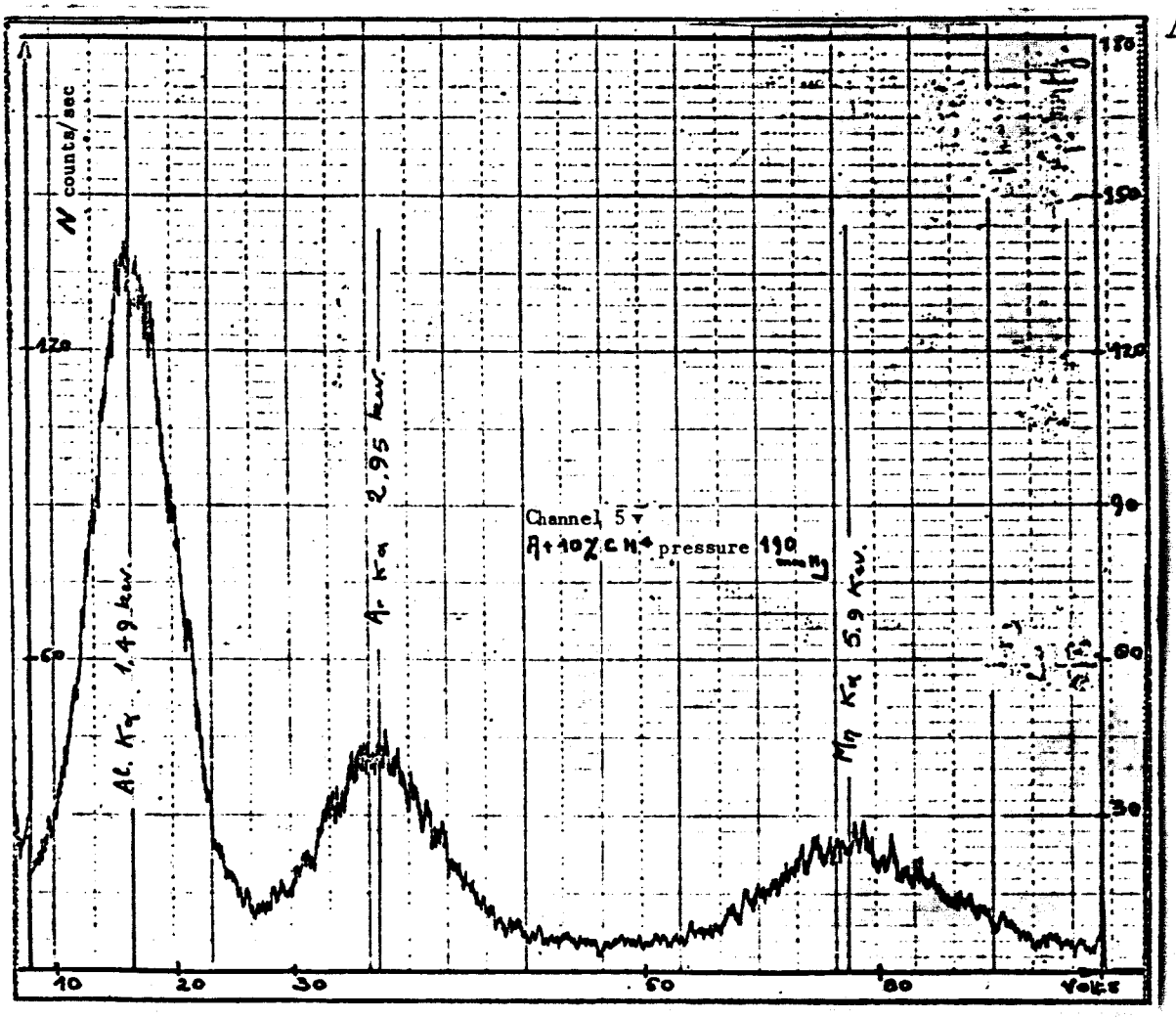

Fig.20 Kα Al Line, Excited by an Fe^{55} Source

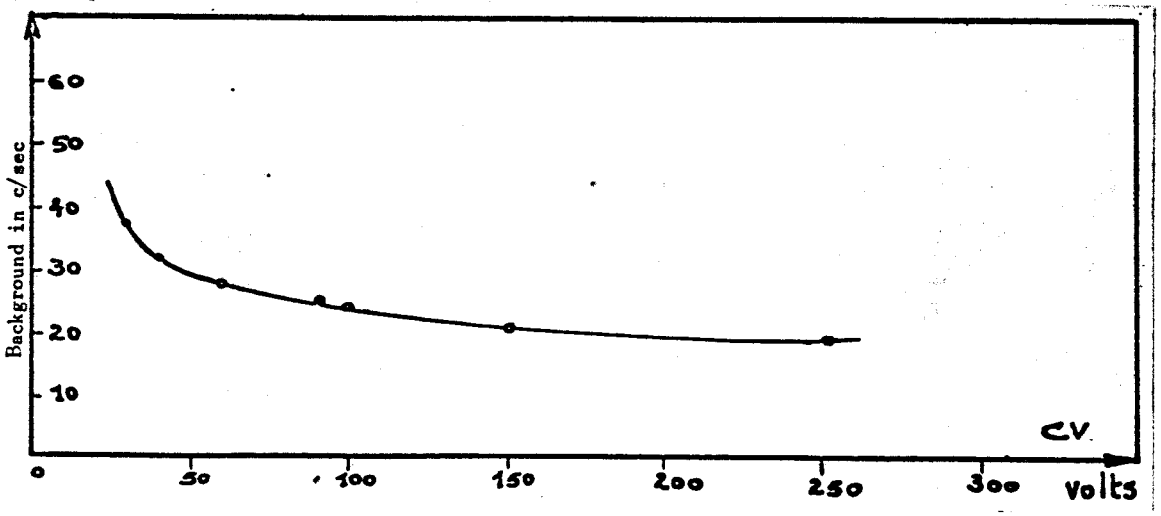

Fig.21 Background as a Function of the Auxiliary Field

In Fig.21, the variations in the background at 6 v on the spectrum No.20 are plotted as a function of the CV.

The peaks, appearing at 5.9 Kev, are due to back scattering, on the target, of exciter photons of 5.9 Kev energy.

The intensity of the peaks of light elements, such as Al and Mg, could be increased by using excitation sources of higher activity.

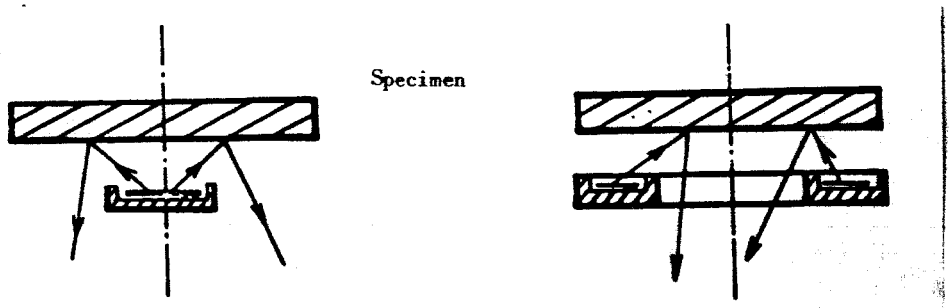

Excitation by central source

Excitation by ring source

In the central geometry, the increase in activity of the source will /76 lead to an increase in its surface and thus to a shadow effect which becomes prohibitive. The use of a ring source would permit a greater activity at an acceptable shadow effect.

For a high activity, the central geometry can be retained if a Fe^{55} source of high specific activity is available. This particular Fe^{55} is produced in the Oak Ridge cyclotron over the reaction Mn + p. Specific activities of 800 mC/mg are obtained, permitting the production of quasi-point sources.

III.2.3 Po^{210} Source

The practically pure Po^{210} emitter of α-particles with 5.3 Mev has a half-life of 138 days. This radioisotope has been used in the form of a standard C.E.A. source, of the SA 2 type:

outer diameter, 16 mm

mica window of 1 mg/cm^2

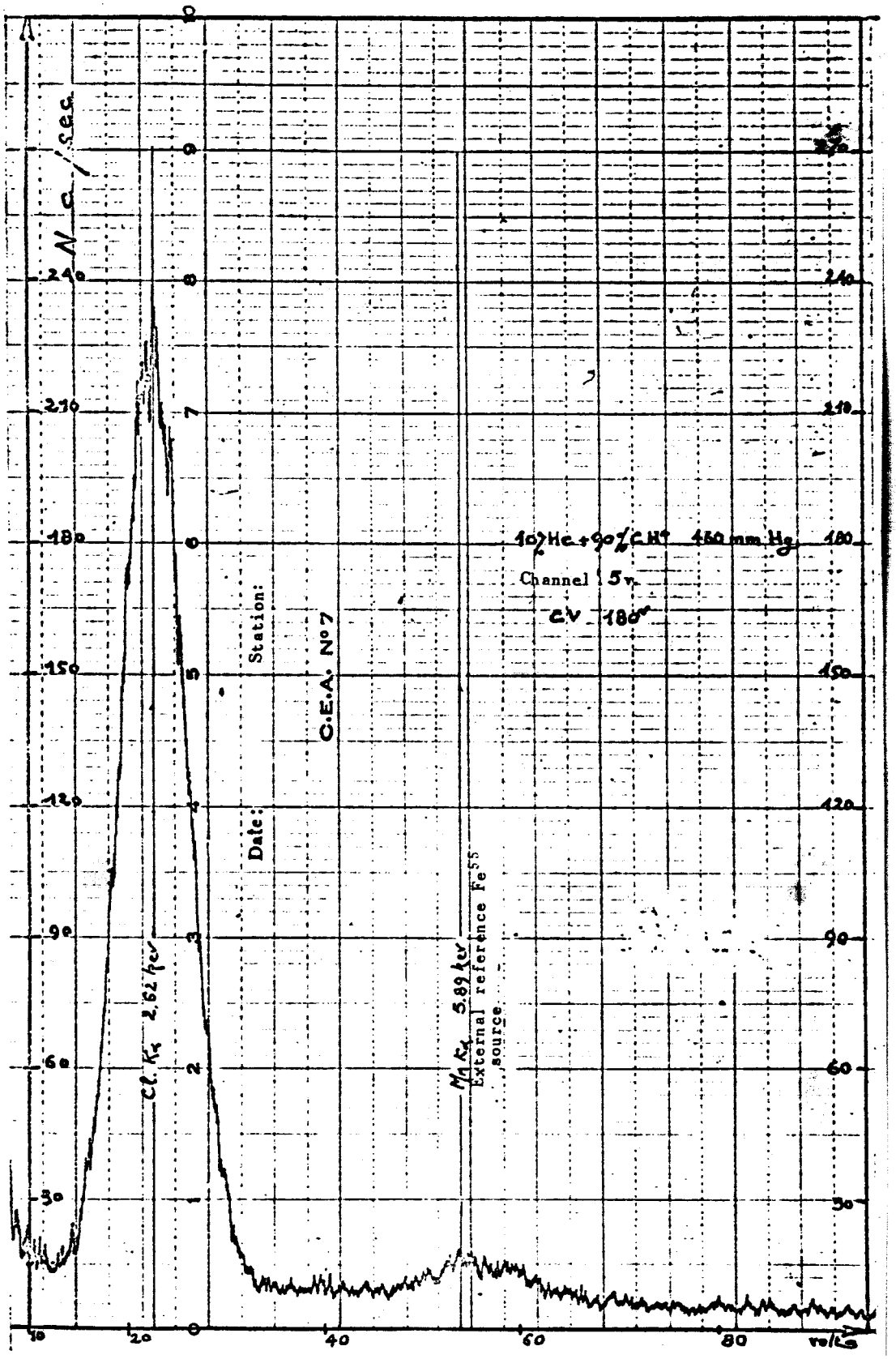

Fig.22 Kα Peak of Chlorine

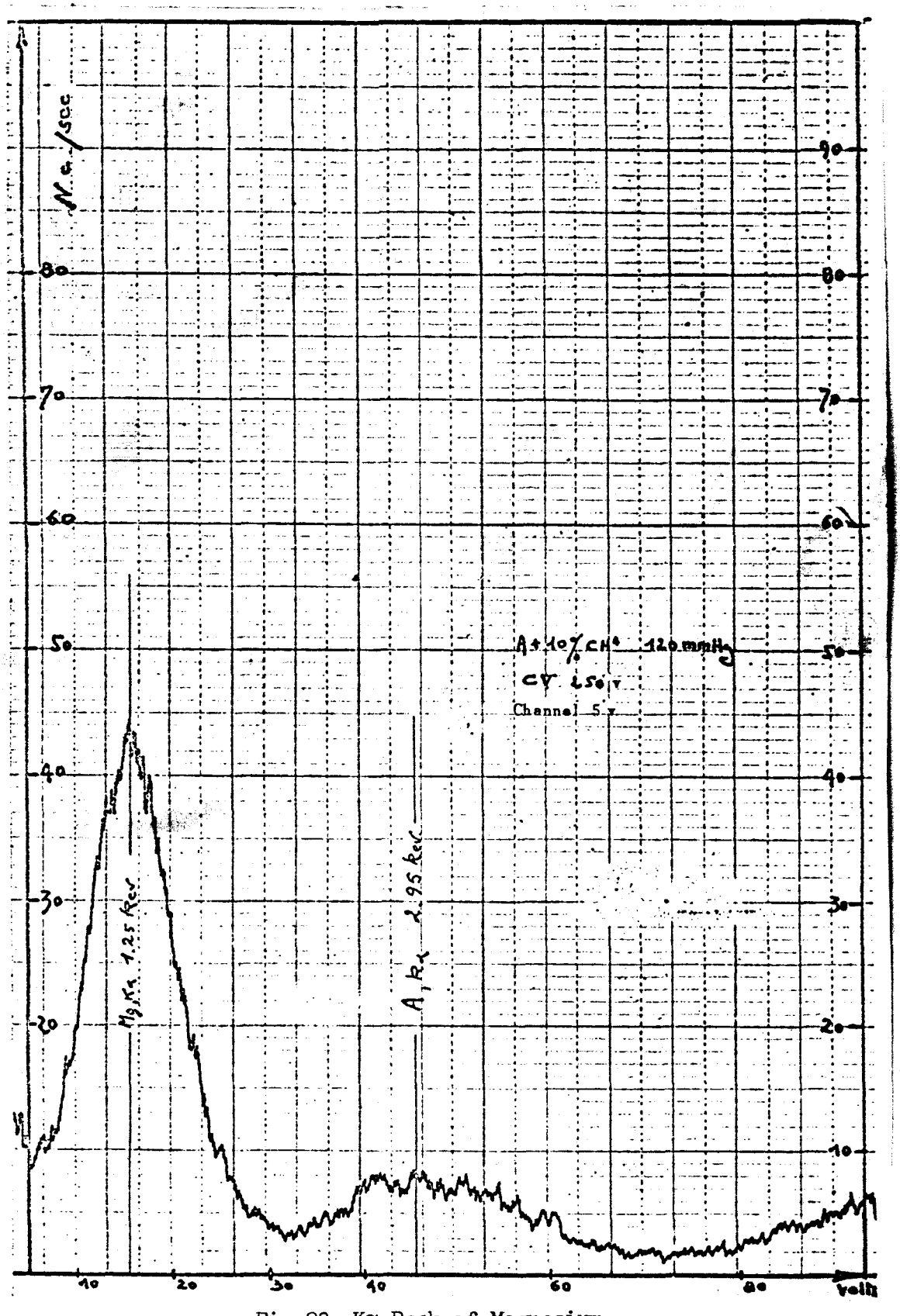

Fig.23 Kα Peak of Magnesium

activity of the source, 6 mC

adopted geometry, a = 0.4 to 0.5 cm.

In exciting an aluminum target, a strong background is observed at the optimum pressure of 190 mm Hg. The fluorescence peak separates from the background on increasing the pressure. The α path and the volume of the plasma can be limited by increasing the pressure.

Figure 24 shows the characteristic Kα peak of aluminum, for a pressure of 725 mm Hg.

The intensity of the peak is particularly high; we counted 2460 c/sec at a reduced background and a peaking ratio of 10.

The experiments with this particular source had to be interrupted, due to contamination of the counter with Po^{210}. The fact that a pressure drop occurred in the counter no doubt permitted the polonium to migrate through the mica.

Bouteiller (D.R.E.) studied and developed a model source of the type SA 3 of reduced dimensions, provided with a stainless steel window of 6 μ thickness. After vacuum tests and practical operation over a period of several months, these sources were found perfectly tight and thus completely uncontaminated.

The accompanying sketch shows the geometry of the irradiation used, with the type SA 3 source.

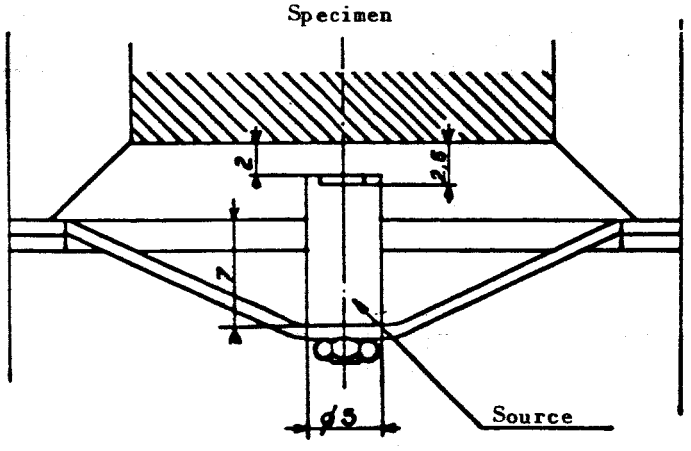

/80

This steel window noticeably decreases the energy of the emitted α-particles, but imparts a much greater ruggedness to this type of source.

At the time of its use, the source had an activity of about 0.8 mC.

The excitation by this source of elements of the second period gave interesting results; the Kα lines of fluorine and carbon were detected in a satisfactory manner.

A plate of LiF constitutes the irradiated target and the X-ray fluorescence emitted by it is detected in pure methane.

Figure 26 gives three radiation spectra detected at various pressures of the gas.

At a pressure of 500 mm Hg, the detection yield is low for the KαF line of the target. Conversely, the Kα line of the carbon of the CH_4 gas is strongly excited in the absorption volume and manifests itself in a relatively intense peak.

Detection of the X-ray radiation Kα of fluorine gives a peak of an intensity increased at the expense of that of carbon, at a pressure of 200 mm Hg.

The optimum pressure for the detection of the KαF line is 70 mm Hg. The peak of carbon is practically nonexistent in the spectrum.

To reduce the contribution of the Kα line of the carbon in the gas to the spectrum, it is suggested to use a gas mixture of, for example, He + CH_4 which would have the advantage of increasing the optimum detection pressure for the elements of the second period.

The use of an α-source does not permit application of the relation for the optimum pressure, as derived in Section II.3. In this case, the energy loss of the α-particle in the gas must be taken into consideration, since the efficiency of excitation of a given element depends on the energy of the particle, in

/81

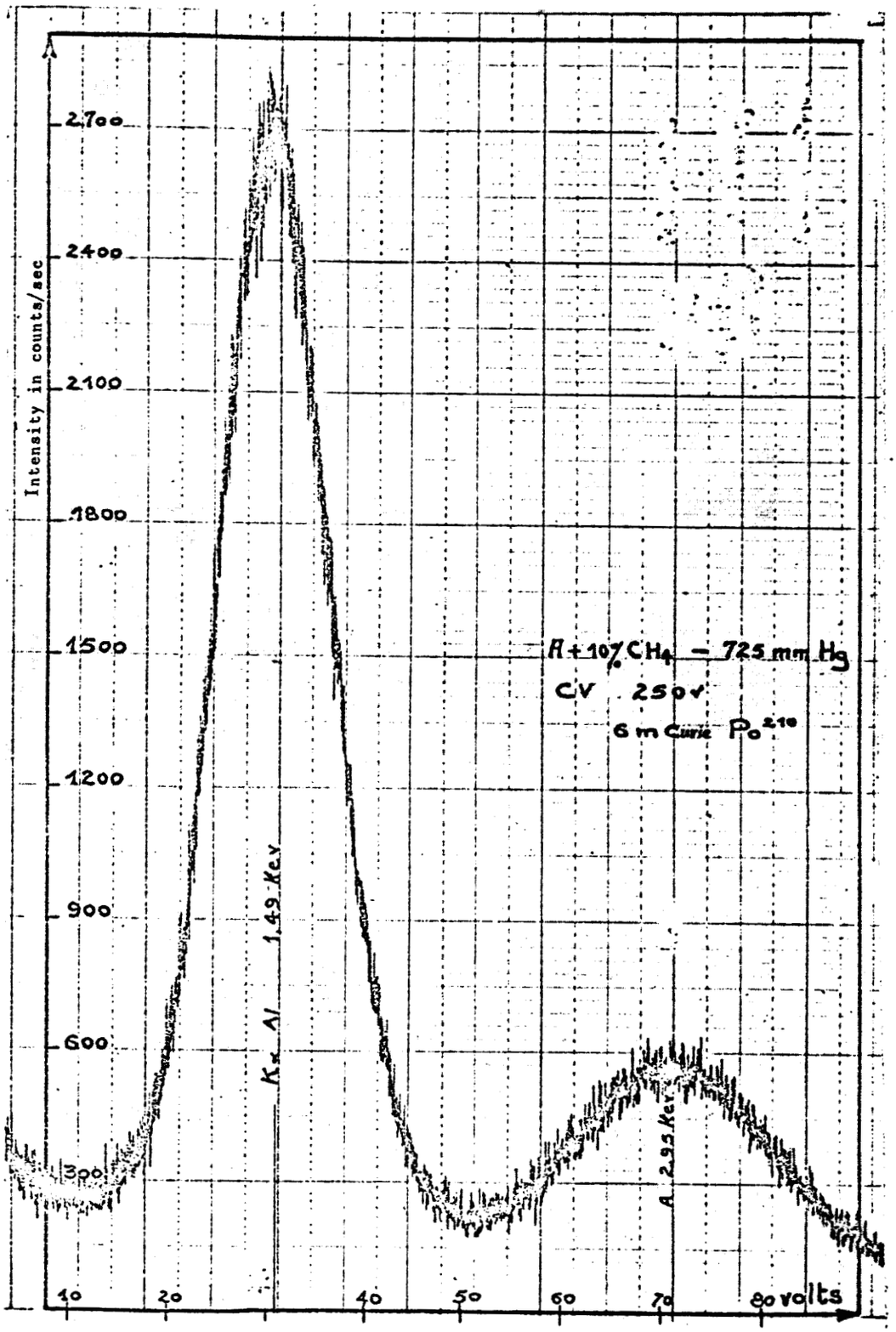

Fig.24 Kα Al Line, Excited by a Po^{210} Source

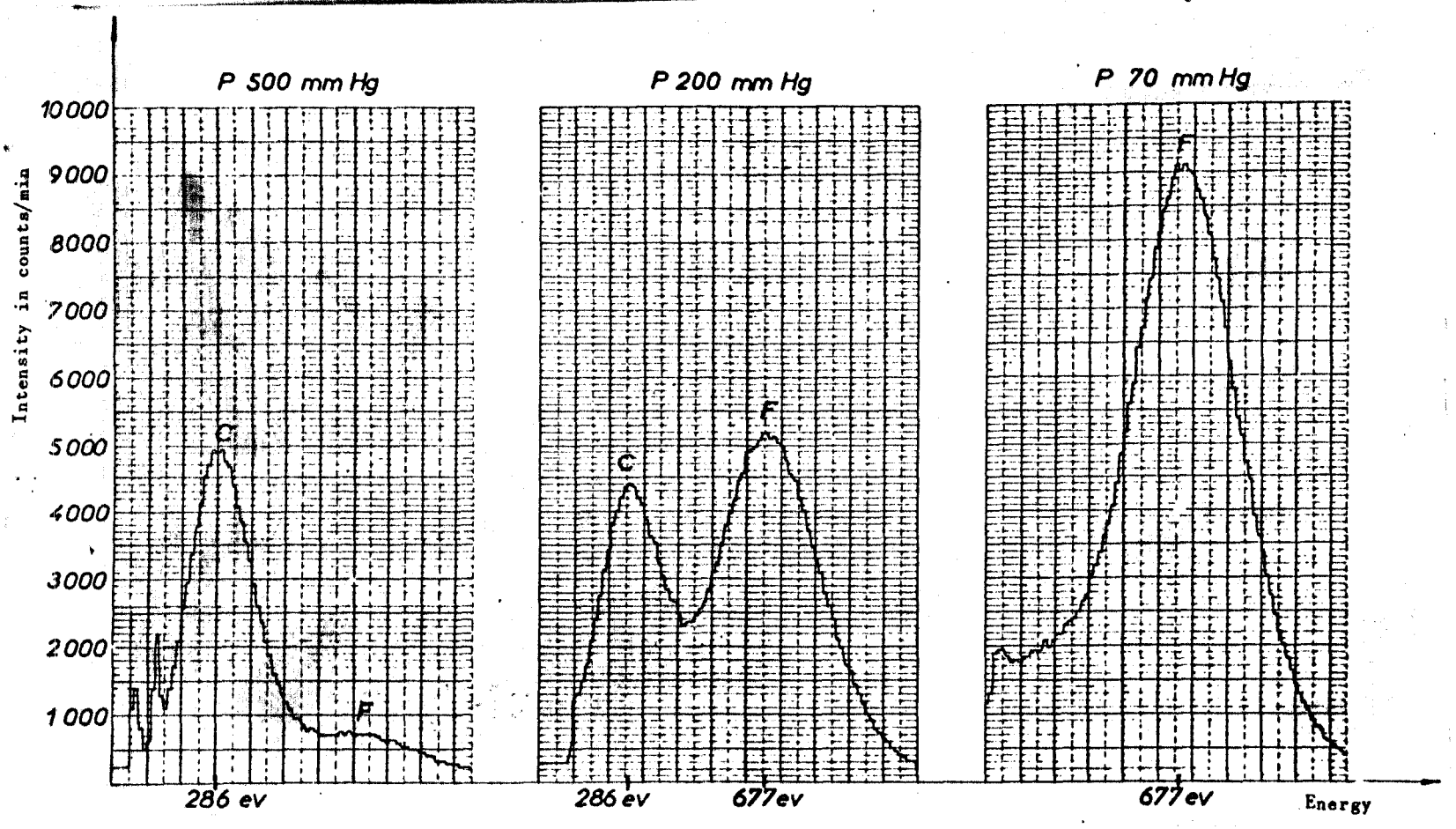

Fig.26 Excitation of the Fluorine Line (LiF Target); Detection in Methane

accordance with a relation of the form kE^n (Part I, Section III.3).

IV. BACKGROUND AT LOW ENERGY /84

The elimination of the counter window introduces two new factors with respect to conventional detection. The first is the possibility to detect electrons coming from the auxiliary volume and the second is the creation of a strongly ionized zone in the atmosphere of the proportional counter. The basic phenomena, accompanying these two factors, are schematically given below:

Creation of a plasma	ion recombination
	gas scintillation
	scattering of free electrons
Windowless proportional counter	deformation of the electric field
	detection of Auger electrons
	detection of low-energy free electrons.

Under these conditions, the fluorescence to be detected is masked by a continuous spectrum having an intensity that increases toward low energies.

In this Chapter, we will discuss the phenomena believed to be correlated with the background. For certain hypotheses (Auger electrons, distortion of the electric field), experiments were made in an attempt to substantiate these assumptions.

IV.1 Auger Electrons and Free Electrons

The Auger electrons, created in the target, have a kinetic energy of $E_K - 2E_L$; on arriving in the detection volume, this energy is decreased on traversal of a portion of the target and the gas in the auxiliary volume. The electrons, on arriving in the detection volume, exhibit a continuous spectrum of

the maximum energy $E_K - 2E_L$.

IV.1.1 Countervoltage

After having stipulated the hypothesis that the obtained continuous spectrum was due to a detection of low-energy electrons resulting from the creation of Auger electrons in the target, to scattering of free electrons of the /85 plasma, and to scattering by electrons ejected from the walls of the counter by X-ray radiation, we studied the possibility of collecting these undesirable electrons by an electric field. For this, an electric field E_2, as described in Section II.1, is established in the auxiliary volume. Figure 11 shows a deformation of the continuous spectrum under the influence of this field, together with the fluorescence peak emerging from the background, for a sufficiently high value of the countervoltage.

IV.1.2 Mylar Window

An experimental assembly was constructed for stopping the electrons emerging from the auxiliary volume and thus preventing their detection. It is assumed that the energy of these electrons does not exceed 5.89 Kev, which would correspond to that of the photons of the Fe^{55} excitation source.

A Mylar window of 1 mg/cm^2 stops most of these electrons (Bibl.55). The design was so arranged that the auxiliary volume was at the same atmosphere and pressure as the counter.

At the indicated dimensions, the Fe^{55} excites an aluminum target, Kα Al = = 8.34 Å or 1.48 Kev.

The detection gas used was A + 10% CH_4, at a pressure of 190 mm Hg.

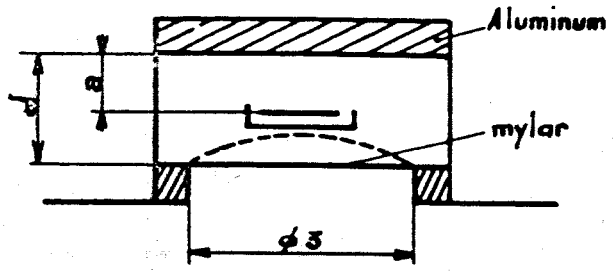

a = 0.5 cm

d = 0.8 ± 0.4 cm

The obtained results are given below:

	Without Window	Mylar Window
	CV = 250 v	CV = 0
K α Al peak	73 c/sec	31
Background	15 c/sec	8
Intensity of the peak	73 - 15 = 58 c/sec	23
r, peaking ratio	4.9	3.9

Let us use a ratio between peaks of /86

$$\frac{23}{58} = 0.397 .$$

The transmission of the window for a radiation of 8.34 Å will then be

$$\mu_m = 850 \text{ cm}^2/\text{gm} \quad \text{(Bibl.56)}$$

from which we obtain the transmission as $e^{-850 \times 1 \times 10^{-3}} = 0.428$.

Transmission of the gas:

Assuming that the Mylar is deformed and follows the contours of the source holder, as mentioned above, the distance d will be equal to a, i.e., 0.5 cm.

In the experiments without window, we must take into consideration an absorbing gas layer (Section II.3.2) whose thickness of 0.1 cm is known with an accuracy of the order of 20%. In experiments with window, the absorbing gas layer will then be d = 0.1, i.e., 0.5 - 0.1 = 0.4 cm.

The mass absorption coefficient of the gas reads:

$$\mu_m = 1050 \text{ cm}^2/\text{gm}$$

and the transmission then is $e^{-1050 \times 1.56 \times 10^{-3} \frac{190}{760} \times 0.4} = 0.903$. This value is determined to within 3.3%, because of the inaccuracy of the geometry.

The total transmission then becomes $0.903 \times 0.428 = 0.387$.

This value differs by -2.5% from the intensity ratio of the peaks, but can be explained by the geometric indeterminacy.

According to the above statements, the detection of electrons coming from the auxiliary volume is a demonstrated cause of the low-energy background. The auxiliary electric field permits collecting the free electrons of the lowest energies and thus prevents their scattering toward the counter.

For a = 0.5 and CV = 250 v, the maximum electric field will be 500 v/cm. In the source - specimen space, the electrons of an energy below 500 ev can then be collected.

IV.1.3 Pressure /87

To permit proper collection of the electrons supposed to be in energy equilibrium, it would be useful to decrease their velocity. In a plasma, the collisions between ions impart a velocity ω to these ions, whose expression $\omega = \mu \frac{E}{P}$ demonstrates that this velocity depends on the mobility μ of the ion in question, on the electric field E, and on the pressure P.

Thus, it is obvious that P must be increased in order to decrease ω. Consequently, to obtain the peak of fluorescence, it became necessary to increase the pressure above the optimum pressure, in cases of excitation of the target by relatively intense sources of H^3/Zr and of Po^{210}.

It should also be mentioned that an increase in pressure, within the range

of 0 to 1 atm, will increase the recombination coefficient α (Bibl.50). Thus, from 150 to 450 mm Hg, the coefficient α of the air will change from 1.1×10^6 to 2×10^6.

IV.2 Deformation of the Electric Field

We were interested to determine whether the perturbation produced in the principal electric field E_1 by the aperture zone of the auxiliary volume, may be responsible for a flattening of the peak, leading to a deterioration in the signal-to-noise ratio. However, it seems that this phenomenon is of minor significance with respect to the results given below.

IV.2.1 Aluminized Mylar

The idea of separating the volumes of the counter by Mylar, as described in Section IV.1, has been picked up again, using aluminized Mylar of less thickness. The results for the Kα peak of aluminum were as follows:

peak	35 c/sec
background	8 c/sec
r	4.4.

Thus, the ratio r has become more favorable, by changing from 3.9 to 4.4.

IV.2.2 Grid /88

An attempt at an electric separation of the two volumes by a metal grid, carrying the excitation source, did not give encouraging results. With the grid connected to ground, the ratio r does not exceed 2.5 and increases to 3.2 when bringing the grid to a potential of +80 v.

IV.3 Phenomena Accompanying Ion Recombination

In the strongly irradiated zone, close to the source, the high ion density and the weak electric field favor an intense ion recombination. The rate of recombination $\frac{dn}{dt}$ is a function of the density M^+ and M^- of the positive and negative ions per cm^3, having the form

$$\frac{dn}{dt} = -\alpha \cdot M^+ \cdot M^-$$

where α is the recombination coefficient of the gas which, in turn, is a function of the type of gas, the electric field, and the pressure (Section IV.1.3).

IV.3.1 Incomplete Detection of the Fluorescence Quantum

For the photoelectrons produced by fluorescence in the vicinity of the target, there is a recombination probability with the existing population of positive ions. This phenomenon will prevent complete detection of the electrons produced by the quantum $h\nu$, so that the detected spectrum will contain a tail at low energy.

This effect can be counteracted by lowering the coefficient α over an increase in the electric field E_2 or by lowering the pressure. Another possibility is to diminish the distance d that limits the recombination zone. Figure 12 shows that the decrease in d will lead to an increase in the peaking ratio.

IV.3.2 Gas Scintillation

Gas scintillation can be induced by radiative and dissociative recombination of the ions produced in the detection gas. Such a scintillation would give an intense continuous spectrum in the ultraviolet region. This radiation band, for the case of xenon, is located between 3000 and 5000 Å (Bibl.52). /89

Stacking phenomena would have to be expected here, since the duration of the luminescence is extremely short. L.Koch (Bibl.54) obtained pulses with pure xenium whose width at midheight was 3.3×10^{-9} sec at a pressure of 740 mm Hg.

With the gas mixtures used here, the scintillation will be greatly attenuated by the presence of polyatomic gases such as methane. It is well known that small amounts of oxygen, carbon monoxide, carbon dioxide, ammonia, methane, and various organic vapors would be sufficient to suppress the luminescence of the rare gas.

CONCLUSIONS

After excitation of the specimen by a radioactive source, the generated fluorescence is detected by a gas-filled proportional counter and then analyzed by spectrometry of the pulse amplitude. A special proportional counter was constructed, permitting the fluorescence emitted by the target to penetrate into the detection volume without traversing a window. The window of conventional detectors strongly absorbs the soft or ultrasoft X-rays but also eliminates the electrons traveling toward the detector. Therefore, it was necessary to provide an auxiliary electric field, to be used as a stopping medium for the electrons scattered toward the detection volume. This system has the advantage of adjusting the absorption volume to the range of the Auger electrons and thus to permit optimum transmission of the fluorescence photons from the target to the detection volume.

An optimum filling pressure of the detector is defined in accordance with the geometry of the device, the nature of the gas, and the respective energies of the X-ray radiation of excitation and fluorescence. This optimum pressure corresponds to a maximum efficiency of the detector, for a given X-ray energy

and thus plays a selective role with respect to other energies.

For circulation operation of the detector, the principle of peak stabilization is presented.

We also gave the main characteristics of X-ray fluorescence excitation for X-rays, β-radiation, and α-radiation. In this investigation, the excitation of the target was obtained either by X-ray radiation (Fe^{55} and H^3/Zr sources) or by α-radiation (Po^{210}). Some results obtained for the detection of X-Kα rays of elements are given, ranging from chlorine to carbon.

It must be taken into consideration that, in these experiments, the /90 sources which are not comparable in activity, nature of emission, and geometry, will naturally determine different parameters.

The optimum excitation and detection parameters were defined only for the Fe^{55} source.

However, a qualitative comparison for these experiments is readily possible.

The X-ray spectrum, emitted by a H^3/Zr source, is highly suitable for the excitation of elements of the third period; however, the liberation of tritium from such sources constitutes a major obstacle to their use.

The Fe^{55}, at satisfactory yield, excites the last elements of the third period and can also be used for the first elements; however, starting from aluminum and magnesium, preference should be given to α-sources which are the only ones useful for elements of the second period.

Consequently, an excitation of light elements by α-sources, using the described detection system, made it possible to obtain fluorescence spectra of low energy which, until now, could only be demonstrated by means of complex instruments such as the Castaing microprobe (Bibl.20) or by the use of X-ray

tubes of special design (Bibl.21).

The advantages obtained from the possibility of analyzing elements of the second period are obvious when taking into consideration that all organic materials contain carbon and, in numerous cases, large amounts of nitrogen and oxygen.

The described process, in a suitably adapted version, could be used for dosing and controlling light elements contained in industrial products.

Acknowledgement

The author wishes to express his deep gratitude to Prof. Grinberg who demonstrated interest in this work and procured the possibility of publishing this paper.

Sincere gratitude is also expressed to Messrs. Fisher, Cornuet, and Hours for making the facilities of the Department of Radioelements available, as well as to Mr. Martinelli who suggested this particular work and who always was ready to assist with valuable advice.

The author also wishes to thank all those who participated in the material realization of this study. Thanks are also expressed to the members of the /91 Department for Application of Radioelements for their friendly cooperation, specifically to Messrs. Kuntschmann, Lemaire, and Jacquet who made frequent contributions.

BIBLIOGRAPHY /93

1. Compton and Allison: X-Rays in Theory and Experiment. D. Van Nostrand Company Inc., New York, 1935.

2. Fine, S. and Hendee, C.F.: X-Ray Critical Absorption and Emission Energies

in Kev. Nucleonics, March 1955.

3. Martinelli, P. and Seibel, G.: Recent Developments in the Analysis and Measurement of Thicknesses by Excitation of Fluorescence Lines over the Intermediary of β-Particles (Nouveaux développements de l'analyse et de la mesure des épaisseurs par excitation des raies de fluorescence au moyen des particules β). Comm. Energie At. (France), Rappt., No.1786.

4. Henke, B.L., White, R., and Lundberg, B.: Semi-Empirical Determination of Mass Absorption Coefficient for the 5 to 50 Å X-Ray Region. J. Appl. Phys., Vol.28, No.1, 1957.

5. Broyles, C.D., Thomas, D.A., and Haynes, S.K.: The Measurement and Interpretation of the K-Auger Intensities. Phys. Rev., Vol.89, p.715, 1953.

6. Reiffel, L.: Beta-Ray-Excited Low-Energy X-Ray Sources. Nucleonics, March 1955.

7. Filosofo, I. et al.: Design and Characteristics of Beta-Excited X-Ray Sources. Conference on the Use of Radioisotopes, 1960.

8. Cameron and Rhodes: Beta-Excited Sources of Electromagnetic Radiation. Conference on the Use of Radioisotopes, RICC/14, 1960.

9. Cook, Mellish, and Payne: Application of Fluorescence X-Ray Production by EC Isotopes. Conference on the Use of Radioisotopes, 1958.

10. Enomoto and Mori: Coefficient of the Production of Beta-Excited X-Rays (Coefficient de la production des rayons X excités par les beta). Transl. Comm. Energie At., No.471, 1962.

11. Blokhin, M.A.: The Physics of X-Rays. A.E.C., Tr. 4502, Moscow, 1957. /94

12. Korff: Electron and Nuclear Counters. Van Nostrand, N.Y., 1946.

13. Kiser, R.W.: Characteristic Parameters of Gas-Tube Proportional Counters. Appl. Sci. Res., Sect.B, Vol.8, pp.183-200, 1959.

14. Holton, P. and Shape, J.: Rise Times of Pulses from a Proportional Counter. At. Energy Res. Estab., Harwell, March 1950.

15. Labeyrie, J.: Detection of Nuclear Radiations (Détection des rayonnements nucléaires). Course, University of Paris, 1957.

16. Korolev, G.A. and Kocharov, G.E.: Concerning the Operation of Proportional Counters. Izv. Akad. Nauk SSSR, Ser. Fiz., Vol.25, pp.866-870, 1961.

17. Arnot, E.L.: Collision Processes in Gases. Methuen, London, 1933.

18. Pontecorvo, B.: Recent Development in CP Technique. At. Energy Res. Estab. Harwell, 1949.

19. Langevin, M.: The Proportional Counter, its Principles and Applications (Le compteur proportionnel, principes, applications). Electronique, No.121.

20. Dolby: Brit. J. Appl. Phys., pp.64-66, February 1960.

21. Henke, B.L.: Measurement in the 10 to 100 Å X-Ray Region. Advan. X-Ray Anal., Vol.4, p.244, 1960.

22. Martinelli, P. and Seibel, G.: VIII International Colloq. Spectr., Lucerne, 1959.

23. Starfelt, Cederlund, and Liden: Intern. J. Appl. Radiation Isotopes, /95
Vol.2, p.265, 1957.

24. Leveque, P., Martinelli, P., and Chauvin, R.: Paper Presented by the C.E.A. (Atomic Energy Commission) at the Geneva Conference of 1955 (Communication du C.E.A. à la Conference de Genève 1955). Comm. Energie At. (France), Rappt., No.426.

25. Seibel, G. and Letraon, J.Y.: IRSID RAD 137, 1962.

26. Friedman, H.: Advances in Spectroscopy, edited by Thomson. John Wiley & Sons, 1962.

27. Hendee, C.F., Fine, S., and Brown, W.B.: Gas-Flow Proportional Counter for Soft X-Ray Detection. Rev. Sci. Instr., Vol.27, No.7, 1956.

28. Bühring, W. and Haxel, O.: Excitation of the X-K Rays of Nickel, Copper, Molybdenum by Particles of Po^{210} (Excitation des rayons X-K du Ni, Cu, Mo par les particules du Po^{210}). Z. Physik, Vol.148, p.653, 1957.

29. Curie, I. and Joliot, F.: J. Phys. Radium,Vol.11, p.116, 1931.

30. Rotwell and West: Proc. Phys. Soc. (London), Vol.63, Part 5(365A), 1950.

31. Holliday, J.E.: A Soft X-Ray Spectrometer Using Flow CP. Rev. Sci. Instr., Vol.31, p.891, August 1960.

32. Bothe and Franz: Z. Physik, Vol.49, p.1, 1928; Vol.52, p.466, 1929.

33. Dowell, L.G. and Berwaldt, O.E.: Experiments with Fluorescent X-Ray in the 10 - 50 Å Region. Rev. Sci. Instr. (USA), Vol.33, No.3, pp.340-341, 1962.

34. Tellez-Placencia, H.: K,L Absorption Discontinuity; Fluorescence Yield (Discontinuité d'absorption K,L; rendement de fluorescence). J. Phys. Radium, Vol.49, p.16, 1955.

35. Scobie, Molerr, and Fink: Capture Ratio L/K in Fe^{55} (Rapport de capture L/K dans le Fe^{55}). Phys. Rev., Vol.3, No.9, p.452, 1959.

36. Henke, B.L.: Auger Photoelectron Spectroscopy in the 10 to 1000 ev Range. Private Communication. /96

37. Hanna, Kirkwood, and Pontecorvo: High Multiplication Proportional Counter for Energy Measurement. Phys. Rev., Vol.75, pp.982-986, 1949.

38. Szymanski, A. and Herman, J.A.: Luminescence of Rare Gases Subjected to Ionizing Radiation in an Electric Field (Luminescence des gaz rares soumis à un rayonnement ionisant dans un champ électrique). J. Chim. Phys. Canada, Vol.60, No.3, 1963.

39. Kurepin and Maduyev: Low-Pressure Proportional Counter (Compteur propor-

tionnel à basse pression). Khim. i Tekhnol. Eksp. SSSR, Vol.5, pp.48-50, 1961.

40. Kramer, P.: A Double Proportional Counter for Absolute Measurement of Low-Energy Photons and Electrons. Nucl. Instr. Methods, Vol.15, p.289, 1962.

41. Lang, A.R.: Some Notes on the Design and Performance of X-Ray Proportional Counters. J. Sci. Instr., Vol.33, March 1956.

42. Taylor, J. and Parrish, W.: Absorption and Counting Efficiency Data for X-Ray Detection. Rev. Sci. Instr., Vol.26, 1955.

43. Holloway, J.T.: Large CP Spectrometer for the Study of Radioactive Samples with Low Specific Activity.

44. Riggs, F.B.: New Design for a Gas Flow Proportional Counter. Rev. Sci. Instr., Vol.34, April 1963.

45. Crawford, R.C.: A Proportional Counter Spectrometer Study of Low-Energy Auger and Fluorescence Radiation. Thesis TID 15693, 1954.

46. C.F.*: A Study of Mechanism of Poisoning of Proportional Counters. Thesis TID 13491, 1961.

47. Cameron, J.F. and Rhodes, J.R.: Nucleonics, Vol.19, No.3, 1961. /97

48. Laporte: Electric Discharge in Gases (Décharge électrique dans les gaz).

49. Townsend: Electricity in Gases. Clarendon Press, Oxford, 1915.

50. Loeb: Fundamental Process of Electrical Discharge in Gases. John Wiley & Sons, New York, 1939.

51. Blanc, D.: Particle Detectors (Détecteurs de particules). Masson & Cie.

52. Samour, C.: Thesis, Paris, 1963.

53. Muttel: Rapport S.A.R., 1963.

54. Koch, L.: Thesis, Paris, 1959.

* Last name of author omitted from document (translator).

55. Lane, P.O. and Zaffarano, D.J.: I S C, p.439, 1953.

56. Henke, B.L.: Transmission Coefficients, 4 - 44 Å (Coefficients de transmission 4 à 44 Å). Private Communication.

57. Lansiart, A. and Morucci, J.P.: Gas Amplification in a Proportional Counter (Amplification gazeuse dans un compteur proportionnel). J. Phys. Radium, Vol.23, p.102 A, June 1962.

58. Siegbahn, K.: Beta and Gamma Spectroscopy.

59. Mitchell, B.J.: Anal. Chem. U.S.A., Vol.33, No.7, pp.917-921, 1961.

60. Lucas, H.J. and Price, B.J.: Metallurgia, Vol.64, No.383, pp.149-152, 1961.

61. Felten, L.J.: Anal. Chem. U.S.A., Vol.31, No.11, p.1771, 1959. /98

62. Birks, L.S. and Harris, D.L.: Anal. Chem., July 1962.

63. Mulvey, T. and Campbell, A.: Brit. J. Appl. Phys., Vol.9, p.406, October, 1958.

64. Bisi, A. and Zappa, L.: Nuovo Cimento, Vol.2, p.988, 1955.

65. Laverlochere, J.: Microtecnic, Vol.XVI, No.5, 1962.

66. Born, M.: Z. Physik, Vol.38, p.803, 1926.

67. Thomson, J.J.: Phil. Mag., Vol.23, p.449, 1912.

68. Rutherford and Richardson: Phil. Mag., Vol.25, p.722, 1913.

69. Henneberg, W.: Z. Physik, Vol.86, p.592, 1933.

70. Chadwick, J.: Phil. Mag., Vol.24, p.594, 1912.

Received June 1, 1964